Future Climate Projections
Benton County, Oregon

April 2023

Oregon Climate Change Research Institute

OCCRI

Future Climate Projections: Benton County, Oregon

Meghan Dalton, Erica Fleishman, Dominique Bachelet, and David Rupp
Oregon Climate Change Research Institute
College of Earth, Ocean, and Atmospheric Sciences
104 CEOAS Administration Building
Oregon State University
Corvallis, OR 97331

April 2023

Table of Contents

Executive Summary

Climate change is expected to increase the occurrence of many climate-related natural hazards and to increase climate-related risks to assets, such as people, buildings, and other infrastructure. Confidence that the risk of heat waves will increase is very high (Table 1) given strong evidence in the peer-reviewed literature, consistency among the projections of different global climate models, and robust scientific principles that explain why temperatures increase in response to ongoing emissions of greenhouse gases. In areas where the human population is growing, and especially where it is aging, both the absolute number and the proportion of people at risk of negative health outcomes from heat exposure is increasing. Confidence that the risk of many other natural hazards will increase as climate changes is high or medium (Table 1), reflecting moderate to strong evidence and consistency among models. The latter risks are influenced by multiple factors in addition to increasing temperatures. Confidence that the risk of windstorms will change is low given that projections suggest relatively few to no changes and evidence is limited.

Table 1. Projected direction and level of confidence in changes in the risks of climate-related natural hazards and associated risks to assets. Very high confidence means that the direction of change is consistent among nearly all global climate models and there is robust evidence in the peer-reviewed literature. High confidence means that the direction of change is consistent among more than half of models and there is moderate to robust evidence in the peer-reviewed literature. Medium confidence means that the direction of change is consistent among more than half of models and there is moderate evidence in the peer-reviewed literature. Low confidence means that the direction of change is small compared to the range of model responses or there is limited evidence in the peer-reviewed literature.

	Low Confidence	Medium Confidence	High Confidence	Very High Confidence
⬆ Risk Increasing		💧 Drought 🐛 Expansion of Non-native Invasive Species ⚠ Reduced Air Quality 💧 Loss of Wetlands	🌧 Heavy Precipitation 🏠 Flooding 🔥 Wildfire	☀ Heat Waves
= Risk Unchanging	🌬 Windstorms			
⬇ Risk Decreasing				❄🌡 Cold Waves

In this report, we present future projections of climate and climate-related natural hazards in Benton County for the 2020s (2010–2039) and 2050s (2040–2069) relative to the 1971–2000 historical baseline. The projections are based on multiple global climate models for both a lower greenhouse gas emissions scenario (RCP 4.5) and a higher emissions scenario (RCP 8.5). Unless otherwise noted, all projections in this executive summary refer to the 2050s, relative to the historical baseline, under the higher emissions scenario. Projections for both time periods and emissions scenarios, and potential consequences for assets given current demographic data and projected population trends, are in the main report.

Heat Waves

The number, duration, and intensity of extreme heat events will increase as temperatures continue to warm. In Benton County, the number of extremely hot days (those on which the temperature is 90°F or higher) and the temperature on the hottest day of the year are projected to increase by the 2020s and 2050s under both the lower and higher emissions scenarios. The number of days per year with temperatures 90°F or higher is projected to increase by an average of 18 (range 6–33) by the 2050s, relative to the 1971–2000 historical baselines, under the higher emissions scenario. The temperature on the hottest day of the year is projected to increase by an average of about 6°F (range 2–9°F) by the 2050s. Projected demographic changes in Benton County, such as an increase in the proportion of older adults and the absolute number of children, will increase the number of people in some of the populations that are most vulnerable to extreme heat.

Cold Waves

Cold extremes will become less frequent and intense as the climate warms. The number of cold days (maximum temperature 32°F or lower) per year in Benton County is projected to decrease by an average of 0.5 (range -1.1–0.3). The temperature on the coldest night of the year is projected to increase by an average of 5°F (range 1–10°F). The number of county residents vulnerable to extreme cold is likely to grow, although this increase may be offset somewhat by the decrease in incidence of cold extremes.

Heavy Precipitation

The intensity of extreme precipitation is expected to increase as the atmosphere warms and holds more water vapor. In Benton County, the number of days per year with at least 0.75 inches of precipitation is not projected to change substantially. Nevertheless, the amount of precipitation on the wettest day and wettest consecutive five days per year is projected to increase by an average of 13% (range 1–29%) and 10% (range 2–19%), respectively. The number of days per year that exceed a threshold for landslide risk, which is based on prior 18-day precipitation accumulation, is not projected to change substantially. However, landslide risk depends on multiple factors, and this metric does not reflect all aspects of the hazard.

River Flooding

Winter flood risk at mid- to low elevations in Benton County, where temperatures are near freezing during winter and precipitation is a mix of rain and snow, is projected to increase as winter temperatures increase. The temperature increase will lead to an increase in the percentage of precipitation falling as rain rather than snow. An estimated 7% of residences in the county are within the 100-year floodplain, and another 7% are within the 500-year floodplain.

Drought

Drought, as represented by low summer soil moisture, low spring snowpack, low summer runoff, and low summer precipitation, is projected to become more frequent in Benton County. The incidence of related negative physical and mental health outcomes, especially among low income, tribal, rural, and agricultural communities, is likely to increase.

Wildfire

Wildfire frequency, intensity, and area burned are projected to continue increasing in the Northwest. Wildfire risk, expressed as the average number of days per year on which fire danger is very high, is projected to increase in Benton County by 11 days (range -7–25). The average number of days per year on which vapor pressure deficit is extreme is projected to increase by 26 (range 9–43).

Reduced Air Quality

Climate change is expected to reduce outdoor air quality. The risks to human health from wildfire smoke in Benton County are projected to increase. From 2004–2009 to 2046–2051, under a moderate emissions scenario, the number of days per year with poor air quality due to elevated concentrations of wildfire-derived fine particulate matter is projected to increase modestly (3%), but the concentration of fine particulate matter on those days is projected to increase by 80%.

Loss of Wetlands

In Benton County, losses of wetlands in recent decades largely were caused by conversion to agriculture. Projected effects of climate change on wetlands in the Northwest include reductions in water levels and hydroperiod duration. If withdrawals of ground water do not increase, then wetlands that are fed by ground water rather than surface water may be more resilient to climate change.

Windstorms

Wind patterns affect provision of electricity, transportation safety, and the spread of wildfires and pollutants. Mean wind speeds in Oregon are projected to decrease slightly, but extreme winter wind speeds may increase, especially in western Oregon. The frequency of strong easterly winds during summer and autumn, however, is projected to decrease slightly.
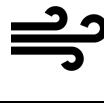
Expansion of Non-native Invasive Species

In general, non-native invasive plants in Benton County are likely to become more prevalent in response to projected increases in temperature and the frequency, duration, and severity of drought. However, many of these responses are uncertain, are likely to vary locally, and may change over time. Over the next several decades, changes in the distribution and abundance of non-native invasive animals in the county may not be strongly related to climate change.

Introduction

Industrialization has increased the amount of greenhouse gases emitted worldwide, which is causing Earth's atmosphere, oceans, and lands to warm (IPCC, 2021). Climate change and its effects already are apparent in Oregon (Dalton *et al.*, 2017; Mote *et al.*, 2019; Dalton and Fleishman, 2021; Fleishman, 2023). Climate change is expected to increase the likelihood of natural hazards such as heavy precipitation, flooding of rivers and streams, drought, heat waves, wildfires, and episodes of poor air quality, and to decrease the likelihood of cold waves.

We analyzed the influence of climate change on natural hazards in Benton County, Oregon, and explored potential effects of those natural hazards on the county's assets. Products of our analysis include county-specific data, graphics, and narrative summaries of climate projections related to ten climate-related natural hazards (Table 2). This information will be integrated into the county's Natural Hazards Mitigation Plan and can be used in other county plans, policies, and programs.

Table 2. Selected natural hazards and related climate metrics.

Heat Waves Hottest Day, Warmest Night Hot Days, Warm Nights	**Cold Waves** Coldest Day, Coldest Night Cold Days, Cold Nights
Heavy Precipitation Wettest Day, Wettest Five Days Wet Days, Landslide Risk Days	**River Flooding** Annual Maximum Daily Flows Atmospheric Rivers Rain-on-Snow Events
Drought Summer Flow, Spring Snow Summer Soil Moisture Summer Precipitation	**Wildfire** Fire Danger Days Extremely Dry Air Days
Reduced Air Quality Days with Unhealthy Smoke Levels	**Loss of Wetlands**
Windstorms	**Expansion of Non-native Invasive Species**

As of 2020, an estimated 94,665 people lived in Benton County (PRC, 2023a). The county's population is projected to increase by 27% by 2040, and by another 22% (or 55% relative to 2020) by 2070 (PRC, 2023b). Social factors affect the probability that natural hazards will negatively affect individuals and communities. For example, inequities in housing, education, income, and transportation access affect how different populations respond to heat, drought, and other climate extremes (Ho *et al.*, 2021). The U.S. Centers for Disease Control and Prevention developed and maintains a social vulnerability index for use in planning and response to hazardous events (Flanagan *et al.*, 2011; ATSDR, 2022). The index

encompasses 16 variables, which are aggregated into four themes: socioeconomic status, household characteristics, racial and ethnic minority status, and housing type and transportation. The numbers of cost-burdened housing units, multiple-unit homes, and people in group quarters in Benton County from 2016–2020 (Table 3) were among the highest 10% relative to other counties in Oregon; higher values indicate higher vulnerability (ATSDR, 2022).

Table 3. Measures of social vulnerability in Benton County, Oregon, as estimated on the basis of the 2016–2020 American Community Survey (ATSDR, 2022). Housing cost burden is defined as an occupied housing unit with a household annual income below $75,000 and monthly housing costs that equal or exceed 30 percent of annual income. Single-parent households include one or more persons under the age of 18. Racial and ethnic minority status includes individuals who identify as Hispanic, Latino (of any race), Black, African American, American Indian, Alaska Native, Asian, Native Hawaiian, Pacific Islander, two or more races, and other non-White races. Multi-unit housing refers to housing structures with ten or more units. Crowded housing is defined as an occupied housing unit with more people than rooms. Number of households without a broadband internet subscription is not included in calculation of the overall social vulnerability index. CI, confidence interval. Percentage, percentage of population or number. Percentages for some variables do not correspond exactly to raw values.

Social vulnerability metric	Population or number	CI	Percentage	CI
Total population	92168			
Number of housing units	38713	38464–38962		
Number of households	36051	35516–36586		
Socioeconomic status				
Below 150% poverty	22003	20872–23134	25.4	24.1–26.7
Unemployed	2927	2487–3367	6.1	5.2–7.0
Number of cost-burdened housing units	12156	11432–12880	33.7	31.8–35.6
No high school diploma	2149	1798–2500	3.8	3.2–4.4
No health insurance	4906	4256–5556	5.3	4.6–6.0
Household characteristics				
Aged 65 or older	14774	14674–14874	16.0	15.9–16.1
Aged 17 or younger	14935	14889–14981	16.2	
Civilian with a disability	10224	9529–10919	11.1	10.3–11.9
Single-parent household	1542	1256–1828	4.3	3.5–5.1
Speaks English less than well	1325	978–1672	1.5	1.1–1.9
Racial and ethnic minority status				
Minority	18792	18128–19456	20.4	19.7–21.1
Housing type and transportation				
Number of multiple-unit homes	5104	4593–5615	13.2	11.9–14.5
Number of mobile homes	2366	2084–2648	6.1	5.4–6.8
Number of crowded housing units	618	429–807	1.7	1.2–2.2
Number of households with no vehicle	2445	2089–2801	6.8	5.8–7.8
People in group quarters	5860	5298–6422	6.4	5.8–7.0

| People in households without a broadband internet subscription | 5240 | 4062–6418 | 6.1 |

Future Climate Projections Background

Introduction

The county-specific future climate projections presented here are derived from 10–20 global climate models and two scenarios of future global emissions of greenhouse gases. The spatial resolution of projections from global climate models has been increased to better represent local conditions. County-level summaries of changes in climate metrics (Table 2) are projected to the beginning and middle of the twenty-first century relative to a historical baseline. More information about the data sources is in the appendix.

Global Climate Models

Global climate models are computer models of Earth's atmosphere, ocean, and land and their interactions over time and space. Climate models generally refer to both general circulation models (GCMs) and Earth system models (ESMs). GCMs simulate the interactions between the atmosphere and the land and ocean, whereas ESMs also simulate more-detailed chemical and biological processes that interact with the physical climate. The models are grounded in the fundamental laws of physics and are the most sophisticated tools for understanding Earth's climate. However, they still necessarily simplify the climate system. Because there are several ways to simplify climate in a global model, different climate models yield somewhat different projections. Accordingly, it is best practice to analyze and present an average and range of projections from at least ten global climate models.

Over time, the spatial resolution of GCMs has increased and more physical, chemical, and biological processes, such as wildfire emissions and dynamic vegetation change, have been included (Figure 1). The climate models from the sixth phase of the Coupled Model Intercomparison Project (CMIP6), the climate modeling foundation of the Sixth Assessment Report of the Intergovernmental Panel on Climate Change (IPCC), generally have higher resolution, better represent Earth system processes, and improve simulation of recent mean values of climate change indicators relative to climate models from fifth phase of the Coupled Model Intercomparison Project (CMIP5) (IPCC, 2021). However, some CMIP6 models overestimate observed temperatures in the twentieth century, likely because they yielded a greater increase in temperature in response to modeled changes in cloud patterns (Dalton *et al.*, 2021; IPCC, 2021). The latter increase may not be realistic (Hausfather *et al.*, 2022). Consequently, the IPCC ranked climate models on the basis of their ability to reproduce twentieth-century temperatures, and used only the most accurate models to project warming given different scenarios of greenhouse gas emissions (Hausfather *et al.*, 2022).

A Climate Modeling Timeline
(When Various Components Became Commonly Used)

| 1890s | 1960s | | 1970s | 1990s | 2000s | 2010s |
| Radiative Transfer | Non-Linear Fluid Dynamics | Hydrological Cycle | Sea Ice and Land Surface | Atmospheric Chemistry | Aerosols and Vegetation | Biogeochemical Cycles and Carbon |

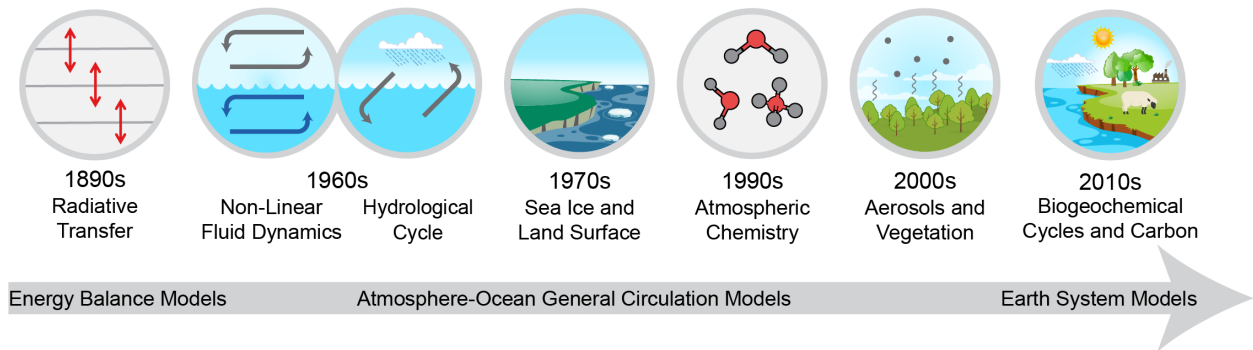Energy Balance Models — Atmosphere-Ocean General Circulation Models — Earth System Models

Figure 1. As scientific understanding of climate has evolved over the last 120 years, increasing amounts of physics, chemistry, and biology have been incorporated into global climate calculations. Over the second half of the twentieth century, as computing resources became available, such knowledge also was incorporated into global climate models. (Source: science2017.globalchange.gov)

Differences in simulations of Oregon's projected average temperature between CMIP5 and CMIP6 were estimated in the fifth Oregon Climate Assessment (Dalton *et al.*, 2021). The group of CMIP6 models generally projected greater warming over Oregon than the group of CMIP5 models. This outcome was due to the inclusion of several of the CMIP6 models that produce greater warming than most models given the same concentration of greenhouse gases.

One measure of climate sensitivity, the equilibrium climate sensitivity (ECS), is an estimate of the increase in global temperature after it stabilizes over hundreds to thousands of years following a doubling of carbon dioxide concentrations. On the basis of observations, paleoclimate data, and other evidence, the ECS of Earth was estimated to be within 4.5–7.2°F (66% likelihood) or 3.6–9.0°F (90% likelihood) (Forster *et al.*, 2021). The scientific community typically evaluates climate model outputs on the basis of how close they are to this range of ECS. ECS in all CMIP5 models was less than 9°F, whereas about one-fifth of the CMIP6 models had an ECS above 9°F (Hausfather *et al.*, 2022). Although there is a 5% likelihood that Earth's ECS is above 9°F, the CMIP6 climate models with ECS >9°F overestimate the observed warming and therefore are considered less valid and reliable than those with ECS ≤9°F. Consequently, use of the average and range of the CMIP6 model ensemble likely will yield inaccurate projections of future climate (Hausfather *et al.*, 2022).

It is best practice to analyze and present an average and range of projections from at least ten global climate models with realistic climate sensitivity that simulate the historical climate well (Mote *et al.*, 2011; Hausfather *et al.*, 2022; Dalton and Bachelet, 2023). In this report, we rely on projections from 10–20 CMIP5 models (see *Appendix*), all of which have realistic climate sensitivities and are still considered valid and useful in evaluating future climate (Dalton and Bachelet, 2023). Additionally, locally relevant, high-resolution projections from these models are readily available. It will be advantageous to consider CMIP6 climate projections after the scientific community has further evaluated the

projections and associated impacts and high-resolution projections become more widely available and vetted (Dalton and Bachelet, 2023).

Greenhouse Gas Emissions

When scientists use global climate models to project climate, they make assumptions about the future volume of global emissions of greenhouse gases. The models then simulate the effects of those emissions on the atmosphere, oceans, and land over the coming centuries. Because the precise amount of greenhouse gases that will be emitted in the future is unknown, scientists use multiple scenarios of greenhouse gas emissions that correspond to plausible societal trajectories.

The CMIP5 models used scenarios called Representative Concentration Pathways (RCPs), which describe concentrations of greenhouse gases, aerosols, and other factors through the year 2100. These concentrations affect the level of outgoing long-wave radiation from Earth's surface, thus radiative forcing. Radiative forcing is the total amount of energy retained in the atmosphere after absorption of incoming solar radiation, which is affected by the reflectivity of Earth's surface, and emission of outgoing long-wave radiation. The higher the volume of global emissions, the greater the radiative forcing and projected increase in global temperature (Figure 2).
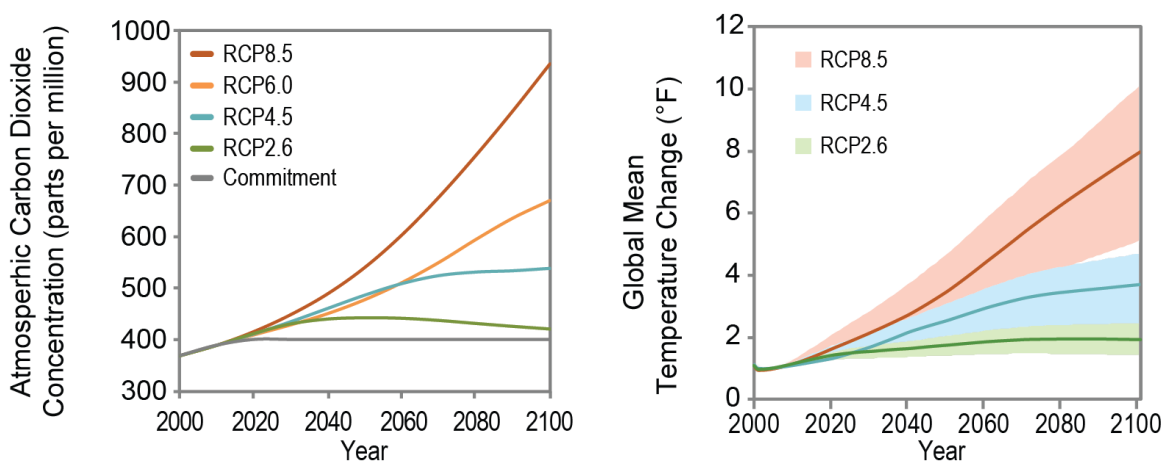

Figure 2. Future scenarios of atmospheric carbon dioxide concentrations (left) and projections of global temperature change (right) resulting from several different emissions scenarios, called Representative Concentration Pathways (RCPs), that were considered in the fourth National Climate Assessment (Hayhoe *et al.*, 2017). In the left plot, the gray line represents a scenario in which atmospheric carbon dioxide concentrations remain constant after reaching 400 parts per million; this concentration was exceeded in 2013 and continues to increase. In the right plot, the solid line and shading represent the mean and range of simulations from global climate models included in CMIP5. (Source: science2017.globalchange.gov/chapter/4/)

CMIP6 models used scenarios called Shared Socio-economic Pathways (SSPs). The SSPs reflect assumptions about future population, technological, and economic growth that were paired with the different levels of emissions associated with the CMIP5 RCPs (IPCC, 2021). Projections in this report are based on both a lower emissions pathway (RCP 4.5) and a higher emissions pathway (RCP 8.5) that are often described as representing moderate reductions and business-as-usual increases in greenhouse gas emissions, respectively (Hayhoe *et al.*, 2017). These two RCPs are the most common scenarios in the peer-reviewed literature, and high-resolution data representing the effects of these scenarios on local climate are available.

Downscaling

Global climate models simulate the climate across large, contiguous grid cells. One to three grid cells cover the state of Oregon. To make these coarse-resolution simulations more locally relevant, outputs are combined statistically with historical observations, yielding higher-resolution projections. This process is called statistical downscaling. The future climate projections in this report were statistically downscaled to a resolution of about 2.5 by 2.5 miles (Abatzoglou and Brown, 2012). More information about downscaling is in the appendix.

Future Time Periods

When analyzing global climate model projections, it is best practice to compare the average of simulations across at least 30 future years to the average of simulations across at least 30 recent past years. The average over those 30 past years is called the *historical baseline*. We present projections averaged over two future 30-year periods, 2010–2039 (2020s) and 2040–2069 (2050s), relative to the historical baseline from 1971–2000 (Table 4).

Table 4. Historical and future time periods over which projections were averaged.

Historical Baseline	2020s	2050s
1971–2000	2010–2039	2040–2069

Because each of the 20 CMIP5 models from which we obtained projections is based on slightly different assumptions, each yields a slightly different value for the historical baseline. Therefore, we do not present the average and range of projected absolute values of variables. Instead, we present the average and range of projected changes in values of climate variables relative to each model's historical baseline. We also present the average of the 20 historical baselines to aid in understanding the relative magnitude of projected changes. The average projected change can be added to the average historical baseline to infer the average future value of a given variable. The average projected change and historical baseline are included in the tables.

How to Use the Information in this Report

Because the observational record may not include plausible future values of some climate variables or the plausible future frequency of some climate extremes, one cannot reliably anticipate future climate by considering only past climate. Future projections from GCMs

enable exploration of a range of plausible outcomes given the climate system's complex response to increasing atmospheric concentrations of greenhouse gases. Projections from GCMs should not be interpreted as predictions of the weather on a given date, but rather as projections of climate, which is the long-term statistical aggregate of weather (Walsh *et al.*, 2014).

The projected direction and magnitude of change in values of climate variables in this report are best interpreted relative to the historical climate under which a particular system or asset evolved or was designed to operate. For this reason, considering the projected changes between the historical and future periods allows one to envision how natural and human systems may respond to future climate conditions that are different from past conditions. In some cases, the projected change may be small enough for the existing system to accommodate. In other cases, the projected change may be large enough to require adjustments, or adaptations, to the existing system. However, engineering or design projects would require an analysis that is more detailed than we present in this report.

The information in this report can be used to

- Explore a range of plausible future outcomes that reflect the climate system's complex response to increasing concentrations of greenhouse gases
- Envision how current systems may respond to climate conditions different from those under which the systems evolved or were designed to operate
- Inform evaluation of potential mitigation actions within hazard mitigation plans
- Inform assessment of the likelihood of occurrence of a particular climate-related hazard

Average Temperature

Oregon's average temperature warmed at a rate of 2.2°F per century from 1895 through 2021 (Fleishman, 2023). Average temperature is expected to continue increasing during the twenty-first century if global emissions of greenhouse gases continue; the rate of warming depends on the level of emissions (IPCC, 2021). By the 2050s (2040–2069), relative to the 1970–1999 historical baseline, Oregon's average temperature is projected to increase by 3.6°F (range 1.8–5.4°F) under a lower emissions scenario (RCP 4.5) and by 5.0°F (range 2.9–6.9°F) under a higher emissions scenario (RCP 8.5) (Dalton *et al.*, 2017, 2021; Fleishman, 2023). Summers are projected to warm more than other seasons (Dalton *et al.*, 2017, 2021; Fleishman, 2023).

During the twenty-first century, average temperature in Benton County is projected to warm at a rate similar to that of Oregon as a whole (Figure 3). Projected increases in average temperature in the county, relative to the 1971–2000 historical baseline in each global climate model (GCM), range from 0.9–3.3°F by the 2020s (2010–2039) and 1.4–6.3°F by the 2050s (2040–2069), depending on emissions scenario and GCM (Table 5).
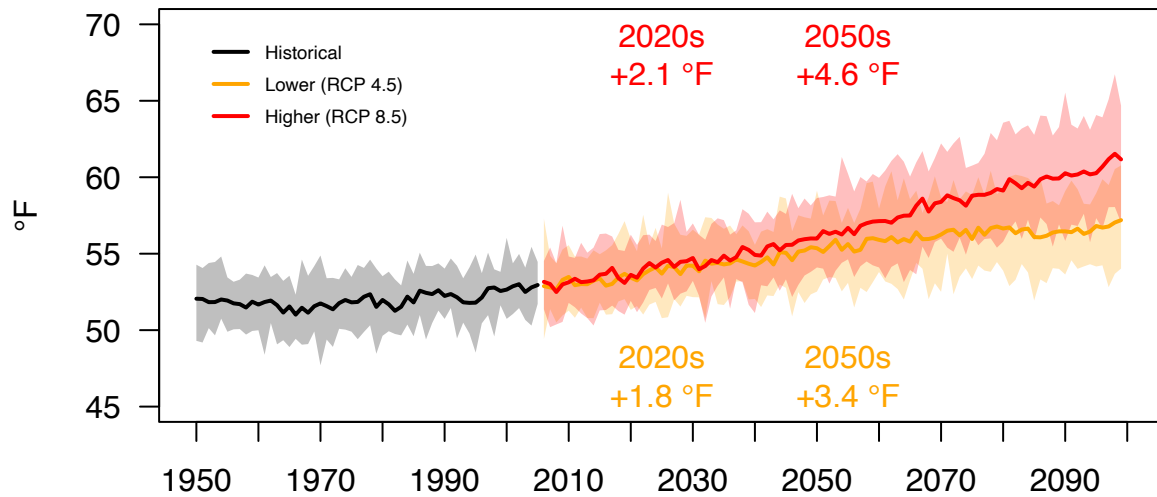

Figure 3. Projected annual average temperature in Benton County as simulated by 20 downscaled global climate models under a lower (RCP 4.5) and a higher (RCP 8.5) greenhouse gas emissions scenario. Solid lines and shading represent the 20-model mean and range, respectively. The figure shows the multiple-model mean differences between the average historical (1971–2000) baseline and the 2020s (2010–2039 average) and 2050s (2040–2069 average).

Table 5. Projected changes in annual temperature in Benton County between the 1971–2000 baseline period and future periods. Values are averages across 20 global climate models (range in parentheses).

Emissions Scenario	Future Period	
	2020s (2010–2039 average)	2050s (2040–2069 average)
Lower (RCP 4.5)	+1.8°F (0.9–2.9)	+3.4°F (1.4–4.8)
Higher (RCP 8.5)	+2.1°F (1.3–3.3)	+4.6°F (2.7–6.3)

Heat Waves

Heat is the leading cause of weather-related deaths in the United States (Khatana *et al.*, 2022). Extreme heat and home air conditioning are less common in Oregon than in many other parts of the country, leaving residents more vulnerable when extreme heat occurs. For example, record-breaking heat in June 2021 caused more than 100 deaths in Oregon, mostly inside homes without air conditioning (O'Neill *et al.*, 2023). Dangerous heat is almost always associated with a weather event called a heat wave (O'Neill *et al.*, 2023). Heat waves occur periodically as a result of natural variability in temperature, but human-caused climate change is increasing their frequency and intensity (Vose *et al.*, 2017; IPCC, 2021). In the absence of human-caused climate change, the intensity of the June 2021 heat wave would have been virtually impossible (Philip *et al.*, 2022).

Extreme heat can refer to extremely warm daytime highs or overnight lows (days on which maximum or minimum temperatures are above a threshold or a probability relative to past decades), seasons in which temperatures are well above average, and heat waves, or multiple consecutive days on which maximum or minimum temperatures are above a threshold or a probability. In the Pacific Northwest, a day on which the maximum temperature is at least 90°F often is considered to be an extremely warm day. The number of such days increased significantly across Oregon since 1951 (O'Neill *et al.*, 2023). The heat index is a measure of perceived heat that reflects both temperature and relative humidity and is more relevant to human health impacts than temperature alone. As relative humidity increases, a given temperature can feel hotter. The National Weather Service issues heat warnings when the heat index exceeds given local thresholds. Across Oregon, heat waves rarely are humid (Rastogi *et al.*, 2020), and the heat index generally is similar to the actual temperature. Nevertheless, the average number of hours per year that Oregonians experience a heat index of at least 90°F increased significantly since 1981 (O'Neill *et al.*, 2023).

The number of extremely warm nights is also increasing. In western Oregon, nights on which the minimum temperature was at least 65°F were rare before 1990, but the number of such nights has increased significantly in some areas during the past two decades (O'Neill *et al.*, 2023). In addition, evidence of increases in the number of summer extreme heat events that are defined by nighttime minimum temperatures is stronger than evidence of increases in the number of those defined by maximum temperatures (Dalton and Loikith, 2021).

The number, duration, and intensity of extreme heat events in Oregon is projected to increase due to continued increases in mean temperatures (Dalton and Loikith, 2021; O'Neill *et al.*, 2023). Climate models generally agree that changes in temperature extremes largely are linearly correlated with changes in the mean temperature. However, some mechanisms, which are the subject of active research, might cause a more substantial increase in extreme temperature than mean temperature (O'Neill *et al.*, 2023). For example, Arctic amplification (the decrease in the equator-to-pole temperature gradient, caused in part by the melting of Arctic sea ice) may alter the shape and position of the midlatitude jet stream, thereby contributing to an increase in the number of summer heat waves in Oregon (O'Neill *et al.*, 2023; Rupp and Schmittner, 2023). In addition, dry soils can

amplify extreme heat events through their relative lack of evaporative cooling (O'Neill *et al.*, 2023).

Here, we present projected changes in three metrics of extreme daytime heat (maximum temperature) and nighttime heat (minimum temperature) (Table 6).

Table 6. Metrics and definitions of heat extremes.

Metric	Definition
Hot Days	Number of days per year on which maximum temperature is 90°F or higher
Warm Nights	Number of days per year on which minimum temperature is 65°F or higher
Hottest Day	Highest value of maximum temperature per year
Warmest Night	Highest value of minimum temperature per year
Daytime Heat Waves	Number of events per year in which the maximum temperature on at least three consecutive days is 90°F or higher
Nighttime Heat Waves	Number of events per year in which the minimum temperature on at least three consecutive days is 65°F or higher

In Benton County, the number of hot days and warm nights, and the temperature on the hottest day and warmest night, are projected to increase by the 2020s (2010–2039) and 2050s (2040–2069) under both the lower (RCP 4.5) and higher (RCP 8.5) emissions scenarios (Table 7, Figure 4, Figure 5). For example, by the 2050s under the higher emissions scenario, the number of hot days, relative to each GCM's 1971–2000 historical baseline, is projected to increase by 6–33. The average number of hot days per year is projected to be 18 more than the average historical baseline of 4 days. The average number of days per year with a heat index of 90°F or higher is projected to be 21 more than the average historical baseline of 4 days (Dalton and Loikith, 2021). The average number of warm nights per year is projected to be 3 more than the average historical baseline of less than 1.

Under the higher emissions scenario, the temperature on the hottest day of the year is projected to increase by 1.5–8.7°F by the 2050s relative to the GCMs' historical baselines. The average projected increase in temperature on the hottest day is 5.9°F above the average historical baseline of 92.9°F. The average projected increase in temperature on the warmest night is 5.1°F above the average historical baseline of 61.5°F.

Under the higher emissions scenario, the numbers of daytime and nighttime heat waves are projected to increase by 0.9–3.8 and 0.0–1.1, respectively, by the 2050s relative to the GCMs' historical baselines. The average number of daytime and nighttime heat waves is

projected to increase by 2.6 and 0.4, respectively, above the average historical baselines of 0.7 and 0 (Table 7, Figure 6).

Table 7. Projected future changes in extreme heat metrics in Benton County. Changes from the 1971–2000 baseline were calculated for each of 20 global climate models and averaged across the 20 models (range in parentheses) for a lower (RCP 4.5) and higher (RCP 8.5) emissions scenario and for the 2020s (2010–2039 average) and 2050s (2040–2069 average). The average projected change can be added to the average historical baseline to infer the average projected future value of a given variable.

	Average Historical Baseline	2020s		2050s	
		Lower	Higher	Lower	Higher
Hot Days	4.4 days	4.2 days (1.7-7.9)	5.5 days (2.5-7.9)	10.8 days (5.4-18.6)	17.6 days (5.6-32.5)
Warm Nights	0.3 days	0.3 days (-0.1-1)	0.5 days (0-1.5)	1.3 days (0.1-3.8)	2.9 days (0.5-9.2)
Hottest Day	92.9°F	1.8°F (-0.2-3.1)	2.6°F (1-4.6)	4.4°F (1.4-6.6)	5.9°F (1.5-8.7)
Warmest Night	61.5°F	1.6°F (-0.2-3)	2.1°F (0.3-3.5)	3.8°F (1.9-6.2)	5.1°F (2.1-7.6)
Daytime Heat Waves	0.7 events	0.7 events (0.1-1.4)	0.9 events (0.4-1.4)	1.7 events (0.9-2.7)	2.6 events (0.9-3.8)
Nighttime Heat Waves	0 events	0 events (0-0.2)	0.1 events (0-0.2)	0.2 events (0-0.5)	0.4 events (0-1.1)

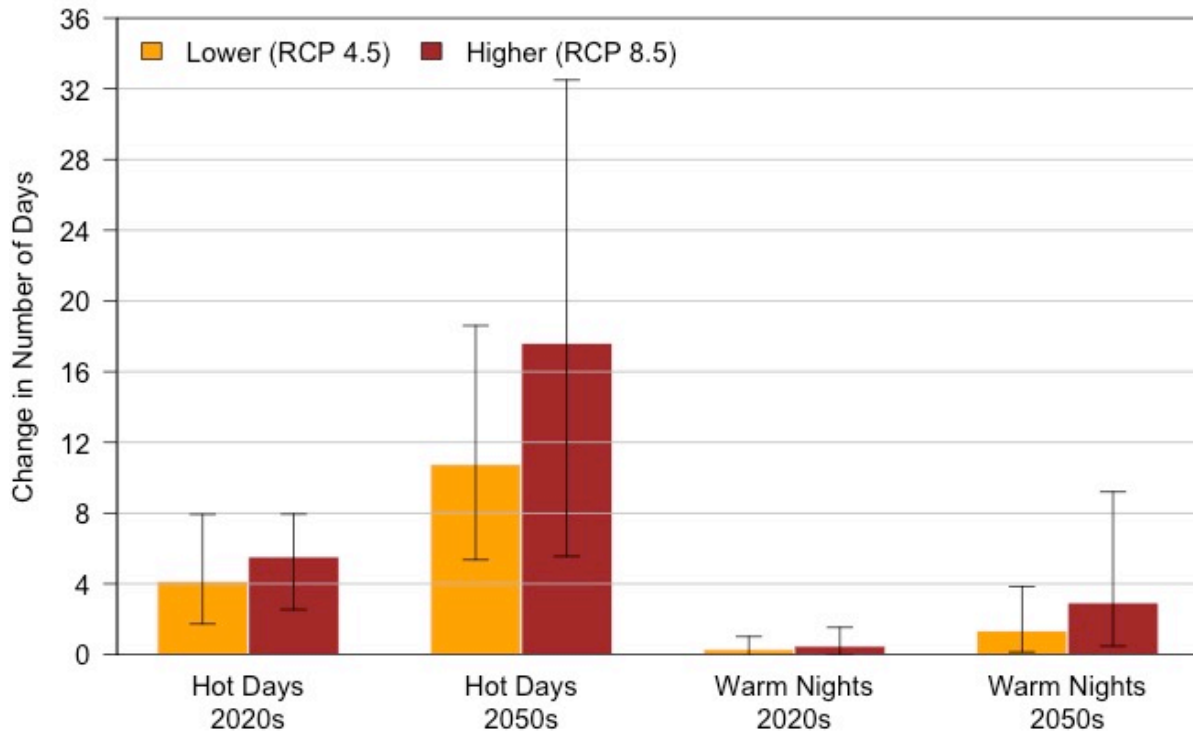**Change in Number of Extreme Heat Days in Benton County**

Figure 4. Projected changes in the number of hot days (left two sets of bars) and warm nights (right two sets of bars) in Benton County by the 2020s (2010–2039 average) and 2050s (2040–2069 average), relative to the historical baseline (1971–2000 average), under two emissions scenarios. Changes were calculated for each of 20 global climate models relative to each model's historical baseline, then averaged. Whiskers represent the range of changes across the 20 models. Hot days are those on which the maximum temperature is 90°F or higher; warm nights are those on which the minimum temperature is 65°F or higher.

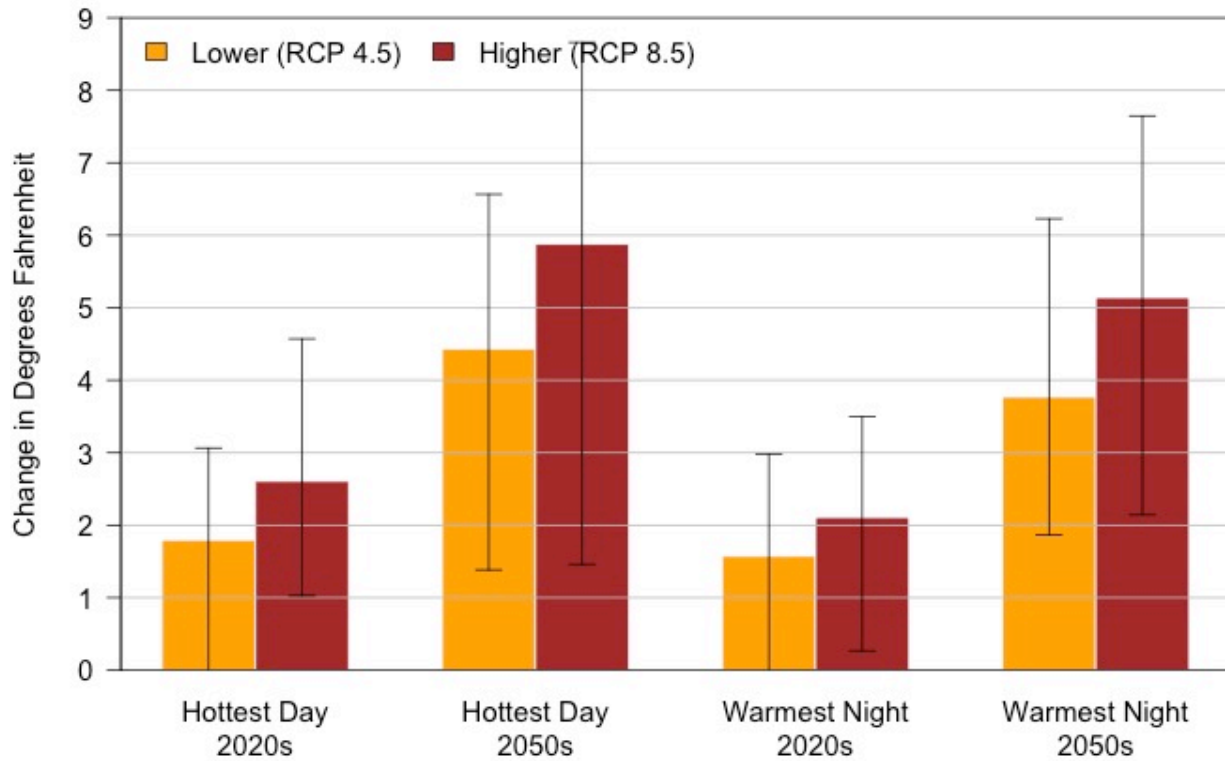**Change in Magnitude of Extreme Heat in Benton County**

Figure 5. Projected changes in the temperature on the hottest day of the year (left two sets of bars) and warmest night of the year (right two sets of bars) in Benton County by the 2020s (2010–2039 average) and 2050s (2040–2069 average), relative to the historical baseline (1971–2000 average), under two emissions scenarios. Changes were calculated for each of 20 global climate models relative to each model's historical baseline, then averaged. Whiskers represent the range of changes across the 20 models.

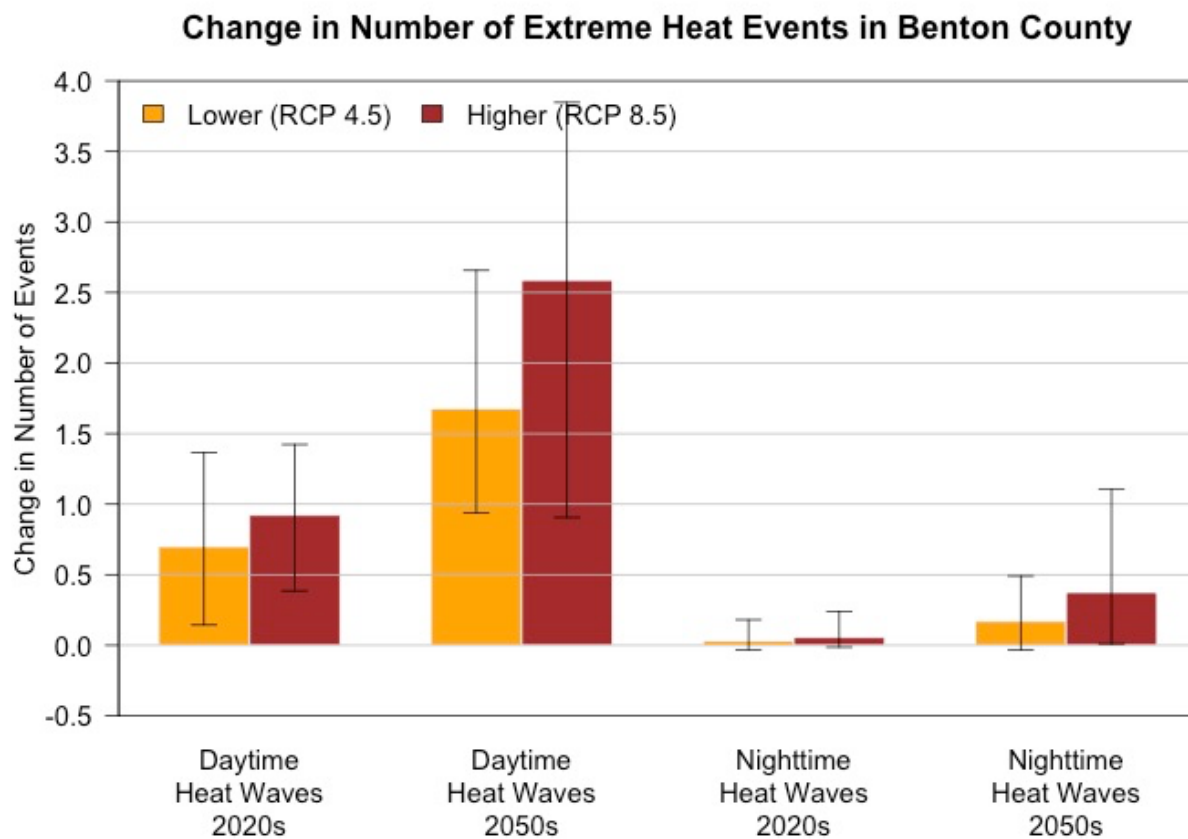**Change in Number of Extreme Heat Events in Benton County**

Figure 6. Projected changes in the number of daytime heat waves (left two sets of bars) and nighttime heat waves (right two sets of bars) in Benton County by the 2020s (2010–2039 average) and 2050s (2040–2069 average), relative to the historical baseline (1971–2000 average), under two emissions scenarios. Changes were calculated for each of 20 global climate models relative to each model's historical baseline, then averaged. Whiskers represent the range of changes across the 20 models. Daytime heat waves are defined as three or more consecutive days on which the maximum temperature is 90°F or higher; nighttime heat waves are three or more consecutive days on which the minimum temperature is 65°F or higher.

Potential Effects of Extreme Heat on People

Certain populations are considered especially vulnerable to heat-related illness and death; extreme heat also exacerbates interpersonal violence (Miles-Novelo and Anderson, 2019; Stechemesser et al., 2022). These populations include agricultural, forestry, and other outdoor workers; residents of urban heat islands; people with preexisting conditions or without housing or air conditioning; pregnant women; older adults; children; low-income communities; and communities of color (York et al., 2020; Ho et al., 2021).

Outdoor workers. The U.S. Bureau of Labor Statistics does not track occupational employment and wages in Benton County, although data for Corvallis are available. However, the Oregon Employment Department includes Benton, Clatsop, Columbia, Lincoln, and Tillamook Counties in its Northwest Oregon employment data and projections

(OED, 2023). Within Northwest Oregon in 2021, an estimated 2837 individuals were employed in farming, fishing, and forestry and 4661 were employed in construction and extraction. Employment in those two sets of occupations was projected to increase by 2% and 13%, respectively, by 2031.

The 2012 Census of Agriculture estimated that 572 migrant farmworkers (including those producing livestock) and 1135 seasonal farmworkers were employed in Benton County (Rahe, 2018). A 2016 survey of agricultural workers in the Monroe area indicated that 90% were Latino, half were migrant workers, and 38% were seasonal (BCHD, 2017).

Urban areas. As of 2020, about 83% of Benton County's population (78,456 people) lived within the urban growth boundaries of Adair Village, Albany (within county lines), Corvallis, Monroe, and Philomath (PRC, 2023b). A projected 84% and 86% of the county's residents will live within urban growth boundaries by 2040 and 2070, respectively (PRC, 2023b).

Preexisting conditions. Two national surveys provide estimates of preexisting conditions at the county level. The American Community Survey (ACS), conducted by the U.S. Census Bureau, surveys more than 3.5 million households each year (https://www.census.gov/programs-surveys/acs/about.html). The Behavior Risk Factor Surveillance System (BRFSS), sponsored by the U.S. Centers for Disease Control and Prevention's National Center for Chronic Disease Prevention and Health Promotion, other Centers for Disease Control and Prevention centers, and federal agency partners, surveys more than 400,000 adults per year (https://www.cdc.gov/brfss/about/index.htm). Data from the ACS indicated that from 2011–2015, 10% of Benton County residents, including about 8% of those aged 18–64 and 31% of those aged 65 and older, were living with a disability (BCHD, 2017). The BRFSS data indicated that 28% of residents ages 18 and older were living with a disability (BCHD, 2017). The most prevalent disability reported by individuals aged 5–64 was cognitive difficulty, whereas that among individuals aged 65 and older was ambulatory disability (BCHD, 2017).

Data from the BRFSS and the U.S. Census suggested that as of 2022, 5.6% of Benton County residents had cardiovascular disease (coronary heart disease, stroke, and heart attack) (American Lung Association, 2022). As of 2014, about 0.07% of female residents and 0.11% of male residents in Benton County were living with ischemic heart disease (coronary artery disease) (IHME, 2016).

As of 2022, about 4.5% of county residents had chronic obstructive pulmonary disease (chronic bronchitis and emphysema) (American Lung Association, 2022). About 9–10% of adults in Benton County have asthma (BCHD, 2017; American Lung Association, 2022). In 2015, 10% of Benton County 8th graders and 13% of 11th graders reported living with asthma (BCHD, 2017).

Without housing or air conditioning. As of 2017, the unhoused population in Benton County was estimated to be 3.2 people per 1000 residents, or roughly 287 people (OHA, 2019). A separate estimate indicated that 28.5 per 1000 students enrolled in kindergarten through grade 12, or about 259 children, were unhoused (OHA, 2019). Statewide, an estimated 34% of housing units did not have air conditioning in 2020 (EIA, 2022).

Vulnerable life stage or age class. The percentage of Oregon residents of reproductive age (15–44) is projected to decrease from an estimated 39% in 2020 to 36% in 2045 (PRC, 2023c). If 49.8% of Benton County's population in that age range is female (U.S. Census Bureau, 2023), and about 5% of women of reproductive age are pregnant at any given time (CDC, n.d.), then the estimated number of pregnant women in Benton County will increase by about 193 (21%) from 2020 to 2045 (PRC, 2023b).

If trends in Benton County mirror statewide projections, then the percentage of county residents aged 65 and older will increase from an estimated 19% in 2020 to 23% in 2045 (PRC, 2023c). From 2011–2015, 10% of households in the county were individuals aged 65 and older who lived alone (BCHD, 2017), which can increase health risks. The percentage of Oregon's population that is under the age of 15 is projected to decrease from 17% in 2020 to 14% in 2045 (PRC, 2023c). Accordingly, the projected number of residents aged 15 and younger in Benton County will increase by 1770 (11%) from 2020 to 2045 (PRC, 2023b).

Low income. Statewide, the income inequality ratio (the 80th income percentile divided by the 20th income percentile) is 4.7. Benton County's income inequality ratio of 6.0 is the highest within the state and within the highest two percent of counties nationwide (BCHD, 2017). An estimated 25.4% of Benton County's population is low-income (Table 3), and across the county in 2015, approximately 25% of children aged 0–4 and 15% of children aged 0–17 were living in households that earned less than the federally designated poverty level (BCHD, 2017).

Approximately 5% of Benton County's residents do not live close to a grocery store, where close is defined as within 1 mile for urban residents or within 10 miles for rural residents (BCHD, 2017). In 2015, 16% of all county residents and 20% of children were considered food insecure (did not have enough to eat or were unable to purchase or obtain food in socially acceptable ways) (BCHD, 2017).

Communities of color. An estimated 20.4% of Benton County's population identify as non-White (Table 3).

Summary

The number, duration, and intensity of extreme heat events will increase as temperatures continue to warm. In Benton County, the number of extremely hot days (those on which the temperature is 90°F or higher) and the temperature on the hottest day of the year are projected to increase by the 2020s and 2050s under both the lower and higher emissions scenarios. The number of days per year with temperatures 90°F or higher is projected to increase by an average of 18 (range 6–33) by the 2050s, relative to the 1971–2000 historical baselines, under the higher emissions scenario. The temperature on the hottest day of the year is projected to increase by an average of about 6°F (range 2–9°F) by the 2050s. Projected demographic changes in Benton County, such as an increase in the proportion of older adults and the absolute number of children, will increase the number of people in some of the populations that are vulnerable to extreme heat.

❄🌡 Cold Waves

Extremely cold temperatures in Oregon generally occur when Arctic air moves into the state from the north and east (O'Neill *et al.*, 2023). As a result of human-caused climate change, Arctic air is warming more rapidly than the global mean temperature. This change in Arctic temperature has led to a decrease in the intensity and frequency of cold extremes in the Northwest and worldwide over the past century (Vose *et al.*, 2017; IPCC, 2021; O'Neill *et al.*, 2023). At many locations across Oregon, the annual number of days on which the minimum temperature is below freezing has decreased significantly since 1940 (O'Neill *et al.*, 2023).

The frequency of cold extremes is expected to continue decreasing (Vose *et al.*, 2017; IPCC, 2021), although more slowly than the frequency of heat extremes will increase (O'Neill *et al.*, 2023). Extreme cold will still be possible during the next several decades, but will become increasingly rare as winter temperatures warm and become less variable (O'Neill *et al.*, 2023; Rupp and Schmittner, 2023).

Older adults, infants and children, rural residents, unhoused individuals, and people with preexisting cardiovascular or respiratory conditions are considered most susceptible to extreme cold (Conlon *et al.*, 2011; NCHH, 2022). Recent and projected estimates of these populations are summarized in *Heat Waves*.

Here, we present projected changes in three metrics of extreme daytime cold (maximum temperature) and nighttime cold (minimum temperature) (Table 8).

Table 8. Metrics and definitions of cold extremes.

Metric	Definition
Cold Days	Number of days per year on which the maximum temperature is 32°F or lower
Cold Nights	Number of days per year on which the minimum temperature is 0°F or lower
Coldest Day	Lowest value of maximum temperature per year
Coldest Night	Lowest value of minimum temperature per year
Daytime Cold Waves	Number of events per year in which maximum temperature on at least three consecutive days is 32°F or lower
Nighttime Cold Waves	Number of events per year in which minimum temperature on at least three consecutive days is 0°F or lower

In Benton County, the number of cold days and nights is projected to decrease by the 2020s (2010–2039) and 2050s (2040–2069) under both the lower (RCP 4.5) and higher (RCP 8.5) emissions scenarios (Table 9, Figure 7). For example, climate models projected that by the 2050s under the higher emissions scenario, the number of cold days will change by -1.1–0.3 relative to each GCM's 1971–2000 historical baseline. The average projected number of

26

cold days per year is 0.5 less than the average historical baseline of 0.9 days. Nighttime temperatures in Benton County rarely are lower than 0°F.

Similarly, the temperatures on the coldest day and night are projected to increase by the 2020s and 2050s under both emissions scenarios (Table 9, Figure 8). For example, by the 2050s under the higher emissions scenario, the temperature on the coldest night of the year is projected to increase by 0.8–9.9°F relative to the GCMs' historical baselines. The average projected increase in the temperature on the coldest night is 5.3°F above the average historical baseline of 17.6°F. The average projected increase in the temperature on the coldest day is 4.8°F above the average historical baseline of 32.9°F. Daytime and nighttime cold waves are rare in Benton County (Table 9, Figure 7, Figure 9).

Table 9. Projected future changes in extreme cold metrics in Benton County. Changes from the 1971–2000 baseline were calculated for each of 20 global climate models and averaged across the 20 models (range in parentheses) for a lower (RCP 4.5) and higher (RCP 8.5) emissions scenario and for the 2020s (2010–2039 average) and 2050s (2040–2069 average). The average projected change can be added to the average historical baseline to infer the average projected future value of a given variable.

	Average Historical Baseline	2020s		2050s	
		Lower	Higher	Lower	Higher
Cold Days	0.9 days	-0.1 days (−0.8 – 0.8)	-0.3 days (−0.9 – 0.5)	-0.5 days (−1 – 0.3)	-0.5 days (−1.1 – 0.3)
Cold Nights	0 days	0 days (0 – 0.1)	0 days (0 – 0.1)	0 days (0 – 0.1)	0 days (0 – 0.1)
Coldest Day	32.9°F	1.1°F (−2.8 – 3.5)	2.3°F (−1.4 – 4.9)	3.7°F (−0.2 – 7.4)	4.8°F (0.8 – 8.1)
Coldest Night	17.6°F	1.3°F (−2.2 – 3.8)	2.4°F (−0.6 – 5.1)	4.3°F (0.7 – 8.3)	5.3°F (0.8 – 9.9)
Daytime Cold Waves	0.1 events	0 events (−0.1 – 0.1)	0 events (−0.2 – 0.1)	-0.1 events (−0.1 – 0.1)	-0.1 events (−0.2 – 0)
Nighttime Cold Waves	0 events	0 events	0 events	0 events	0 events

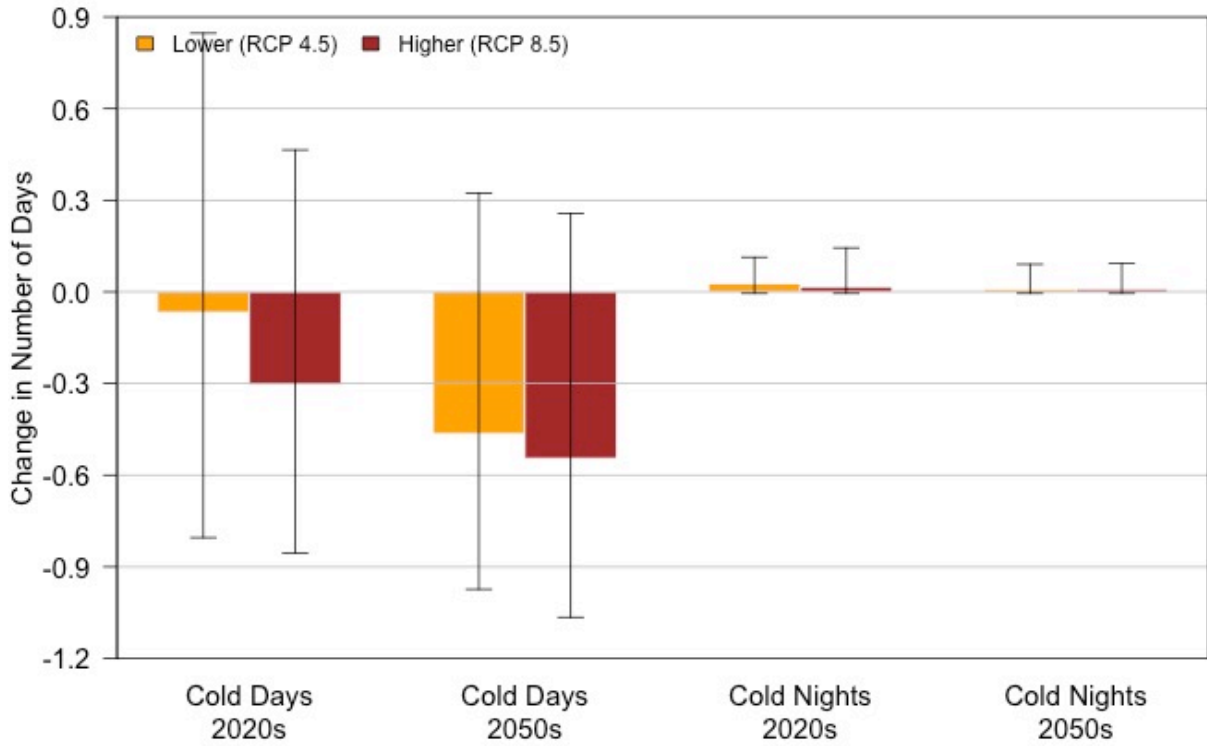**Change in Number of Extreme Cold Days in Benton County**

Figure 7. Projected changes in the number of cold days (left two sets of bars) and cold nights (right two sets of bars) in Benton County by the 2020s (2010–2039 average) and 2050s (2040–2069 average), relative to the historical baseline (1971–2000 average), under two emissions scenarios. Changes were calculated for each of 20 global climate models relative to each model's historical baseline, then averaged. Whiskers represent the range of changes across the 20 models. Cold days are those on which the maximum temperature is 32°F or lower; cold nights are those on which the minimum temperature is 0°F or lower.
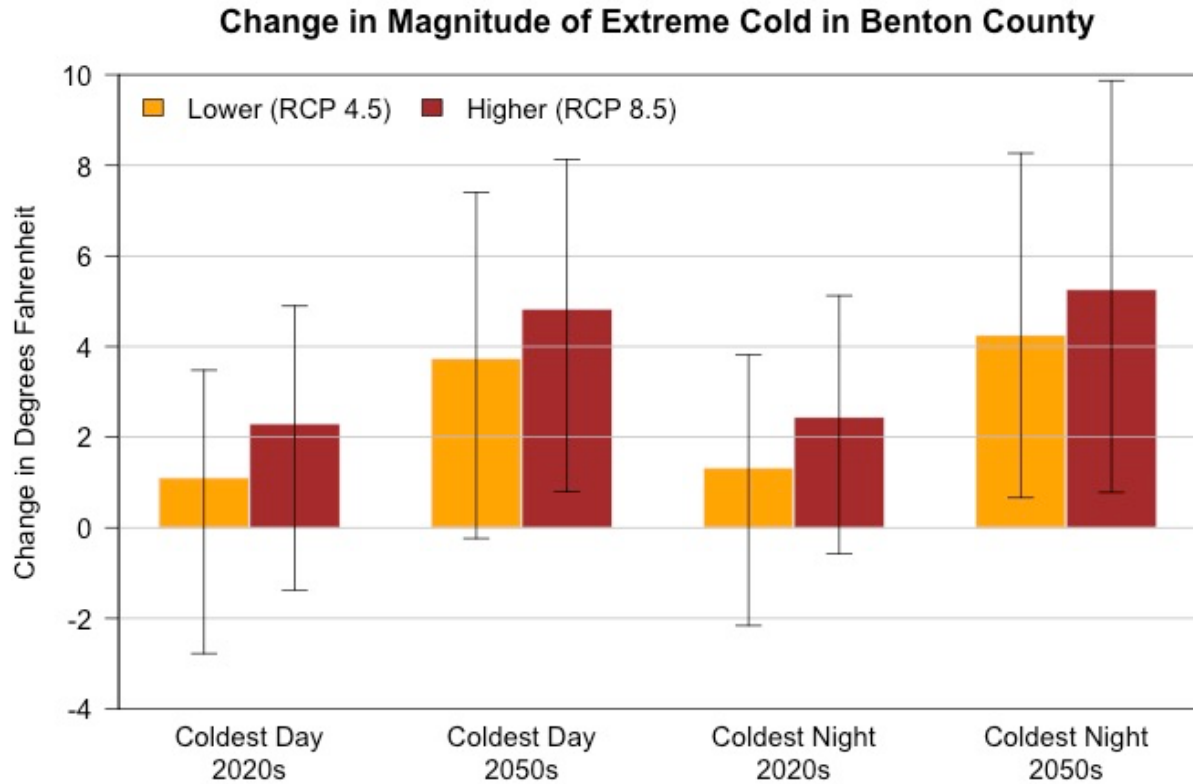
Figure 8. Projected changes in the temperature on the coldest day of the year (left two sets of bars) and coldest night of the year (right two sets of bars) in Benton County by the 2020s (2010–2039 average) and 2050s (2040–2069 average), relative to the historical baseline (1971–2000 average), under two emissions scenarios. Changes were calculated for each of 20 global climate models relative to each model's historical baseline, then averaged. Whiskers represent the range of changes across the 20 models.

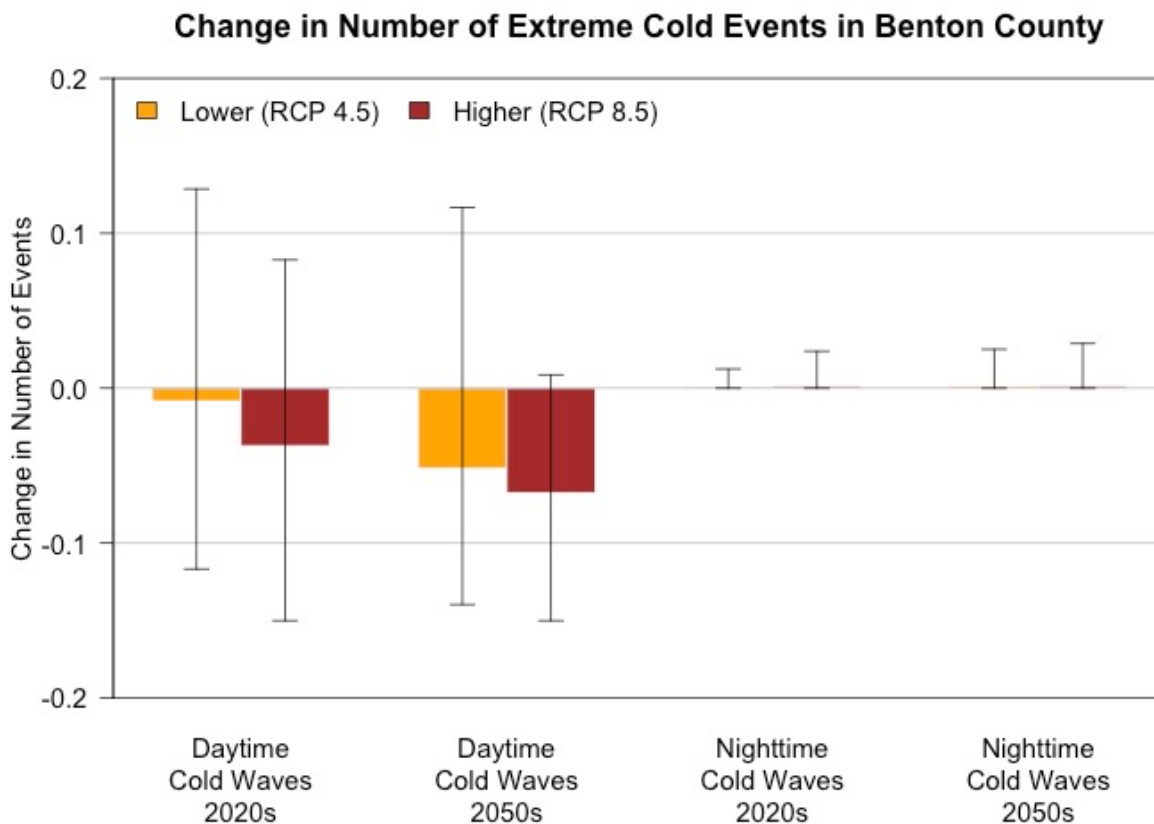**Change in Number of Extreme Cold Events in Benton County**

Figure 9. Projected changes in the number of daytime cold waves (left two sets of bars) and nighttime cold waves (right two sets of bars) in Benton County by the 2020s (2010–2039 average) and 2050s (2040–2069 average), relative to the historical baseline (1971–2000 average), under two emissions scenarios. Changes were calculated for each of 20 global climate models relative to each model's historical baseline, then averaged. Whiskers represent the range of changes across the 20 models. Daytime cold waves are defined as three or more consecutive days on which the maximum temperature is 32°F or lower; nighttime cold waves are three or more consecutive days on which the minimum temperature is 0°F or lower.

Summary

Cold extremes will become less frequent and intense as the climate warms. The number of cold days (maximum temperature 32°F or lower) per year in Benton County is projected to decrease by an average of 0.5 (range -1.1–0.3) by the 2050s, relative to the 1971–2000 historical baselines, under the higher emissions scenario. The temperature on the coldest night of the year is projected to increase by an average of 5°F (range 1–10°F) by the 2050s. The number of county residents vulnerable to extreme cold is likely to grow, although this increase may be offset somewhat by the decrease in incidence of cold extremes.

Heavy Precipitation

There is greater uncertainty in projections of future precipitation than projections of future temperature. Precipitation has high natural variability, and the atmospheric patterns that influence precipitation are represented differently among GCMs. Globally, mean precipitation is likely to decrease in many dry regions in the subtropics and mid-latitudes and to increase in many mid-latitude wet regions (IPCC, 2013; Stevenson *et al.*, 2022). Because the location of the boundary between mid-latitude increases and decreases in precipitation varies among GCMs, some models project increases and others decreases in precipitation in Oregon (Mote *et al.*, 2013).

Observed annual precipitation in Oregon has high year-to-year variability and has not changed significantly over the period of record. Annual precipitation in Oregon is projected to increase somewhat over the twenty-first century, although natural variability will continue to dominate this trend (Dalton *et al.*, 2017, 2021; Fleishman, 2023). On average, summers in Oregon are projected to become drier and other seasons to become wetter. However, some models project increases and others decreases in each season (Dalton *et al.*, 2017, 2021; Fleishman, 2023). In addition, regional climate models project larger increases in winter precipitation east of the Cascade Range than west of the Cascade Range, which suggests a weakened rain shadow effect in winter (Mote *et al.*, 2019).

Extreme precipitation in the Northwest is governed by atmospheric circulation and its interaction with complex topography (Parker and Abatzoglou, 2016). Atmospheric rivers— long, narrow swaths of warm, moist air that carry large amounts of water vapor from the tropics to mid-latitudes—generally result in extreme precipitation across large areas west of the Cascade Range, and are associated with the majority of fall and winter extreme precipitation events in Oregon. By contrast, low pressure systems that are not driven by westerly flows from offshore often lead to locally extreme precipitation east of the Cascade Range (Parker and Abatzoglou, 2016).

The frequency and intensity of heavy precipitation has increased across most land areas worldwide since the 1950s (IPCC, 2021). Observed trends in the frequency of extreme precipitation across Oregon vary among locations, time periods, and metrics, but overall, the frequency has not changed substantially. As the atmosphere warms, it holds more water vapor. As a result, the frequency and intensity of extreme precipitation is expected to increase (Dalton *et al.*, 2017, 2021; Kossin *et al.*, 2017). Regional climate models project a larger percentage increase in precipitation extremes east of the Cascade Range than west of the Cascade Range (Mote *et al.*, 2019; Rupp *et al.*, 2022). Additionally, the projected percentage increase in extreme precipitation tends to be larger on the leeward side of the Coast and Cascade Ranges than on the windward side (Rupp *et al.*, 2022). Climate models also project an increase in the number of days on which an atmospheric river is present, and that atmospheric rivers will account for an increasing proportion of total annual precipitation across the Northwest (Dalton *et al.*, 2021).

Here, we present projected changes in four metrics of precipitation extremes (Table 10).

Table 10. Metrics and definitions of precipitation extremes.

Metric	Definition
Wettest Day	Highest one-day precipitation total per water year (1 October–30 September)
Wettest Five Days	Highest consecutive five-day precipitation total per water year
Wet Days	Number of days per water year on which precipitation exceeds 0.75 inches
Landslide Risk Days	Number of days per water year that exceed the landslide threshold developed by the US Geological Survey for Seattle, Washington (see https://pubs.er.usgs.gov/publication/ofr20061064). $P3/(3.5-.67*P15)>1$, where - P3 = Precipitation accumulation on prior days 1–3 - P15 = Precipitation accumulation on prior days 4–18

In Benton County, the amount of precipitation on the wettest day and wettest consecutive five days per year is projected to increase on average by the 2020s (2010–2039) and 2050s (2040–2069), relative to the 1971–2000 historical baseline, under both the lower (RCP 4.5) and higher (RCP 8.5) emissions scenarios (Table 11, Figure 10). Some models project decreases in these metrics for certain time periods and scenarios.

Climate models project that by the 2050s under the higher emissions scenario, the amount of precipitation on the wettest day of the year, relative to each GCM's 1971–2000 historical baseline, will increase by 1.2–28.5% (Figure 10). The average projected amount of precipitation on the wettest day of the year is 13.2% greater than the average historical baseline of 2.6 inches.

By the 2050s under the higher emissions scenario, the amount of precipitation on the wettest consecutive five days of the year is projected to increase by 2.4–19.1% (Figure 10). The average projected amount of precipitation on the wettest consecutive five days is 10.2% above the average historical baseline of 6.5 inches.

Table 11. Projected future changes in extreme precipitation metrics in Benton County. Changes from the 1971–2000 baseline were calculated for each of 20 global climate models and averaged across the 20 models (range in parentheses) for a lower (RCP 4.5) and higher (RCP 8.5) emissions scenario and for the 2020s (2010–2039 average) and 2050s (2040–2069 average). The average projected change can be added to the average historical baseline to infer the average projected future value of a given variable.

	Average Historical Baseline	2020s		2050s	
		Lower	Higher	Lower	Higher
Wettest Day	2.6 inches	6.5% (–4.8-17.6)	5.6% (–6.4-19.8)	10.8% (2.7-24.3)	13.2% (1.2-28.5)
Wettest Five-Days	6.5 inches	5.2% (–3.7-18.6)	3.9% (–5.7-17.5)	8.5% (–0.1-21.6)	10.2% (2.4-19.1)
Wet Days	22.9 days	0.4 days (–1.4-2.6)	0.1 days (–2.5-2)	1 days (–2-2.7)	0.9 days (–3-3.8)
Landslide Risk Days	25.7 days	–0.4 days (–3-3)	–0.5 days (–3-1.6)	–0.5 days (–3.2-2.3)	–0.1 days (–2.6-3.6)

**Change in Precipitation Totals on Wettest Day and Wettest Five Days
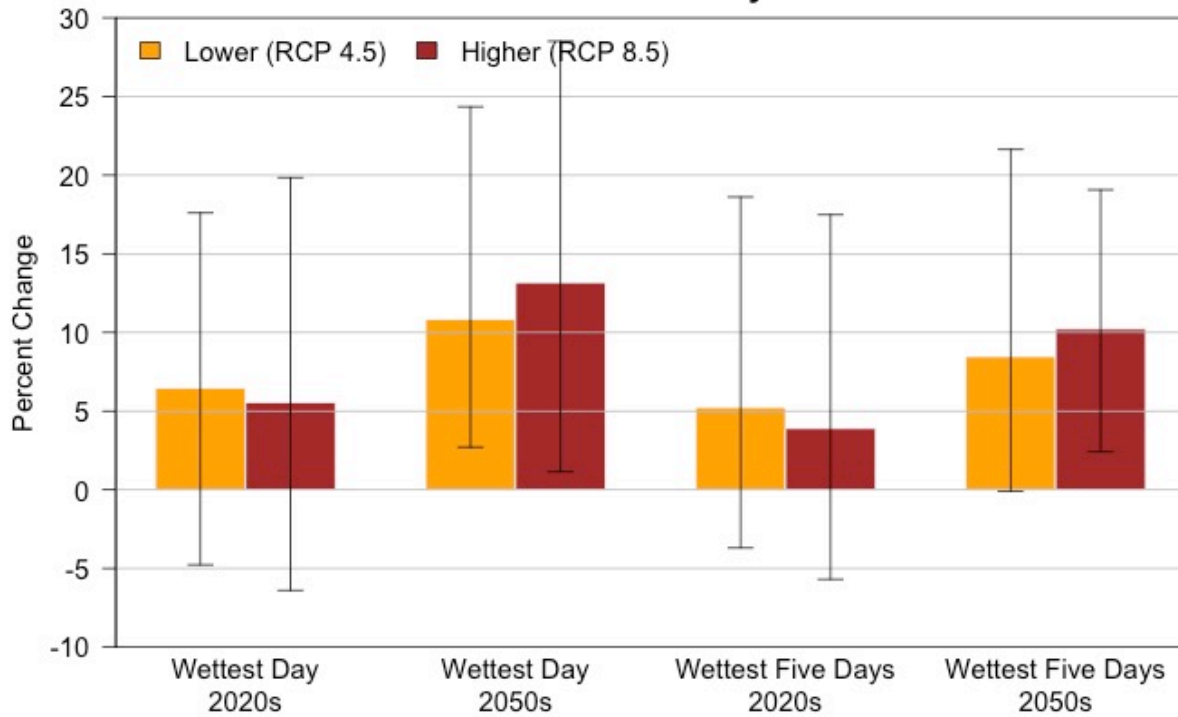Benton County**

Figure 10. Projected percent changes in the amount of precipitation on the wettest day of the year (left two sets of bars) and wettest consecutive five days of the year (right two sets of bars) in Benton County by the 2020s (2010–2039 average) and 2050s (2040–2069 average), relative to the historical baseline (1971–2000 average), under two emissions scenarios. Changes were calculated for each of 20 global climate models relative to each model's historical baseline, then averaged. Whiskers represent the range of changes across the 20 models.

The average number of days per year on which precipitation exceeds 0.75 inches is not projected to change substantially (Figure 11). For example, by the 2050s under the higher emissions scenario, the number of wet days per year is projected to increase by 0.9 (range -3.0–3.8). The historical baseline is an average of 22.9 days per year.

Landslides are often triggered by rainfall when the soil becomes saturated. As a surrogate measure of landslide risk, we present a threshold based on recent precipitation (cumulative precipitation over the previous 3 days) and antecedent precipitation (cumulative precipitation on the 15 days prior to the previous 3 days). By the 2050s under the higher emissions scenario, the average number of days per year in Benton County on which the landslide risk threshold is exceeded is projected to remain about the same, with a change of -0.1 (range -2.6–3.6) (Figure 11). The historical baseline is an average of 25.7 days per year. Landslide risk depends on multiple site-specific factors, and this metric does not reflect all aspects of the hazard. Also, the landslide risk threshold was developed for Seattle, Washington, and may be less applicable to other locations.
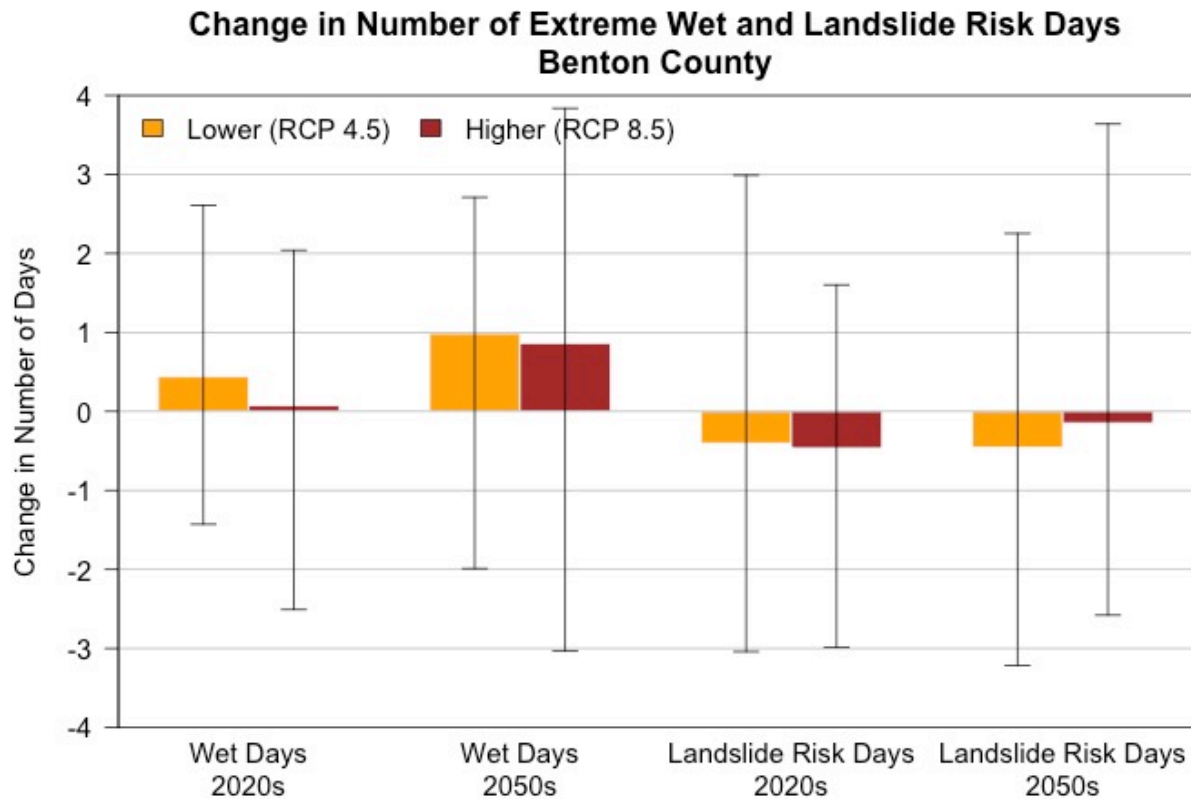
Figure 11. Projected changes in the number of wet days (left two sets of bars) and landslide risk days (right two sets of bars) in Benton County by the 2020s (2010–2039 average) and 2050s (2040–2069 average), relative to the historical baseline (1971–2000 average), under two emissions scenarios. Changes were calculated for each of 20 global climate models relative to each model's historical baseline, then averaged. Whiskers represent the range of changes across the 20 models.

The occurrence and magnitude of landslides in western Oregon is largely influenced by past clearcutting and construction of logging roads. In the Lookout Creek watershed in the Willamette National Forest, the major floods of 1964–1965, which occurred during the peak of logging, produced more and larger landslides than major floods in 1996 and 2011, decades after logging in the area ended (Goodman *et al.*, 2023). Landslide risk also can become high when heavy rain falls on an area that burned within approximately the past five to ten years. The probability that extreme rainfall will occur within one year after an extreme fire-weather event in Oregon or Washington was projected to increase by 700% from 1980–2005 to 2100 under the higher emissions scenario (Touma *et al.*, 2022). Similarly, projections suggested that by 2100, 90% of extreme fire-weather events across Oregon and Washington are likely to be succeeded within five years by three or more extreme rainfall events (Touma *et al.*, 2022). Although fire weather is not synonymous with wildfire, these results highlight the increasing likelihood of compounded climate extremes that elevate the risk of natural hazards.

Populations considered particularly vulnerable to the direct and indirect effects of extreme precipitation, from the storms themselves to floods and landslides, include people

dependent on medical equipment that requires electricity, older adults, and children and pregnant women (York *et al.*, 2020; Ho *et al.*, 2021). Recent and projected estimates of populations that are older, younger, and of childbearing age are included in previous sections. Some utility companies, such as Pacific Power, provide consultation and additional outreach to individuals who are dependent on electricity for a medical device. Among the diverse health risks associated with extreme precipitation are injuries, toxic exposures, displacement, disruptions in medical care, and negative mental health outcomes (York *et al.*, 2020; Ho *et al.*, 2021).

Summary

The intensity of extreme precipitation is expected to increase as the atmosphere warms and holds more water vapor. In Benton County, the number of days per year with at least 0.75 inches of precipitation is not projected to change substantially. Nevertheless, by the 2050s, the amount of precipitation on the wettest day and wettest consecutive five days per year is projected to increase by an average of 13% (range 1–29%) and 10% (range 2–19%), respectively, relative to the 1971–2000 historical baselines, under the higher emissions scenario. The number of days per year on which a threshold for landslide risk, which is based on prior 18-day precipitation accumulation, is exceeded is not projected to change substantially. However, landslide risk depends on multiple factors, and this metric does not reflect all aspects of the hazard.

River Flooding

Streams in the Northwest are projected to shift toward higher winter runoff, lower summer and fall runoff, and earlier peak runoff, particularly in snow-dominated regions (Raymondi *et al.*, 2013; Naz *et al.*, 2016). These changes are expected as a result of increases in the intensity of heavy precipitation; warmer temperatures that cause more precipitation to fall as rain and less as snow, and snow to melt earlier in spring; and increasing winter precipitation and decreasing summer precipitation (Dalton *et al.*, 2017, 2021; Mote *et al.*, 2019).

Warming temperatures and increasing winter precipitation are expected to increase flood risk in many basins in the Northwest, particularly mid- to low-elevation, mixed rain-and-snow basins in which winter temperatures are near freezing (Tohver *et al.*, 2014). The greatest projected changes in peak streamflow magnitudes are at intermediate elevations in the Cascade Range and Blue Mountains (Safeeq *et al.*, 2015). Recent regional hydroclimate models project increases in extreme high flows throughout most of the Northwest, especially west of the Cascade crest (Salathé *et al.*, 2014; Najafi and Moradkhani, 2015; Naz *et al.*, 2016). One study that used a single climate model projected an increase in flood risk in fall due to earlier, more extreme storms, including atmospheric rivers; and an increase in the proportion of precipitation falling as rain rather than snow (Salathé *et al.*, 2014). Rainfall-driven floods are more sensitive to increases in precipitation than snowmelt-driven floods. Therefore, the projected increases in total precipitation, and in rain relative to snow, likely will increase flood magnitudes in the region (Chegwidden *et al.*, 2020).

The Willamette River at Albany is within a rain-dominated basin with peak flow during winter (Figure 12). By the 2050s (2040–2069), under both emissions scenarios, winter streamflow in the Willamette River at Albany is projected to increase due to increased winter precipitation. Winter streamflow at Rock Creek, a tributary of the Marys River, similarly is projected to increase (Rupp, 2019). Mean monthly flows do not translate directly to flood risk because floods occur over shorter periods of time. Nevertheless, increases in monthly flow may imply increases in flood likelihood, particularly if increases are projected to occur during months in which flood occurrence historically has been high.

Willamette River at Albany
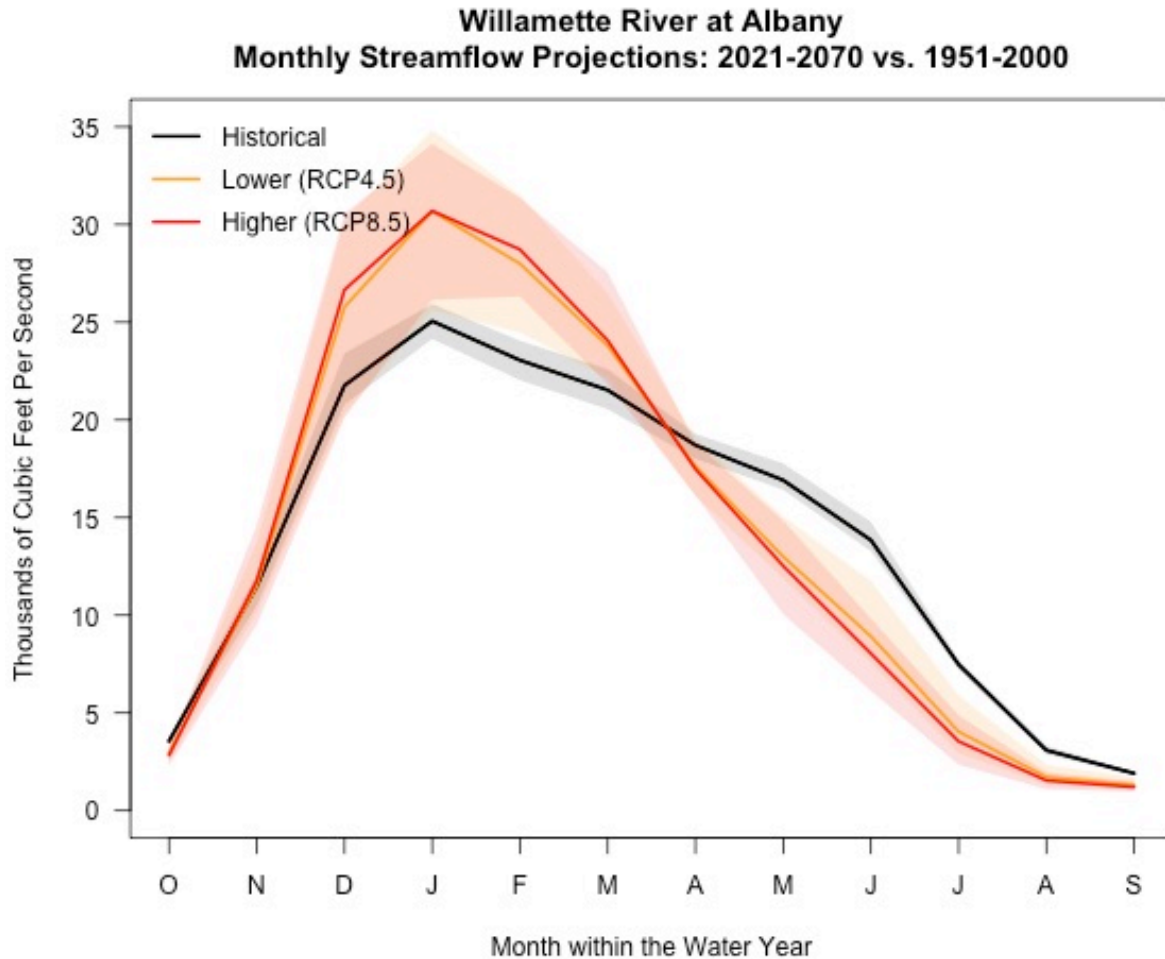**Monthly Streamflow Projections: 2021-2070 vs. 1951-2000**

Figure 12. Simulated monthly non-regulated streamflow at the Willamette River at Albany from 1951–2000 to 2021–2070. Solid lines and shading represent the mean and range across ten global climate models. (Data source: Columbia River Climate Change, https://www.hydro.washington.edu/CRCC/)

Across the western United States, the average magnitudes of major floods are projected to increase by 14–19% by 2010–2039, 21–30% by 2040–2069, and 31–43% by 2070–2099, compared to the 1971–2000 historical baseline, under the higher emissions scenario (Maurer *et al.*, 2018). Major floods are defined as daily peak flow magnitudes that are associated with 100-year to 10-year return periods (1–10% probability that this daily flow magnitude will be exceeded in a given year). Likewise, within the Columbia River basin, projected major flood magnitudes increased nearly everywhere and varied by the dominant precipitation type (Queen *et al.*, 2021). On the Willamette River at Albany, flood levels with 10-year and 100-year return periods were projected to increase by 40% and 47%, respectively, from 1950–1999 to 2050–2099 under the higher emissions scenario (Queen *et al.*, 2021) (Table 12).

We estimated projected changes in the average magnitude of single-day flood levels with 25-year, 100-year, and 500-year return periods (4%, 1%, and 0.2% probability, respectively, that this daily flow magnitude will be exceeded in a given year) along the

Willamette River at Albany in Benton County (Table 12). We then compared flood magnitudes between 1951–2000 and 2021–2070 under the lower and higher emissions scenarios. Depending on emissions scenario, the average magnitudes of single-day floods with 25-year, 100-year, and 500-year return periods were projected to increase by 22–26%, 25–29%, and 29–32%, respectively (Table 12, Figures 13). Some models projected no change or decreases in the magnitude of maximum daily flows for each return period. These results can be interpreted as either an increase in flood magnitude given a flood frequency, or an increase in flood frequency given a flood magnitude. These analyses were exploratory and should not be applied to engineering or design.

Table 12. Average projected percent change in annual maximum flow associated with multiple return periods for the Willamette River at Albany by 2021–2070, relative to 1951–2000. (Source: Rupp, 2019)

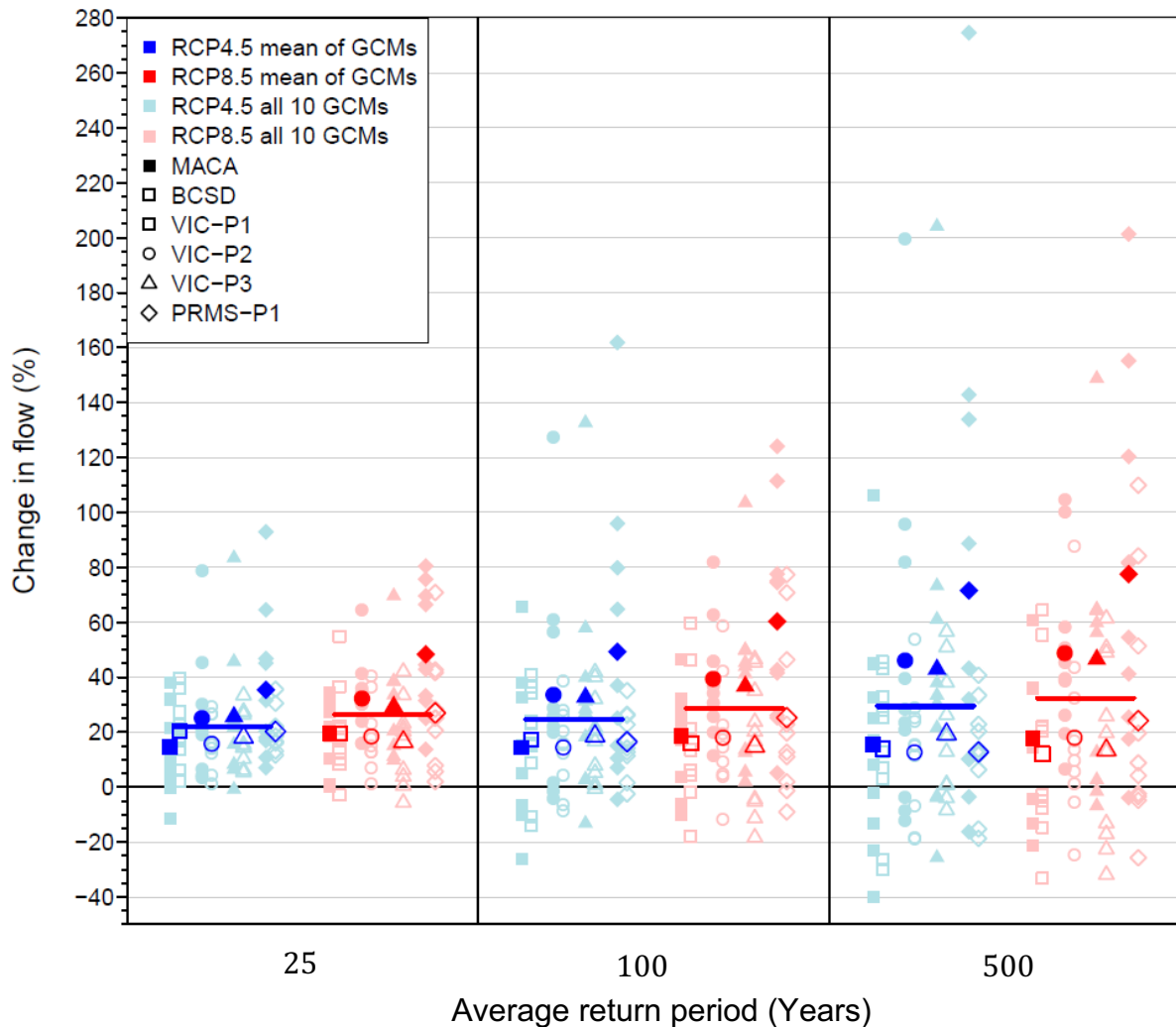| Return Period (Probability that this level will be exceeded in a given year)	Lower Emissions (RCP 4.5)	Higher Emissions (RCP 8.5)
25-year (4%)	22	26
100-year (1%)	25	29
500-year (0.2%)	29	32

Figure 13. Projected change in water-year maximum daily, non-regulated streamflows with 25-year, 100-year, and 500-year return periods at the Willamette River at Albany from 1951–2000 to 2021–2070. Changes estimated from 80 hydrological simulations under each of the lower (RCP 4.5; blue) and higher (RCP 8.5; red) emissions scenarios (see *Appendix*). Larger symbols represent the average across ten global climate models. Only ten of the full set of 20 models that were used to project temperature and precipitation simulated future hydrology. Horizontal line segments represent the average of all simulations under each emissions scenario for each return period. Smaller, light-colored dots represent projections from individual models. The shading and shape of the symbol indicates the downscaling method (Multivariate Adaptive Constructed Analogs [MACA] or bias correction spatial disaggregation [BCSD]) and hydrological model, respectively, from which the estimate was derived (Data source: Columbia River Climate Change, www.hydro.washington.edu/CRCC/; Figure source: Rupp, 2019)

Some of the Northwest's highest floods occur when large volumes of warm rain from atmospheric rivers fall on a deep snowpack (Safeeq *et al.*, 2015). The frequency and amount of moisture transported by atmospheric rivers is projected to increase along the

West Coast in response to increases in air temperature (Kossin *et al.*, 2017), which in turn increases the likelihood of flooding (Konrad and Dettinger, 2017).

Future changes in the frequency of rain-on-snow events likely will vary along elevational gradients. At lower elevations, the frequency is projected to decrease due to decreasing snowpack, whereas at higher elevations the frequency is projected to increase due to the shift from snow to rain (Surfleet and Tullos, 2013; Safeeq *et al.*, 2015; Musselman *et al.*, 2018). The likely effects on streamflow of such changes in frequency of rain-on-snow events vary. For example, projections for the Santiam River, Oregon, indicated an increase in annual peak daily flows with return intervals less than 10 years, but a decrease in annual peak daily flows with return intervals of 10 or more years (Surfleet and Tullos, 2013). Average runoff from rain-on-snow events in watersheds in northern coastal Oregon was projected to decline due to depletion of the snowpack (Musselman *et al.*, 2018), which may imply that the driver of floods in these areas shifts from rain-on-snow events to rainfall that exceeds soil capacity (Berghuijs *et al.*, 2016; Musselman *et al.*, 2018). Wildfires and shifts in vegetation that affect soil properties also will likely affect water transport, but hydrological models generally have not accounted for these processes (Bai *et al.*, 2018; Wang *et al.*, 2020; Williams *et al.*, 2022).

Potential Effects of Projected Flooding on Infrastructure

First Street Foundation (2023) estimated that 6168 properties in Benton County (25%) have a >26% probability of being severely affected by flooding by 2050. Among the structures that may be affected by flooding are 6208 residences (24%) at moderate risk, 460 commercial properties (38%) at moderate risk, 20 critical infrastructure facilities (e.g., hospitals; police, fire, and power stations; and water treatment facilities) (47%) at moderate risk, and 31 (26%) of social facilities (schools, houses of worship, museums, and government or historic buildings) at moderate risk (Table 13). More than 815 of the 2250 miles of roads in Benton County (36%) were estimated to be at severe risk of flooding (First Street Foundation, 2023).

Table 13. 30-year cumulative probability of flooding to different depths and First Street Foundation's associated risk characterizations.

		30-year cumulative probability					
		≤0.06	>0.06–0.12	>0.12–0.27	>0.27–0.47	>0.47–0.96	>0.96
Flood depth	0–3"	Low	Moderate	Moderate	Major	Major	Severe
	>3–6"	Low	Moderate	Moderate	Major	Major	Severe
	>6–9"	Moderate	Moderate	Major	Major	Severe	Extreme
	>9–12"	Moderate	Moderate	Major	Severe	Severe	Extreme
	>12–24"	Moderate	Major	Major	Severe	Extreme	Extreme
	>24"	Major	Major	Severe	Extreme	Extreme	Extreme

Benton County currently estimates that of 42,936 residential structures in the county, 2970 (7%) are within the 100-year floodplain (the area that has a 1% probability of flooding in a given year) and another 2988 (7%) are within the 500-year floodplain (the area that has a 0.2% probability of flooding in a given year). The majority of these residences (86%) are within city limits or urban growth boundaries (Table 14).

Table 14. Estimated number of residences in Benton County within the 100-year and 500-year floodplains, which correspond to 1% and 0.2% annual probabilities of flooding, respectively. Data provided by Benton County's Information Technology Department.

Jurisdiction and annual probability of flooding	Estimated number of residences	
	Within city limits or urban growth boundary	Outside city limits or urban growth boundary
Adair Village	507	11
1%		
0.2%		
Albany	3629	
1%	430	
0.2%	705	
Corvallis	27,233	1283
1%	1540	43
0.2%	2147	34
Monroe	366	6
1%	9	
0.2%		
Philomath	2651	168
1%	233	11
0.2%	33	1
Other areas		7082
1%		704
0.2%		68

Summary

Winter flood risk at mid- to low elevations in Benton County, where temperatures are near freezing during winter and precipitation is a mix of rain and snow, is projected to increase as winter temperatures increase. The temperature increase will lead to an increase in the percentage of precipitation falling as rain rather than snow. An estimated 7% of residences in the county are within the 100-year floodplain, and another 7% are within the 500-year floodplain.

Drought

Drought can be defined in many ways (Table 14), but most fundamentally is insufficient water to meet needs (Redmond, 2002; O'Neill *et al.*, 2021; O'Neill and Siler, 2023). Drought is common in the Northwest, particularly because seasonal precipitation is lowest during the warmest season (O'Neill and Siler, 2023). The incidence, extent, and severity of drought increased over the last 20 years relative to the twentieth century, and this trend is expected to continue (O'Neill *et al.*, 2021; O'Neill and Siler, 2023).

Table 14. Definitions and characteristics of various drought classes. (Sources: O'Neill *et al.*, 2021; O'Neill and Siler, 2023; Fleishman *et al.*, unpublished)

Drought Class	Definition and Characteristics
Meteorological	• lack of precipitation • evaporative demand that exceeds precipitation for 90 days or longer
Hydrological	• extended periods of meteorological drought affect surface or subsurface water supply, such as streamflow, reservoir and lake levels, or ground water levels • tends to evolve more slowly than meteorological drought and to persist for longer than six months
Agricultural	• occurs when lack of surface or subsurface water adversely affects agricultural production • reflects precipitation shortages, differences between actual and potential evapotranspiration, soil water deficits, and reduced availability of water for irrigation
Socioeconomic	• occurs when meteorological, hydrological, or agricultural drought reduces the supply of an economic or social good or service • often affects state and federal drought declarations
Ecological	• undesirable changes in ecological state caused by deficits in water availability • usually caused by meteorological or hydrological drought • sensitivity to water limitation varies among species and life stages
Flash	• rapid-onset periods of elevated surface temperatures, low relative humidities, precipitation deficits, and a rapid decline in soil moisture • tends to develop and intensify rapidly within a few weeks, and may be generated or magnified by prolonged heat waves
Snow	• snowpack—or snow water equivalent (SWE)—is below average for a given point in the water year, traditionally 1 April • often presages hydrological drought conditions during the ensuing spring and summer in snowmelt-dominated watersheds • warm snow drought—below-average snowpack that results primarily from above-average winter temperatures • dry snow drought—below-average snowpack that results primarily from below-average winter precipitation

Drought often affects human health indirectly, such as through food scarcity and the increased incidence of infectious, chronic, and vector-borne diseases. Moreover, drought affects both physical and mental health (Vins *et al.*, 2015). Low income, tribal, rural, and farming and farmworker communities are especially susceptible to negative health effects as a result of drought and associated water scarcity and poor water quality (York *et al.*, 2020; Ho *et al.*, 2021). Recent and projected estimates of low income, rural, and some farmworker populations are presented in previous sections. As of 2022, an estimated 1% of Benton County residents identified as one race and as American Indian or Alaska Native (U.S. Census Bureau, 2023).

By 2100, annual mean precipitation in Oregon is projected to increase by 5–10% (O'Neill and Siler, 2023). However, summers in the state are expected to become drier and warmer (Dalton *et al.*, 2021; Fleishman, 2023). As winters become warmer, snowpack across Oregon is projected to decline by approximately 25% by 2050 relative to 1950–2000 (Siirila-Woodburn *et al.*, 2021). The decline in snowpack across the western United States is projected to reduce summer soil moisture in the mountains (Gergel *et al.*, 2017). Climate change is also expected to reduce summer streamflows in snow-dominated and mixed rain and snow basins across the Northwest as snowpack melts earlier and summer precipitation decreases (Dalton *et al.*, 2017; Mote *et al.*, 2019). For example, summer flow is projected to decrease in the Willamette River (Figure 12) by the 2050s (2040–2069). As mountain snowpack declines, seasonal drought will become less predictable and snow droughts will increase the likelihood of hydrological and agricultural drought during the following spring and summer (Dalton and Fleishman, 2021; Fleishman, 2023).

We present projected changes in four variables indicative of drought: low spring (April 1) snowpack (snow drought), low summer (June–August) soil moisture from the surface to 55 inches below the surface (agricultural drought), low summer runoff (hydrological drought), and low summer precipitation (meteorological drought). We present drought in terms of a change in the probability of exceeding the magnitude of seasonal drought conditions for which the historical annual probability of exceedance was 50% (snowpack) or 20% (5-year return period) (soil moisture, runoff, and precipitation) (Figure 14).

In Benton County, summer soil moisture, spring snowpack, summer runoff, and summer precipitation are projected to decline by the 2050s under both lower (RCP 4.5) and higher (RCP 8.5) emissions scenarios. Therefore, seasonal drought conditions will occur more frequently by the 2050s (Figure 14). By the 2050s under the higher emissions scenario, the annual probability of snow drought is projected to be about 71% (1.4-year return period). The annual probabilities of agricultural, hydrological, and meteorological drought are projected to be about 34% (2.9-year return period), 38% (2.6-year return period), and 33% (3.0-year return period), respectively. We did not evaluate drought projections for the 2020s due to data limitations, but drought magnitudes in the 2020s likely will be smaller than those in the 2050s.
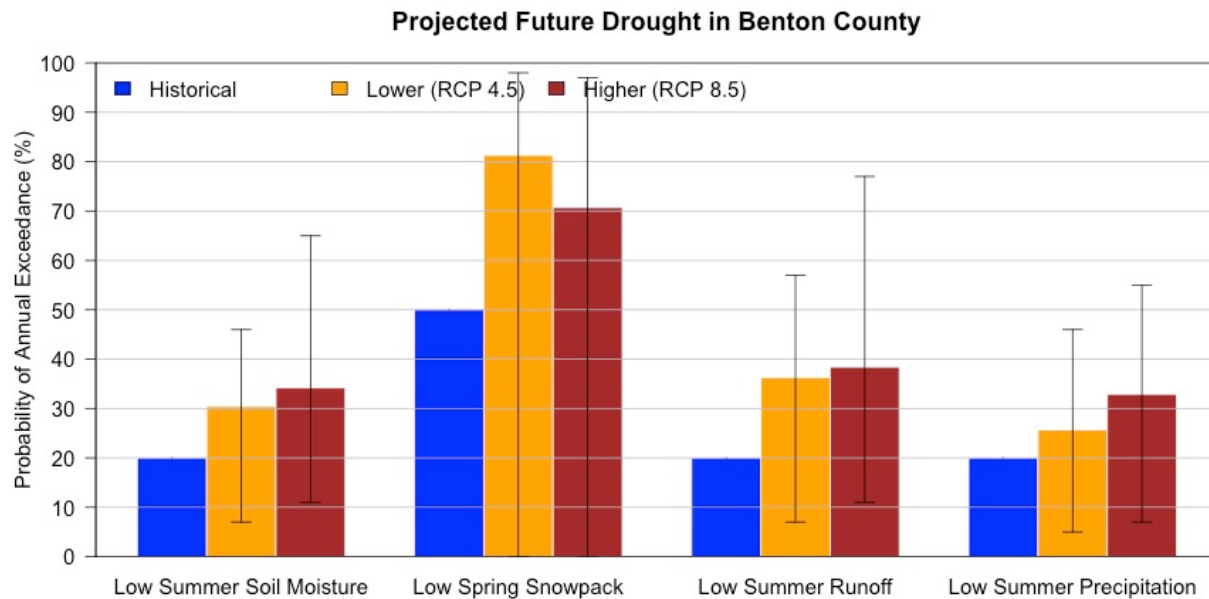
Projected Future Drought in Benton County

Figure 14. Projected probability of exceeding the magnitude of seasonal drought conditions for which the historical annual probability of exceedance was 20% (50% for spring snowpack). Projections are for the 2050s (2040–2069), relative to the historical baseline (1971–2000), under two emissions scenarios. Seasonal drought conditions include low summer soil moisture (average from June through August), low spring snowpack (April 1 snow water equivalent), low summer runoff (total from June through August), and low summer precipitation (total from June through August). The bars and whiskers represent the mean and range across ten global climate models. (Data Source: Integrated Scenarios of the Future Northwest Environment, https://climate.northwestknowledge.net/IntegratedScenarios/)

Summary

Drought, as represented by low summer soil moisture, low spring snowpack, low summer runoff, and low summer precipitation, is projected to become more frequent in Benton County by the 2050s. The incidence of related negative physical and mental health outcomes, especially among low income, tribal, rural, and agricultural communities, is likely to increase.

Wildfire

Projection of contemporary wildfire risk requires an understanding of interactions among plant physiology, climate, and human activities.

Aridity, Heat, and Wildfire Risk

Drought conditions across the western United States have been exacerbated by warmer winters and springs, which drive an overall decline in mountain snowpack and earlier snowmelt (Westerling, 2016), and by longer summers. High temperatures are a major contributor to desiccation of dead vegetation, whereas dry air (in western Oregon, more so than dry soil; Jarecke *et al.*, 2023) reduces moisture in live vegetation. The drier the air, the more plants transpire and lose water. Dry dead or living vegetation is more likely to burn than wet vegetation. If tall trees cannot draw enough water from the soil, they may be at risk of embolism (Olson *et al.*, 2018; Anfodillo and Olson, 2021) and more likely to die. Because concurrent heat and drought are becoming more common (Alizadeh *et al.*, 2020), the volume of stressed or dead vegetation and wildfire risk are increasing.

Trees that become drought-stressed generally are more vulnerable to outbreaks of native and non-native insects and pathogens. For example, Swiss needle cast (*Phaeocryptopus gaeumannii*), a native fungus, killed substantial numbers of Douglas fir (*Pseudotsuga menziesii*) trees in the Tillamook watershed for the first time in 2015. Extreme heat in June 2021 (Heeter *et al.*, 2023) caused mortality of seedlings and saplings in plantations while scorching the canopy of mature trees throughout the Coast Range (Still *et al.*, 2023).

The dryness of the air, also called evaporative demand, is characterized by the vapor pressure deficit (VPD). The VPD is the difference in atmospheric pressure between the current amount of water vapor in the air and the maximum amount of water the air can hold at a given temperature (dew point). VPD is increasing globally, and CMIP6 climate models indicate that human emissions of greenhouse gases explained 68% of the observed VPD increase between 1979 and 2020 (Zhuang *et al.*, 2021). These models also project that across the western United States, given a higher emissions scenario, warm season VPD over the next 30 years will increase at a rate similar to that observed from 1979 through 2020 (Zhuang *et al.*, 2021).

From 1985 through 2017, the annual area burned by high-severity fires across forests in the western United States increased eightfold (Parks and Abatzoglou, 2020). The frequency of large forest fires has also increased: such fires now occur nearly every year in the Northwest (Rupp and Holz, 2023). About half of the observed increase in vegetation dryness in the western United States from 1984 through 2015—again, driven mainly by the dryness of the air—and 16,000 square miles (4.2 million hectares) of burned area were attributable to human-caused climate change (Abatzoglou and Williams, 2016). Area burned is more strongly correlated with VPD than with other drought indices or variables, such as temperature and precipitation (Sedano and Randerson, 2014; Williams *et al.*, 2014; Seager *et al.*, 2015; Rao *et al.*, 2022). CMIP5 models projected that increases in VPD would contribute substantially to wildfire risk in Oregon (Ficklin and Novick, 2017; Chiodi *et al.*, 2021) and across the West (Abatzoglou *et al.*, 2021a; Zhuang *et al.*, 2021; Juang *et al.*, 2022).

Historically, wildfires were less active overnight, and the probability of fire expansion generally was evaluated on the basis of daytime conditions. However, across the western United States, the number of nights during which atmospheric conditions are conducive to burning has increased by 45% since 1979 (Balch *et al.*, 2022). The intensity and duration of wildfires is expected to increase as nights continue to become hotter and drier (Chiodi *et al.*, 2021; Balch *et al.*, 2022).

Land Use and Wildfire Risk

Stand-replacing fires, such as the Tillamook series between 1933 and 1951 and the Yaquina and Nestucca fires in the latter half of the nineteenth century, periodically occur in the cool, moist coastal forests of the Northwest. Lightning is rare in this region, however, and the number of large fires historically was low (Holz *et al.*, 2021). Yet projections that include concurrent increases in aridity, temperature, and intensification of land use (which leads to an increase in human ignitions; see below) indicate that area burned and the frequency and intensity of wildfires will continue to increase in the Pacific Northwest, even in relatively wet areas of western Oregon (Sheehan *et al.*, 2015; Dalton *et al.*, 2017; Mote *et al.*, 2019; Dalton and Fleishman, 2021; Rupp and Holz, 2023). The average annual area burned in Oregon's forests is expected to increase by at least 50% over the next several decades under the lower emissions scenario (Rupp and Holz, 2023). Within national forests in the western Cascade Range, the number of wildfires is projected to increase by 20–140% from 1986–2015 to 2070–2099 under the higher emissions scenario (Heidari *et al.*, 2021). In addition, an increase in the annual average temperature of 3.6°F above the 2002–2020 average was projected to double the annual number of extreme, single-day spreading wildfires in the Cascade Range and elsewhere in the western United States (Coop *et al.*, 2022). The interactions among housing development, the growth of tourism in forested areas, and increasing atmospheric dryness suggest that past projections of changing wildfire risk in the West may be underestimates (Rao *et al.*, 2022). For example, neither Heidari et al. (2021) nor Coop et al. (2022) considered the response of Coast Range forests to longer, drier, and hotter summers.

Extreme wildfires often occur when weather conditions conducive to fire, including high temperatures, aridity, and wind speeds (Reilly *et al.*, 2022), coincide, particularly when vegetation already is dry. These fires can cause widespread loss of structures and the loss of human lives (Abatzoglou *et al.*, 2021b). The 1933 Tillamook fire was enabled in part by a warm and dry summer (as is typical in Oregon), the accumulation of highly flammable vegetation due to logging operations, and strong and dry east winds. Similar conditions facilitated the 2020 Labor Day fires in the western Cascade Range (Higuera and Abatzoglou, 2021). In both cases the dryness of the air was extraordinary and the ignition was human-caused.

Human activities have modified fire dynamics in western forests through fragmentation and exploitation of these ecosystems, suburban population growth and increased recreational activity, introduction of highly flammable, non-native annual grasses, and replacement of indigenous or natural fires by extensive fire suppression and vegetation management. Over two-thirds of Benton County is classified as evergreen forest (Oregon Explorer, 2023). These forests primarily occur on private land; some also occur on federal

land in the Coast Range (Oregon Explorer, 2023). Twenty-one percent of the county is classified as agricultural and seven percent as urban.

Over 80% of ignitions in the United States are now human-caused (Balch *et al.*, 2017), and human caused ignitions accounted for 86% of the fire starts in Benton County from 2008 to 2019 (Short, 2022). Ignition from power generation, transmission, or distribution, often due to high winds, has been identified as the cause of many fires in California and of the Holiday Farm fire in the western Cascade Range. In Oregon's coastal forests, where the density of housing is low, fire starts seem more likely to be caused by smoking, recreation, fireworks, or equipment and vehicle use. Sparks from logging equipment were responsible for starting the Tillamook fires in the 1930s. The fact that longer summers and human activities have extended the temporal and geographic extent of the fire season (Balch *et al.*, 2017; Bowman *et al.*, 2020; Jones *et al.*, 2022) increases the chances that a late summer fire start could affect large areas of timberland and remnants of old growth.

Management practices likely affected the severity of the 2020 fires in Oregon (Allen *et al.*, 2019; Downing *et al.*, 2022). Uniform canopy structure, which is common in forest plantations and on private lands in the Coast Range, can lead to subcanopy winds that transport moisture out of the watershed (Drake *et al.*, 2022). Crowning and torching associated with dry trees may increase the potential for long-distance spot fires that can cause rapid expansion of the fire front and overwhelm suppression efforts (Rothermel, 1991; Koo *et al.*, 2010; Storey *et al.*, 2020). Firebrands can be carried far by strong winds: in September 2017, embers from the Eagle Creek fire jumped across the Columbia River and started some spot fires on the Washington side.

Duration and Magnitude of Wildfire Risk

The duration of the wildfire season is increasing across the western United States (Dennison *et al.*, 2014; Jolly *et al.*, 2015; Westerling, 2016; Williams and Abatzoglou, 2016), and the duration of the fire weather season in forests of the Northwest increased by 43% from 1979 through 2019 (Jones *et al.*, 2022). Anthropogenic emissions increased the likelihood of extreme fire weather during fall by about 40% over the western United States and about 50% over western Oregon, largely through drier vegetation in fall and warmer temperatures during dry wind events (Hawkins *et al.*, 2022). Similarly, the number of days per year on which fire danger was extreme increased by 166% from 1979 through 2019 (Jones *et al.*, 2022). Extreme fire danger was defined as the highest 5% of values of the Canadian Fire Weather Index, which is based on estimates of fuel moisture derived from temperature, precipitation, humidity, and wind (Van Wagner, 1987; Jones *et al.*, 2022).

The Northwest Interagency Coordination Center (https://gacc.nifc.gov/nwcc/) commonly uses the 100-hour fuel moisture (FM100) index to predict fire danger. FM100 is a measure of the percentage of moisture in the dry weight of dead vegetation with 1–3 inch diameter and is calculated from precipitation, temperature, and relative humidity according to the equations in the National Fire Danger Rating System (Bradshaw *et al.*, 1984). A majority of climate models project that FM100 will decline, resulting in increased fire danger across Oregon by the 2050s (2040–2069) under the higher emissions scenario (Gergel *et al.*, 2017). Projections of the Keetch–Byram Drought Index, a common fire index that is based on the response of vegetation moisture to precipitation and temperature, suggested that

within the Northwest, the area with high fire danger in summer will increase by 345% from 1996–2004 to 2086–2094 under the higher emissions scenario (Brown *et al.*, 2021). All of these methods project that the number of summer days with high fire danger in Oregon will increase through the end of the twenty-first century, particularly in the Cascade Range, Coast Range, and Klamath Mountains (Brown *et al.*, 2021).

Projected Wildfire Risk in Benton County

Here, we estimate the future change in wildfire risk with two metrics, FM100 and VPD, that are proxies for extreme fire danger, or conditions under which wildfire is likely to spread. We present projected changes in the average annual number of days on which FM100 is very high and VPD is extreme for two future periods, both of which we compare to the historical baseline (1971–2000 average), under two emissions scenarios. We define a day with very high fire danger as one on which the FM100 value (moisture on the forest floor) is comparable to the lowest (driest) 10% of values within the historical baseline period (1971–2000). Historically, fire danger in Benton County was very high on 36.5 days per year. By the 2050s under the higher emissions scenario, the average number of days per year on which fire danger is very high is projected to increase by 11 (range -7–25) (Figure 15).

Similarly, we define a day with extreme VPD (dry air) as a day within the warm season (March–October) on which VPD is comparable to the highest (driest) 10% of values within the historical baseline period. Historically, VPD in Benton County was extreme for 24.5 days per year. Under the higher emissions scenario, the average number of days per year on which VPD is extreme is projected to increase by 26 (range 9–43) by the 2050s (Figure 16).

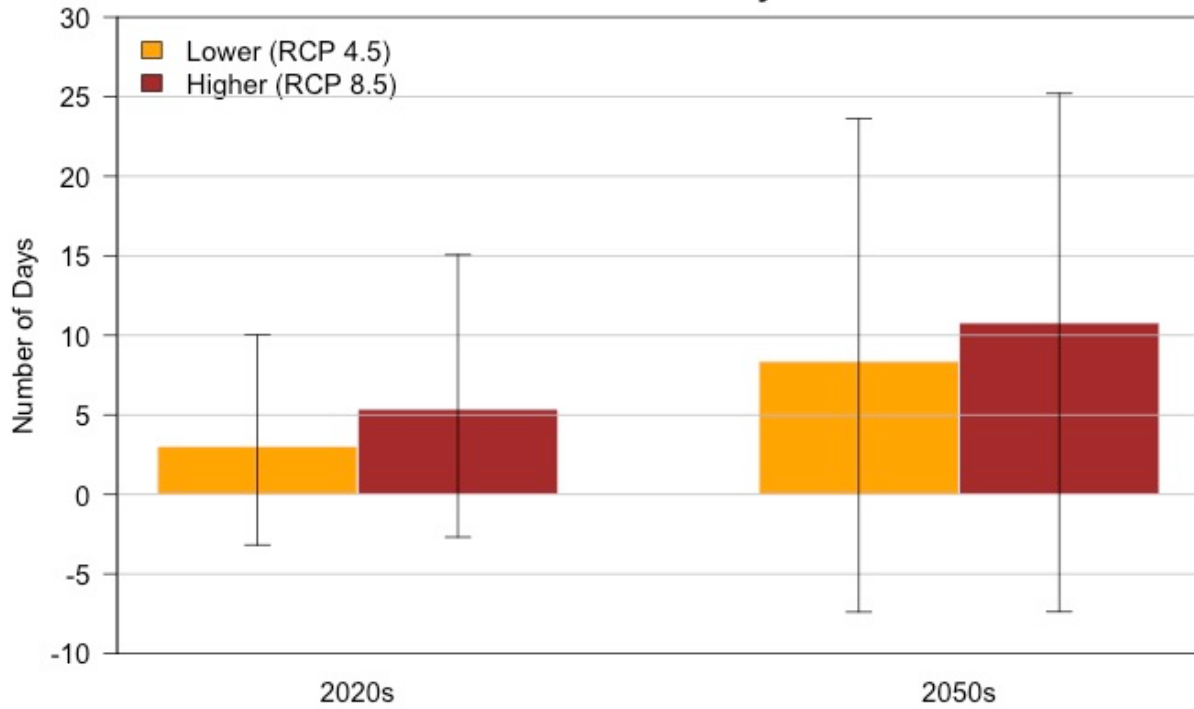**Change in Annual Number of Very High Fire Danger Days**
Benton County

Figure 15. Projected changes by the 2020s (2010–2039 average) and 2050s (2040–2069 average), relative to the 1971–2000 historical baseline and under two emissions scenarios, in the number of days on which fire danger in Benton County is very high. Changes were calculated for each of 18 global climate models relative to each model's historical baseline, then averaged. Whiskers represent the range of changes across the 18 models. Eighteen of the full set of 20 models that were used to project temperature and precipitation included the data necessary to estimate fire danger. (Data Source: Climate Toolbox, climatetoolbox.org/tool/Climate-Mapper)
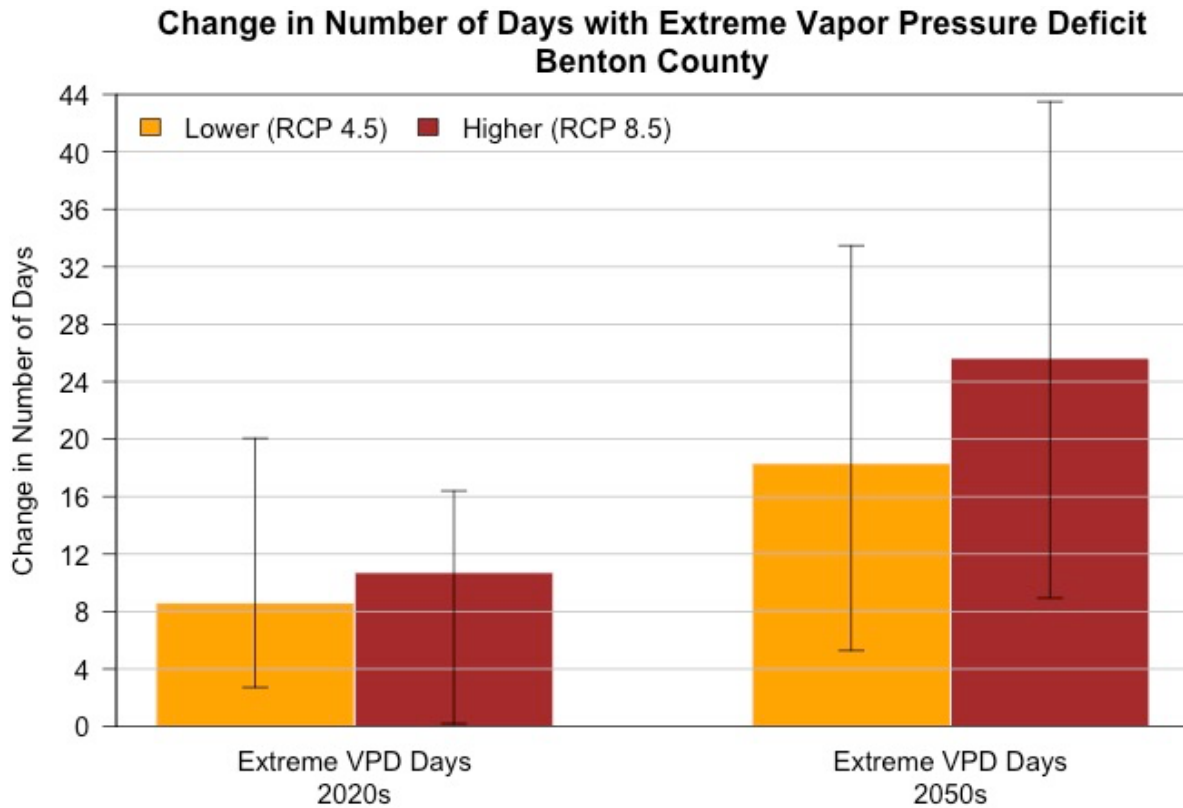
Figure 16. Projected changes by the 2020s (2010–2039 average) and 2050s (2040–2069 average), relative to the 1971–2000 historical baseline and under two emissions scenarios, in the number of days on which vapor pressure deficit in Benton County is extreme. Changes were calculated for each of 20 global climate models relative to each model's historical baseline, then averaged. Whiskers represent the range of changes across the 20 models. (Data Source: Climate Toolbox, climatetoolbox.org/tool/Climate-Mapper)

Summary

Wildfire frequency, intensity, and area burned are projected to continue increasing in the Northwest. Wildfire risk, expressed as the average number of days per year on which fire danger is very high, is projected to increase in Benton County by 11 days (range -7–25) by the 2050s, relative to the historical baseline, under the higher emissions scenario. The average number of days per year on which vapor pressure deficit is extreme is projected to increase by 26 (range 9–43) by the 2050s.

⚠️

Reduced Air Quality

Climate change is expected to reduce outdoor air quality. Warmer temperatures may cause an increase in ground-level ozone concentrations, while more numerous and intense wildfires generate higher concentrations of fine particulate matter (particles less than 2.5 micrometers in diameter [$PM_{2.5}$]) and other pollutants (Rohlman *et al.*, 2023). Moreover, increases in pollen abundance and the duration of the pollen season may cause an increase in airborne allergens.

Poor air quality is expected to exacerbate allergy and asthma conditions and increase the incidence of respiratory and cardiovascular illnesses and death (Fann *et al.*, 2016). Excess asthma events due to $PM_{2.5}$ from wildfire smoke are projected to increase in Oregon by about 42 per 10,000 persons, resulting in a projected increase in cost of more than $250,000 per 10,000 persons (Stowell *et al.*, 2021). Those at high risk of adverse health outcomes as a result of wildfire smoke include people with preexisting conditions, outdoor workers, children, pregnant women, older adults, and rural and tribal communities (York *et al.*, 2020; Ho *et al.*, 2021). Poor air quality and increases in airborne allergens are most likely to affect communities with low incomes, high non-White or farmworker populations, or that are near highways and industrial facilities; outdoor workers, especially in urban areas with stagnant air and during harvest season in agricultural areas such as the Willamette Valley; and those with preexisting conditions (York *et al.*, 2020; Ho *et al.*, 2021). Recent and projected estimates of many of these populations are presented in previous sections.

Wildfire Smoke

Over the past several decades, the wildfire season has increased in length while the intensity and severity of wildfires have increased. This trend is expected to continue as a result of factors including traditional forest management practices (Downing *et al.*, 2022), increasing human population density in areas with high fire risk (Radeloff *et al.*, 2018), and climate change (Sheehan *et al.*, 2015). Wildfire smoke poses a much greater threat, in terms of deaths and total costs to society, than wildfire flames per se (Fleishman, 2023). Wildfire smoke also impairs visibility near ground level and at altitudes where firefighting aircraft and evacuation helicopters fly (Nolte *et al.*, 2018). Hazardous levels of air pollution are most common near wildfires, but extensive fires in the western United States in recent decades have generated taller plumes of smoke and injected a greater volume of $PM_{2.5}$ at high altitudes, increasing long-range transport of these particulates and posing a health hazard to larger numbers of people both near to and far from those wildfires (Wilmot *et al.*, 2022; Rupp and Holz, 2023).

Wildfires are the primary cause of exceedances of air quality standards for $PM_{2.5}$ in western Oregon and parts of eastern Oregon (Liu *et al.*, 2016), particularly in August and September (Wilmot *et al.*, 2021). Woodstove smoke and diesel emissions also contribute to poor air quality in Oregon (Oregon DEQ, 2016; Liu and Peng, 2019). Fine particulate matter from vehicles, woodstoves, and power plants can be regulated, but it is much more difficult to control wildfires. The Oregon Department of Environmental Quality monitors daily levels of $PM_{2.5}$ and ozone in Corvallis. From 2007 through 2015, air quality was good on an average of 336 days per year and moderate on most other days (BCHD, 2017). Wildfires

were the main cause of temporary reductions in air quality, although winter inversion layers also can increase concentrations of fine particulate matter from vehicle exhaust and other pollutants.

Across the western United States, $PM_{2.5}$ concentrations from wildfires are projected to increase 160% by 2046–2051, relative to 2004–2009, under a moderate emissions scenario (SRES A1B) (Liu *et al.*, 2016). The SRES A1B scenario, which is from a generation of emissions scenarios that preceded CMIP5, is most similar to RCP 6.0 (Figure 2). CMIP6 models that were integrated with an empirical statistical model projected that $PM_{2.5}$ concentrations in August and September in the Northwest will double under a lower (SSP5-4.5) emissions scenario and triple under a higher (SSP5-8.5) emissions scenarios by 2080–2100 compared to 1997–2020 (Xie *et al.*, 2022). The Oregon Department of Environmental Quality monitors $PM_{2.5}$ during wildfire seasons with the U.S. Environmental Protection Agency's Air Quality Index (AQI), which classifies air quality on the basis of potential health effects. In the Willamette Valley, concentrations of $PM_{2.5}$ from wildfire smoke from June 1 through October 20 began to increase and become less healthy around 2012 (Oregon DEQ, 2022).

Exposure to $PM_{2.5}$ aggravates chronic cardiovascular and respiratory illnesses (Cascio, 2018). In addition, because exposure to $PM_{2.5}$ increases susceptibility to viral respiratory infections, exposure to wildfire smoke is likely to increase susceptibility to and the severity of reactions from COVID-19 (Henderson, 2020). During the 2020 wildfires in the western United States, in 18 of 19 Oregon counties analyzed, the number of reported COVID-19 cases increased on days with active wildfire smoke (Zhou *et al.*, 2021). Active wildfire smoke was defined as concentrations of $PM_{2.5}$ that exceeded 21 µg m^{-3}, a value within the moderate category of the AQI. Furthermore, wildfire smoke can disrupt outdoor recreational and social activities, in turn affecting physical and mental health (Nolte *et al.*, 2018). For example, on September 11, 2020, Portland's air quality deteriorated to hazardous and was the worst among major cities worldwide, causing many park closures and halting most outdoor activities (Green, 2020).

The negative effects of wildfire smoke extend beyond human health. For example, during the 2020 wildfire season, 62% of Oregon wineries reported not only unhealthy air that delayed harvest but impacts such as ash on grape skins and reduced sunlight that affected the size of grape clusters (IPRE, 2021). Eighteen percent of Oregon wineries reported smoke damage to their wines, with the majority of red wine grape varieties, particularly Pinot Noir, discarded by producers or not harvested (IPRE, 2021). The thin skin of Pinot Noir, Oregon's signature grape, makes smoke exceptionally damaging.

Wildfires emit ozone precursors that in hot and sunny conditions react with other pollutants to increase the concentration of ozone. From 2000 through 2020, the frequency, duration, and area of co-occurrence of $PM_{2.5}$ and ozone increased in the western United States (Kalashnikov *et al.*, 2022), including the Pacific Northwest (Buchholz *et al.*, 2022). The population exposed to persistent extreme $PM_{2.5}$ and ozone levels in the West increased by 25 million person-days per year over the period 2001–2020 (Kalashnikov *et al.*, 2022; Rupp and Holz, 2023).

Projected Changes in Air Quality in Benton County

We present projections of future air quality that are based on $PM_{2.5}$ from wildfire smoke. Smoke wave days are defined as two or more consecutive days on which simulated, county-averaged, wildfire-derived $PM_{2.5}$ values are in the highest 2% of simulated daily values from 2004 through 2009 (Liu *et al.*, 2016). Smoke wave intensity is defined as the concentration of $PM_{2.5}$ on smoke wave days. Liu *et al.* (2016) projected mean number of smoke wave days and mean smoke wave intensity for two six-year periods, 2004–2009 and 2046–2051, under a moderate emissions scenario. More information about their methods is in the appendix. The number of smoke wave days in Benton County is projected to increase by 3% and the intensity of smoke on those days is projected to increase by 80% (Figure 17).
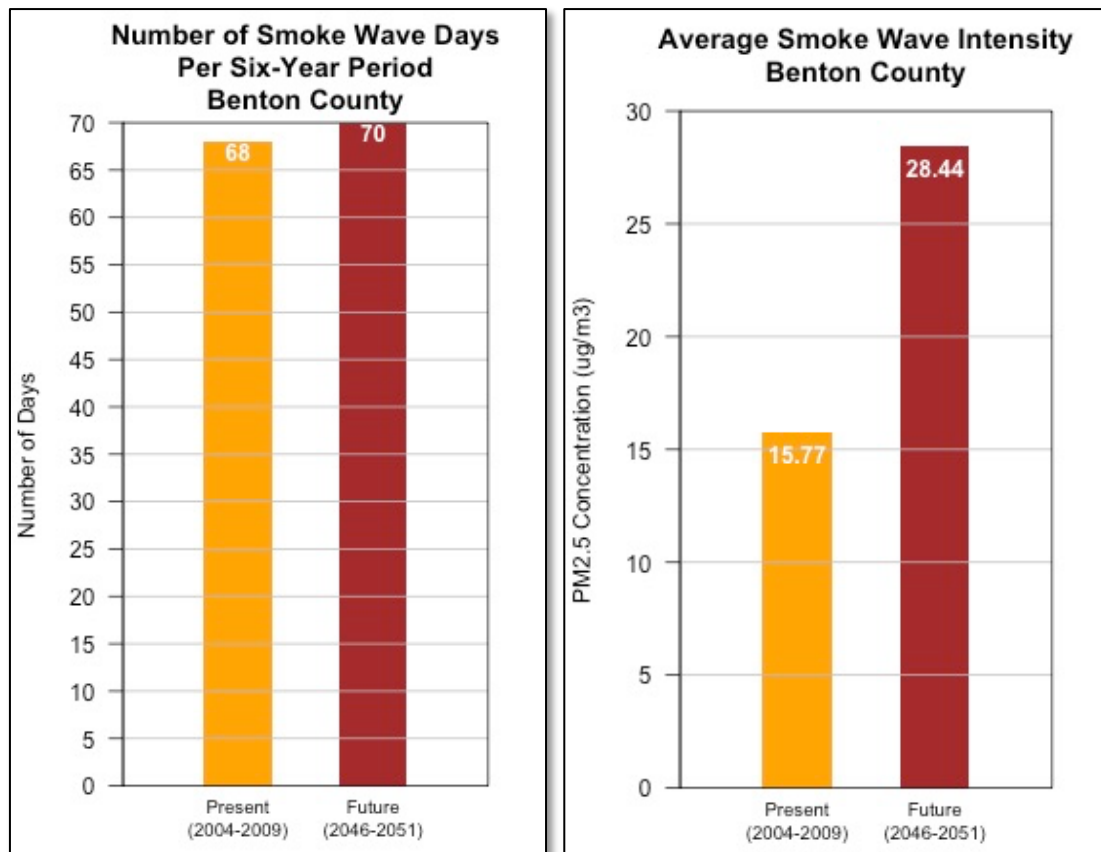

Figure 17. Simulated present (2004–2009) and future (2046–2051) number (left) and intensity (right) of smoke wave days in Benton County under a moderate emissions scenario. Values represent the average among 15 global climate models. (Data source: Liu et al. 2016, khanotations.github.io/smoke-map/)

Allergens and Other Airborne Organic Materials

Plants are responding to changes in climate and atmospheric concentrations of carbon dioxide by producing more pollen, and by producing it earlier in spring and for longer periods of time (Ziska *et al.*, 2009). From 1990 through 2018, pollen seasons increased by about 20 days and pollen concentration increased by 21% in the conterminous United

States (Anderegg *et al.*, 2021), including northern California (Paudel *et al.*, 2021). Wet springs, warm summers, and extensive grass cultivation lead to pollen counts in the Willamette Valley that are among the highest in the country (BCHD, 2017). Pollen counts generally increase markedly in May, reach a maximum in late June or early July, and are relatively low during other months (BCHD, 2017).

Fungal spores could also become more abundant following extreme floods or droughts, which are expected to become more common. The period during which outdoor airborne mold spores are detectable increased in the last 20 years as a result of increasing concentrations of carbon dioxide and changes in climate and land use (Paudel *et al.*, 2021). Furthermore, because both ozone and fine particulate matter affect the sensitivity of respiratory systems to airborne allergens, the combined effects of climate change, air pollution, and changes in vegetation phenology will likely increase the severity of respiratory diseases and allergies (D'Amato *et al.*, 2020).

Summary

Climate change is expected to reduce outdoor air quality. The risks to human health from wildfire smoke in Benton County are projected to increase. From 2004–2009 to 2046–2051, under a moderate emissions scenario, the number of days per year with poor air quality due to elevated concentrations of wildfire-derived fine particulate matter is projected to increase modestly (3%), but the concentration of fine particulate matter on those days is projected to increase by 80%.

Loss of Wetlands

In the United States, wetlands are defined under the Clean Water Act as "areas that are inundated or saturated by surface or ground water at a frequency and duration sufficient to support, and that under normal circumstances do support, a prevalence of vegetation typically adapted for life in saturated soil conditions. Wetlands generally include swamps, marshes, bogs, and similar areas." Wetlands also may be associated with the edges of lakes and with streams and rivers (Halofsky *et al.*, 2019).

The extent of historic wetlands in the Willamette Valley has been reduced by an estimated 57–95% by agriculture, urbanization, timber harvest, and channelization of the Willamette River (Baker *et al.*, 2004; Christy and Alverson, 2011; Fickas *et al.*, 2016). About 4.3% of emergent, lacustrine, riparian, and riverine wetland area within the two-year floodplain inundation zone along the main stem Willamette River changed (became larger or smaller or changed among the latter four classes) from 1972 through 2012 (Fickas *et al.*, 2016). The majority of losses resulted from conversion to agriculture (Daggett *et al.*, 1998; Bernert *et al.*, 1999; Fickas *et al.*, 2016), and the greatest proportion of change reflected conversion of riparian to riverine wetland (Fickas *et al.*, 2016). Some of the gains and losses in area related to agriculture may have been prompted by drought—creation of ponds in the former case, and farming of newly dry lands in the latter—and may not be permanent (Bernert *et al.*, 1999).

Wetlands and their associated plants and animals are likely to be affected by increases in air temperature, which generally are correlated with increases in freshwater temperature; decreases in snowpack and summer stream flows; and increases in evapotranspiration (Lee *et al.*, 2015). Projected effects in the Northwest include reductions in water levels and hydroperiod duration, and may be most pronounced in wetlands that become temporary in dry years (Lee *et al.*, 2015). Wetlands along low-gradient, wide valley bottoms that are dominated by riparian trees and understory species may be most susceptible to decreases in flow and water volume, in part because recruitment of some riparian species depends on seasonal flooding (Dwire *et al.*, 2018). Systems that are fed primarily by ground water may have more consistent temperature, water chemistry, and water levels than wetlands that are fed primarily by surface water (Halofsky *et al.*, 2019). However, effects of climate change on ground water aquifers that are recharged by snowpack are uncertain (Dwire *et al.*, 2018). Moreover, where increasing aridity leads to greater demand for ground water, decreases in ground water availability may affect wetlands.

From 1994 through 1996, The Nature Conservancy of Oregon conducted an inventory of 172 wetlands and stream or river reaches in the Willamette Valley (Titus *et al.*, 1996). Of those 172 locations, the effort identified 21 as particularly high priorities for conservation, including four in Benton County: Bull Run Creek between Fern Road and Peterson Road, Jackson-Frazier County Park, the riparian zones of Muddy Creek and the lower reaches of the Marys River, and William L. Finley National Wildlife Refuge. The reach of Bull Run Creek is on private land and includes vegetation communities dominated by Oregon ash (*Fraxinus latifolia*) and either slough sedge (*Carex obnupta*), dogwood (*Cornus sericea*), or snowberry (*Symphoricarpos albus*). The perennial sedge communities in Jackson-Frazier County Park were highlighted as distinct. Characteristic plant associations in these areas

include green-sheathed sedge (*Carex feta*), dense sedge (*C. densa*) and creeping spike-rush (*Eleocharis macrostachya*), slough sedge, and one-sided sedge (*C. unilateralis*) and meadow barley (*Hordeum brachyantherum*). Benton County is conducting long-term restoration of the Jackson-Frazier Wetland, with a focus on wetland hydrology, diversity of native vegetation, and environmental education and outreach.

The condition of Oregon ash and Oregon oak (*Quercus garryana*) forests along Muddy Creek was considered to be the best remaining in the Willamette Valley (Titus *et al.*, 1996). These forests grow on public lands in William L. Finley National Wildlife Refuge and private lands to the north and south. Small patches of bottomland prairie abut some of the riparian areas along the creek. In addition to riparian forest and prairie, the National Wildlife Refuge contains native emergent marsh.

Summary

In Benton County, losses of wetlands in recent decades largely were caused by conversion to agriculture. Projected effects of climate change on wetlands in the Northwest include reductions in water levels and hydroperiod duration. If withdrawals of ground water do not increase, then wetlands that are fed by ground water rather than surface water may be more resilient to climate change.

Windstorms

Wind patterns in the northwestern United States affect natural disturbances, public health, and multiple sectors. For example, variability in winds affects generation of wind power and, via downed power lines, the reliability of electricity transmission. Changes in winds also affect the safety of transportation by air, land, and sea and the spread of wildfires and pollutants, including wildfire smoke and allergens. In Oregon, average near-surface wind speeds are expected to decrease slightly in the future in response to global climate change (Pryor *et al.*, 2012; Jeong and Sushama, 2019; Chen, 2020; Mass *et al.*, 2022). However, a decrease in the average wind speed may not translate to a decrease in strong winds. Although projections are highly uncertain, climate models tend to agree that the magnitude of extreme wind speed will increase in western Oregon (Pryor *et al.*, 2012; Jeong and Sushama, 2019). Such increases are not projected in eastern Oregon. An extreme wind refers to an annual maximum wind speed with a given average return period, such as 20 or 50 years (annual exceedance probability of 5% or 2%, respectively).

Oregon's location accounts for some of the uncertainty in the response of strong winds to human-caused emissions of greenhouse gases. The state's most severe windstorms occur from October through April and are associated with extratropical cyclones (cyclones that occur from 30–60° latitude) (Read, 2003, 2007; Mass and Dotson, 2010). Future changes in wind speeds in extratropical cyclones are expected to be small, but the projected poleward shift in the tracks of these cyclones could lead to substantial changes in extreme wind speeds in some regions (Seneviratne *et al.*, 2021). One study indicated that by 2081–2099 relative to 1981–1999, assuming the higher emissions scenario, extratropical cyclones that generate severe winds will shift northward by an average of 2.2° over the North Pacific Ocean (Seiler and Zwiers, 2016). Therefore, these extratropical cyclones will become more frequent north of 45°N and less frequent and weaker south of 45°N. Oregon lies between about 42°N and 46°N. Accordingly, although Seiler and Zwiers (2016) did not examine the landfall location of severe cyclones, it is uncertain whether the frequency of severe landfalling extratropical cyclones and the distribution of wind speeds will change in Oregon.

The intensity of strong offshore (easterly) winds, which are most common in summer and in fall before the onset of the rainy season, typically is lower than that of winter windstorms. Nevertheless, offshore winds play a major role in summer heat waves in Oregon, including the record-breaking June 2021 heat wave (Chang *et al.*, 2021), because they displace cooler marine air west of the Cascade Range (Brewer and Mass, 2016). Projections from global climate models, assuming the higher emissions scenario, suggest a decrease in the frequency of strong offshore winds over western Oregon and Washington in July and August, with about a 50% reduction from 1970–1999 to 2071–2100 in the number of days with easterly wind speeds greater than approximately 11 miles per hour (5 meters per second) measured at approximately 5000 feet (1.5 km or 850-hPa) above Earth's surface (Brewer and Mass, 2016).

Easterly winds were key drivers of the largest wildfires on record in western Oregon, including the 2020 Labor Days fires (Abatzoglou *et al.*, 2021b; Mass *et al.*, 2021; Reilly *et al.*, 2022). The results of regional climate models that accounted for topographic effects on

wind indicated that from the preindustrial to the current era, the frequency of fall (September through November) easterly winds along the Cascade Range in Oregon decreased by about 2% (Hawkins *et al.*, 2022). The latter research defined easterly winds as those with horizontal speeds of at least 13 meters per second (approximately 29 miles per hour) and downward speeds of at least 0.6 Pascals per second (at 32°F, approximately 2 inches per second or 10 feet per minute), both measured at 10,000 feet (700 hPa) above Earth's surface, and near-surface relative humidity no greater than 30%. By the year 2099 relative to 1970, assuming the higher emissions scenario, the frequency of 10-meter (approximately 33 feet) easterly winds with a daily maximum exceeding 3.4 meters per second (7.6 miles per hour), which is one standard deviation above the average wind speed, decreased modestly west of the Cascade Range (Mass *et al.*, 2022). For example, in Alpine, Washington, the annual number of days with such winds decreased from 15 to 11 (Mass *et al.*, 2022).

Understanding of how anthropogenic emissions may affect local winds in Oregon remains limited. Due to their coarse spatial resolution, global climate models and all but the highest-resolution regional climate models cannot adequately simulate mountain slope, valley, and coastal winds, sea breezes, and winds associated with mesoscale convective systems (Doblas-Reyes *et al.*, 2021). Large numbers of simulations from multiple high-resolution (1 to 10 km [0.6 to 6 mi]) regional climate models ultimately will be required to estimate changes in these types of winds across Oregon with high confidence.

Summary

Wind patterns affect provision of electricity, transportation safety, and the spread of wildfires and pollutants. Mean wind speeds in Oregon are projected to decrease slightly, but extreme winter wind speeds may increase, especially in western Oregon. The frequency of strong easterly winds during summer and autumn, however, is projected to decrease slightly.

Expansion of Non-native Invasive Species

Changes in climate and atmospheric concentrations of carbon dioxide can affect the distribution and population dynamics of native and non-native species of animals and plants that are considered to be invasive or pests in natural and agricultural systems. Species-environment relations are not static (MacDonald, 2010; Walsworth *et al.*, 2019). Therefore, even when the current ecology of a species is well understood, it often is difficult to predict with confidence how the species will respond to projected changes in climate, especially when climate change interacts with land-use change or other environmental changes. Species adapt not only in response to climate change but in response to all types of environmental change, including management actions (Thomas *et al.*, 1979; Skelly *et al.*, 2007; Winter *et al.*, 2016). These responses may be rapid, on the order of years or decades, particularly among organisms with short generation times (Boughton, 1999; MacDonald *et al.*, 2008; Willis and MacDonald, 2011; Singer, 2017). Adaptive capacity also is affected by whether individuals can move freely or whether habitat fragmentation and other barriers impede movement (Thorne *et al.*, 2008; Willis and MacDonald, 2011; Fleishman and Murphy, 2012). Monocultures, dense populations, and even-aged populations of animals or plants generally are more susceptible to pests and pathogens than individuals in areas with higher species richness or populations with greater demographic diversity.

Animals

The Oregon Conservation Strategy lists 31 non-native invasive species of terrestrial and aquatic animals that have been documented in the Willamette Valley (ODFW, 2016) (Table 15); these species may occur in Benton County. Climate change is unlikely to have a major effect on the status of non-native invasive animals in Benton County given that most are widespread generalists that exploit human-dominated environments and compete effectively with native species. Aquatic species may be adversely affected if the amount or quality of their habitat declines as a function of aridification and human appropriation of surface water and ground water, but it is unclear whether their competitive interactions with native species will change. There is some evidence that as temperature increases, increases in metabolic rate in turtles, such as red-eared and yellow bellied sliders (*Trachemys scripta elegans*, *T. s. scripta*), will reduce their survival and fitness (Willette *et al.*, 2005). Sex ratios of reptiles with temperature-dependent sex determination also may become skewed as temperatures increase (Mitchell and Janzen, 2010). Again, however, these effects will not be limited to non-native taxa.

Table 15. Non-native invasive species of animals with documented occurrences in the Willamette Valley (ODFW, 2016).

Mammals
Black rat (*Rattus rattus*)
Brown rat (*Rattus norvegicus*)
Eastern fox squirrel (*Sciurus niger*)
Eastern gray squirrel (*Sciurus carolinensis*)
Feral swine (*Sus scrofa*)
Nutria (*Myocastor coypus*)

Red fox (*Vulpes vulpes*)
Virginia opossum (*Didelphis virginiana*)
Reptiles and amphibians
American bullfrog (*Lithobates catesbeianus*)
Common snapping turtle (*Chelydra serpentina*)
Red-eared slider (*Trachemys scripta elegans*)
Yellow bellied slider (*Trachemys scripta scripta*)
Birds
Eurasian Collared Dove (*Streptopelia decaocto*)
European Starling (*Sturnus vulgaris*)
House Sparrow (*Passer domesticus*)
Mute Swan (*Cygnus olor*)
Rock Pigeon (*Columba livia*)
Fishes
Amur goby (*Rhinogobius brunneus*)
Common carp (*Cyprinus carpio*)
Fathead minnow (*Pimephales promelas*)
Golden shiner (*Notemigonus crysoleucas*)
Goldfish (*Carassius auratus*)
Grass carp (*Ctenopharyngodon idella*)
Western mosquitofish (*Gambusia affinis*)
Molluscs
Asian clam (*Corbicula fluminea*)
Chinese mysterysnail (*Cipangopaludina chinensis malleata*)
New Zealand mudsnail (*Potamopyrgus antipodarum*)
Invertebrates
Freshwater jellyfish (*Craspedacusta sowerbyi*)
Red swamp crayfish (*Procambarus clarkii*)
Ringed crayfish (*Orconectes neglectus*)
Siberian prawn (*Exopalaemon modestus*)

Plants

The Benton Soil and Water Conservation District maintains a database of 91 non-native invasive plants (Table 16). Although little is known about how many of these species may to respond to climate change, some evidence suggests how others may be affected. In general, non-native invasive plants in Benton County are likely to become more prevalent in response to projected changes in climate. However, many of these responses are uncertain, and are likely to vary locally. Moreover, the responses may change over time.

Table 16. Species of non-native invasive plants in the Benton Soil and Water Conservation District's database. Other jurisdictions may use different common names for some species.

Species	Growth form
African wiregrass (*Ventenata dubia*)	Annual grass
Barbed goat grass (*Aegilops triuncialis*)	Perennial forb
Biddy-biddy (*Acaena novae-zelandiae*)	elsewhere
Brazilian elodea or Brazilian egeria (*Egeria densa*)	Perennial aquatic
Brazilian verbena (*Verbena bonariensis*)	Perennial forb
Bull thistle (*Cirsium vulgare*)	Biennial forb
Canada thistle (*Cirsium arvense*)	Perennial forb
Cheatgrass (*Bromus tectorum*)	Annual grass
Coltsfoot (*Tussilago farfara*)	Perennial forb
Common reed (*Phragmites australis* ssp. *australis*)	Perennial grass
Cutleaf or evergreen blackberry (*Rubus lacinatus*)	Shrub
Cutleaf teasel (*Dipsacus laciniatus*)	Biennial forb
Dalmatian toadflax (*Linaria dalmatica*)	Perennial forb
Dodder (*Cuscuta* spp.)	Annual vine
Dyer's woad (*Isatis tinctoria*)	Annual, biennial, or short-lived perennial forb
English ivy (*Hedera helix*)	Perennial vine
Eurasian watermilfoil (*Myriophyllum spicatum*)	Perennial aquatic
European blackberry (*Rubus vestitus*)	Shrub
European waterchestnut (*Trapa natans*)	Annual aquatic
Evergreen bugloss (*Pentaglottis sempirvirens*)	Perennial forb
False brome (*Brachypodium sylvaticum*)	Perennial grass
Field bindweed (*Convolvulus arvensis*)	Perennial forb
Floating primrose-willow (*Ludwigia peploides*)	Perennial aquatic
Flowering rush (*Butomus umbellatus*)	Perennial aquatic
French broom (*Cytisus monspessulanas*)	Shrub
Garlic mustard (*Alliaria petiolata*)	Perennial forb
Giant hogweed (*Heracleum mantegazzianum*)	Biennial or perennial forb
Giant reed (*Arundo donax*)	Perennial grass
Goats rue (*Galega officinalis*)	Perennial forb
Gorse (*Ulex europaeus*)	Shrub
Hare barley (*Hordeum murinum*)	Grass
Himalayan blackberry (*Rubus bifrons*)	Shrub
Hydrilla (*Hydrilla verticillata*)	Perennial aquatic
Iberian starthistle (*Centaurea iberica*)	Annual forb
Indigo bush (*Amorpha fruticosa*)	Shrub
Italian thistle (*Carduus pycnocephalus*)	Annual or biennial forb
King devil hawkweed (*Hieracium piloselloides*)	Perennial forb
Knotweeds (*Fallopia japonica, F.* x *bohemica, F. sachalinense*)	Perennial forb
Kudzu (*Pueraria lobata*)	Perennial aquatic vine

Large-flower primrose-willow (*Ludwigia grandiflora*)	Perennial aquatic
Leafy spurge (*Euphorbia esula*)	Perennial forb
Lesser celandine (*Ranunculus ficaria*)	Perennial forb
Meadow hawkweed (*Hieracium pratense*)	Perennial forb
Meadow knapweed (*Centaurea pratensis*)	Perennial forb
Medusahead (*Taeniatherum canput-medusae*)	Annual grass
Mile-a-minute (*Persicaria perfoliata*)	Annual vine
Mouse-ear hawkweed (*Hieracium pilosella*)	Perennial forb
Oblong or eggleaf spurge (*Euphorbia oblongata*)	Perennial forb
Old man's beard (*Clematis vitalba*)	Shrub
Orange hawkweed (*Hieracium aurantiacum*)	Perennial forb
Oxeye daisy (*Leucanthemum vulgare*)	Perennial forb
Pampas or jubata grass (*Cortaderia* spp.)	Perennial grass
Parrot feather (*Myriophyllum aquaticum*)	Annual aquatic
Paterson's curse (*Echium plantagineum*)	Annual forb
Perennial peavine (*Lathyrus latifolius*)	Perennial vine
Poison hemlock (*Conium maculatum*)	Biennial forb
Pokeweed (*Phytolacca americana*)	Perennial forb
Policeman's helmet (*Impatiens glandulifera*)	Annual forb
Portuguese broom (*Cytisus striatus*)	Shrub
Prickly lettuce (*Lactuca serriola*)	Annual or biennial forb
Puncturevine (*Tribulus terrestris*)	Annual forb
Purple loosestrife (*Lythrum salicaria*)	Perennial forb
Purple nutsedge (*Cyperus rotundus*)	Perennial sedge
Purple starthistle (*Centaurea calcitrapa*)	Annual, biennial, or perennial forb
Quackgrass (*Elymus repens*)	Perennial grass
Rattail fescue (*Vulpia myuros*)	Annual grass
Reed canarygrass (*Phalaris arundinacea*)	Perennial grass
Ripgut brome (*Bromus diandrus*)	Annual grass
Scotch broom (*Cytisus scoparius*)	Shrub
Scotch thistle (*Onopordum acanthium*)	Annual or biennial forb
Sharp-leaved fluvellin (*Kickxia elatine*)	Perennial forb
Soft brome (*Bromus hordeaceus*)	Annual grass
South American spongeplant or frog's bit (*Limnobium spongia*)	Perennial aquatic
Spanish broom (*Spartium junceum*)	Shrub
Spanish heath (*Erica lusitanica*)	Shrub
Spotted jewelweed (*Impatiens capensis*)	Annual forb
Spotted knapweed (*Centaurea stoebe*)	Short-lived perennial forb
Spurge laurel (*Daphne laureola*)	Shrub
St. Johns wort (*Hypericum perforatum*)	Perennial forb
Sulfur cinquefoil (*Potentilla recta*)	Perennial forb
Tall oatgrass (*Arrhenatherum elatius*)	Perennial grass

Tansy ragwort (*Senecio jacobaea*)	Biennial or short-lived perennial
Uruguayan primrose-willow (*Ludwigia hexapetala*)	Perennial aquatic
Velvetgrass (*Holcus lanatus*)	Perennial grass
Velvetleaf (*Abutilon theophrasti*)	Annual forb
Wild carrot (*Daucus carota*)	Biennial forb
Woold distaff thistle (*Carthamus lanatus*)	Annual forb
Yellow archangel (*Lamiastrum galeobdolon*)	Perennial forb
Yellow flag iris (*Iris pseudocorus*)	Perennial aquatic
Yellow floating heart (*Nymphoides peltata*)	Perennial aquatic
Yellow starthistle (*Centaurea solstitalis*)	Annual forb

Carbon Dioxide, Nitrogen, and Ozone Concentrations

Increasing concentrations of carbon dioxide affect some plants' primary productivity, water-use efficiency, and nutrient content. Increases in photosynthesis in response to increases in carbon dioxide are more common in plants with C3 metabolism than in plants with C4 metabolism. C4 metabolism has evolved multiple times, usually as an adaptation to hot, dry climate. Plants with C4 metabolism lose considerably less water per unit of carbon dioxide absorbed, and tend to photosynthesize more efficiently, than plants with C3 metabolism. By contrast, tolerance of the herbicide glyphosate tends to increase more in C4 than in C3 plants as carbon dioxide increases (Chen *et al.*, 2020).

Experiments suggested that the photosynthetic rate and biomass of Canada thistle, and the number and length of the species' spines, are likely to increase as ambient concentrations of carbon dioxide increase throughout the twenty-first century, and may have increased during the twentieth century (Ziska, 2002). Whether the root biomass of Canada thistle responds positively to increases in carbon dioxide concentrations, especially independent of increases in temperature, is unclear (Ziska *et al.*, 2004; Tørresen *et al.*, 2020), and may vary in space. English ivy also can benefit from increases in carbon dioxide concentrations, especially when temperatures are relatively warm (Manzanedo *et al.*, 2018).

Changes in climate, ongoing human additions of nitrogen to the environment, and their interactions affect the growth and competitive relations among plant and animal species (Greaver *et al.*, 2016). The competitive advantage of non-native forbs and grasses over native species of plants may be strongest in relatively warm and dry areas, which often coincide with lower elevations (Dodson and Root, 2015). Additionally, non-native invasive plants generally gain a competitive advantage from nitrogen deposition. For example, the size of yellow starthistle plants increased substantially in response to experimentally increased nitrogen deposition, whereas co-occurring native plants responded less strongly (Dukes *et al.*, 2011). Japanese knotweed, too, may gain a competitive advantage over native species when nitrogen availability is variable or episodic (Parepa *et al.*, 2013). Nevertheless, how field experiments with supplemental nitrogen relate to changes in nitrogen deposition or availability as a result of climate change is uncertain. Japanese knotweed also is fairly tolerant of high temperatures, drought, saturated soils, and fire (Clements and DiTommaso, 2012).

As tropospheric concentrations of ozone continue to increase, productivity of native and agricultural plants generally is expected to decrease. However, ozone tolerance in weedy, vegetatively reproducing species may increase relatively quickly, allowing them to gain a competitive advantage over some crops (Grantz and Shrestha, 2006).

Heat

Many non-native invasive plants tolerate high temperatures, but responses to interactions between temperature and other climate variables can be complex. A 6.3°F increase in temperature was associated with an increase in aboveground biomass of reed canarygrass early in the growing season, but with earlier senescence and lower biomass later in the growing season, especially when water availability was limited (Ge *et al.*, 2012). Increases in mean monthly temperature and maximum daily temperature, and reduction in the number of spring days with minimum temperatures below 32°F, may lead to earlier seedling emergence and increase reproduction and recruitment of garlic mustard (Blossey *et al.*, 2017; Anderson *et al.*, 2021).

Garlic mustard also may flower earlier as temperature increases (Fox and Jönsson, 2019). Yet germination of garlic mustard seeds currently requires winter chilling, and increases in winter temperature may limit the species' expansion until it evolves tolerance of higher winter temperatures (Footitt *et al.*, 2018). Increases in temperature also can present opportunities for controlling non-native invasive plants. For instance, there is some evidence that heat stress impairs photosynthesis and therefore growth of English ivy (Strelau *et al.*, 2018). The life span of flowers of policeman's helmet (which is associated with duration of pollination) and the amount and sugar concentration of nectar produced responded negatively to temperatures above 81°F (Descamps *et al.*, 2021).

The flowering phenology of purple loosestrife, which readily colonizes wetlands, is adapted to the duration of the growing season. At northern latitudes, including Oregon, purple loosestrife flowers early, at a small size; at southern latitudes, it flowers later, at a larger size (Colautti and Barrett, 2013). Early flowering limits reproductive growth of purple loosestrife, and northern plants generally produce fewer seeds and have less population-level genetic variation than southern plants (Colautti *et al.*, 2010). Climate change is expected to prolong the growing season, and therefore to increase the long-term viability of purple loosestrife, although local adaptation may be relatively slow due to genetic constraints of flowering time (Colautti *et al.*, 2010, 2017).

By contrast, reproduction of false brome along a latitudinal gradient in Europe was independent of temperature (growing degree hours above 41°F after 1 January) (De Frenne *et al.*, 2009). In at least some experimental contexts, growth of kudzu appears to be more sensitive to photoperiod than to temperature (Way *et al.*, 2017).

Cold

Responses of invasive plants to changes in temperature are diverse, even within the same species. For example, although it appears that photosynthesis in Japanese knotweed is constrained by temperatures below freezing (Baxendale and Tessier, 2015), the range of the species is expanding northward, perhaps reflecting evolution of frost tolerance (Clements and DiTommaso, 2012). Therefore, Japanese knotweed may become more

widespread or abundant as minimum temperatures increase. In England, giant hogweed germinated earlier as the number of heat degree days >41°F increased, and the species' overwinter survival decreased as frost incidence increased, but overwinter survival of seeds was not related to winter temperature or the number of days with frost from November through March (Willis and Hulme, 2002).

Biddy-biddy generally is sensitive to frost (Gynn and Richards, 1985). Given that biddy biddy is transported readily by humans, often on socks (Pickering *et al.*, 2011), increases in recreational activity could interact with climate change to facilitate its expansion. Much like biddy-biddy, Atlantic and English ivy and Scotch broom usually are not highly tolerant of frost in autumn, although populations can become more frost-tolerant over time (Strelau *et al.*, 2018; Winde *et al.*, 2020).

Precipitation

Changes in the amount and timing of precipitation may contribute to expansion or contraction of different non-native invasive plants. Normal to high precipitation can decrease the viability of certain non-native invasive plants, at least in some contexts. In forests in western Oregon, occurrence of bull thistle and Canada thistle was associated negatively with annual precipitation, and cover of English ivy was associated negatively with summer precipitation (Gray, 2005). Gorse can spread after wildfire and generally is highly flammable. However, extreme precipitation following wildfire directly or indirectly may reduce seedling survival via movement of soil and litter, which can either expose or bury the small plants (Luís *et al.*, 2005).

Following experimental drought treatment in a seasonally flooded area, percent cover of bull thistle increased five to 13 times (Hogenbirk and Wein, 1991), and in forests in western Oregon, cover of English ivy was associated negatively with summer precipitation (Strelau *et al.*, 2018). By contrast, spotted knapweed may be outcompeted by some native grasses (e.g., bluebunch wheatgrass [*Pseudoroegneria spicata*]) during drought, but may have a competitive advantage when precipitation is closer to average (Pearson *et al.*, 2017). Monocultures of spotted knapweed appear to be less affected by drought (Pearson *et al.*, 2017).

Yellow starthistle is somewhat sensitive to drought and can be outcompeted by natives that are more tolerant of dry conditions (Dlugosch *et al.*, 2015; Young *et al.*, 2017). Evidence of drought tolerance in Scotch broom is equivocal, especially in the field rather than in greenhouse experiments (Potter *et al.*, 2009; Hogg and Moran, 2020). The growth and survival of Scotch broom and Spanish broom in relatively open woodlands and forests may increase as snow depths decrease, especially during the winter after germination (Stevens and Latimer, 2015). Whether drought limits vegetative growth of purple loosestrife is unclear. Increased spring temperatures and decreased precipitation associated with the El Niño–Southern Oscillation in some parts of the species' range were associated with early flowering and aboveground biomass accumulation, but not with total aboveground biomass, inflorescence lengths (an indicator of reproductive output), or timing of senescence (Dech and Nosko, 2004).

Cheatgrass currently is most abundant in areas where precipitation is greatest during autumn and spring, which facilitates the species' germination and growth (Bradley *et al.*,

2016), and with hot, dry summers. Percent cover and biomass of cheatgrass also tends to increase in years with heavy winter and spring precipitation (Knapp, 1998; Garton *et al.*, 2011), and may remain high during the following year (Bradley *et al.*, 2016). Germination, growth, and reproduction of cheatgrass generally are highest at intermediate elevations with moderate temperatures and water availability. At low elevations, cheatgrass is limited by relatively high temperatures and low precipitation, and at high elevations, the species is limited by low soil temperatures (Meyer *et al.*, 2001; Chambers *et al.*, 2007, 2017; Compagnoni and Adler, 2014). Projected increases in temperature at high elevations (as at all elevations) may reduce that constraint on cheatgrass expansion in the future. Furthermore, soil moisture and nutrient levels commonly increase as elevation increases, supporting higher primary productivity and competition between cheatgrass and other species (Chambers *et al.*, 2007; Compagnoni and Adler, 2014), especially perennial grasses, which can reduce the cover and density of cheatgrass (Reisner *et al.*, 2013; Bradley *et al.*, 2016; Larson *et al.*, 2017). Increases in annual precipitation may facilitate expansion of French broom (García *et al.*, 2014).

Wildfire and Other Disturbances

The density and distribution of weedy plants tends to increase in response to ground disturbance, whether from wildfire, livestock grazing, recreational activities, or removal of overstory trees and shrubs. Some non-native plants also contribute to a positive feedback cycle by increasing the probability of disturbances that facilitate their population growth. The rapid expansion of non-native invasive grasses, such as cheatgrass and ventenata grass, has increased fine-fuel biomass and spatial continuity of fuels in sagebrush-dominated ecosystems (Balch *et al.*, 2013; Kerns *et al.*, 2020; Tortorelli *et al.*, 2020). Expansion of cheatgrass leads to a positive feedback loop in which increases in fire frequency and extent facilitate further increases in the distribution and density of cheatgrass. Both bull thistle and Canada thistle can establish readily in soils that have been disturbed by high-severity wildfires or by logging (Reilly *et al.*, 2020).

Summary

In general, non-native invasive plants in Benton County are likely to become more prevalent in response to projected increases in temperature and the frequency, duration, and severity of drought. However, many of these responses are uncertain, are likely to vary locally, and may change over time. Over the next several decades, changes in the distribution and abundance of non-native invasive animals in the county may not be strongly related to climate change.

Appendix

We projected future climate and hydrology on the basis of outputs from twenty global climate models (GCM) and two emissions scenarios (Representative Concentration Pathway [RCP] 4.5 and RCP 8.5) from the fifth phase of the Coupled Model Intercomparison Project (CMIP5) (Table A1).

Table A1. The 20 global climate models (GCMs) from the fifth phase of the Coupled Model Intercomparison Project (CMIP5) represented in this report. Asterisks (*) indicate the ten GCMs used as inputs to the Variable Infiltration Capacity hydrological model in the Integrated Scenarios of the Future Northwest Environment project. Hashes (#) indicate the ten GCMs used as inputs to the hydrological models in the Columbia River Climate Change project. Carets (^) indicate the GCMs that do not include daily relative humidity.

Model Name	Modeling Center
BCC-CSM1-1 BCC-CSM1-1-M*	Beijing Climate Center, China Meteorological Administration
BNU-ESM	College of Global Change and Earth System Science, Beijing Normal University, China
CanESM2*#	Canadian Centre for Climate Modeling and Analysis
CCSM4*#^	National Center for Atmospheric Research, USA
CNRM-CM5*#	National Centre of Meteorological Research, France
CSIRO-Mk3-6-0*#	Commonwealth Scientific and Industrial Research Organization/Queensland Climate Change Centre of Excellence, Australia
GFDL-ESM2G GFDL-ESM2M#	NOAA Geophysical Fluid Dynamics Laboratory, USA
HadGEM2-CC*# HadGEM2-ES*#	Met Office Hadley Center, UK
INMCM4#	Institute for Numerical Mathematics, Russia
IPSL-CM5A-LR IPSL-CM5A-MR*# IPSL-CM5B-LR	Institut Pierre Simon Laplace, France
MIROC5*# MIROC-ESM MIROC-ESM-CHEM	Japan Agency for Marine-Earth Science and Technology, Atmosphere and Ocean Research Institute (The University of Tokyo), and National Institute for Environmental Studies, Japan

MRI-CGCM3	Meteorological Research Institute, Japan
NorESM1-M*^	Norwegian Climate Center, Norway

MACA Downscaling

The coarse horizontal resolution of the GCM outputs (100–300 km) was statistically downscaled to a resolution of about 6 km with the Multivariate Adaptive Constructed Analogs (MACA) statistical downscaling method, which is skillful in complex terrain (Abatzoglou and Brown, 2012). A detailed description of the MACA method is at climate.northwestknowledge.net/MACA/MACAmethod.php. The MACA method uses gridded observational data to train the downscaling. It applies bias corrections and matches the spatial patterns of observed coarse-resolution to fine-resolution statistical relations. The downscaled variables include daily maximum and minimum temperature, maximum and minimum relative humidity, specific humidity, precipitation, wind, and downward solar radiation at the surface from 1950 through 2099. All simulated climate data were bias-corrected with quantile mapping, which adjusts simulated values by comparing the cumulative probability distributions of simulated and observed values. In practice, the simulated and observed values of a variable over the historical time period are sorted and ranked, and each value is assigned a probability of exceedance. The bias-corrected value of a given simulated value is assigned the observed value that has the same probability of exceedance as the simulated value. The historical bias in the simulations is assumed to be constant. Therefore, the relations between simulated and observed values in the historical period were applied to the future scenarios. Climate data in the MACA outputs reflect quantile mapping relations for each non-overlapping 15-day window in the calendar year.

Climate and Fire Danger Variables

We used MACA-downscaled minimum and maximum temperature and precipitation data to characterize heat waves, cold waves, and heavy precipitation. We characterized wildfire risk on the basis of vapor pressure deficit (VPD) and 100-hour fuel moisture (FM100), which were computed by the Integrated Scenarios of the Future Northwest Environment project (climate.northwestknowledge.net/IntegratedScenarios/) with the MACA climate variables according to the equations in the National Fire Danger Rating System (Bradshaw *et al.*, 1984). FM100 projections are only available for 18 GCMs because two models (CCSM4 and Nor-ESM1-M) do not include relative humidity at a daily time step. Calculation of FM100 requires daily relative humidity data.

Hydrological Simulations and Variables

The Integrated Scenarios project used MACA downscaled climate data as the inputs to their simulations of hydrology, which they ran with the Variable Infiltration Capacity (VIC) hydrological model (VIC version 4.1.2.l; Liang *et al.*, 1994 and updates). VIC was applied to ten GCMs and run on a 1/16° x 1/16° (6 km) grid (Table A1). We used the hydrological simulations of snow water equivalent (SWE), runoff, and soil moisture to project drought. The Integrated Scenarios project bias-corrected hydrology variables (excepting SWE) for

each month with quantile mapping. The project estimated daily streamflow by routing daily runoff from VIC grid cells to selected locations along the stream network. Where records of naturalized flow were available, the daily streamflow estimates were bias-corrected for each month with quantile mapping. As a result, their statistical distributions matched those of the naturalized streamflows.

The Columbia River Climate Change (CRCC) project (www.hydro.washington.edu/CRCC/) also generates future streamflow projections for the Columbia River Basin (RMJOC, 2018; Chegwidden *et al.*, 2019). These simulations span the years 1950–2099 and were generated from 160 distinct modeling configurations. The 160 configurations are the product of four hydrological model variants (hereafter *models*) driven with inputs derived from ten GCMs forced with the RCP 4.5 and 8.5 emissions scenarios. Daily temperature and precipitation from the GCM simulations were downscaled with two methods. Eight of the ten GCMs included in the CRCC and Integrated Scenarios projects were the same (Table A1). The CRCC project statistically downscaled GCM outputs to 1/16° (6 km) spatial resolution with two methods, MACA (Abatzoglou and Brown, 2012) and bias correction spatial disaggregation (Wood *et al.*, 2004). Three of the four hydrological models used in the CRCC project are implementations of VIC (Liang *et al.*, 1994), VIC-P1, VIC-P2, and VIC-P3, that vary with respect to calibration method. The fourth hydrological model is a gridded implementation of the Precipitation-Runoff Modeling System (PRMS-P1) (Leavesley *et al.*, 1983), which was calibrated in a manner similar to VIC-P1. All hydrological models simulated variables at 1/16° (6 km), routed gridded daily runoff to selected locations along the stream network, and bias-corrected simulated streamflow against estimated historical naturalized flows.

We used streamflow data from either the Integrated Scenarios project or the CRCC project to characterize changes in the timing of seasonal streamflow, which affects the likelihood of drought and flooding, and changes in extreme flood magnitudes.

Air Quality Data

Our projections of air quality are based on smoke wave data from Liu et al. (2016), which are available at khanotations.github.io/smoke-map/. We used two variables, "Total # of SW days in 6 yrs" and "Average SW Intensity". The former is the number of days within each time period on which the concentration of fine particulate matter ($PM_{2.5}$), averaged within the county, exceeded the 98th quantile of the distribution of daily, wildfire-specific $PM_{2.5}$ values from 2004 through 2009 (smoke wave days). The latter is the average concentration of $PM_{2.5}$ across smoke wave days within each time period. Liu et al. (2016) used 15 GCMs from the third phase of the Coupled Model Intercomparison Project under a moderate emissions scenario (SRES-A1B) as inputs to a fire prediction model and the GEOS-Chem three-dimensional global chemical transport model. The available data include only the multiple-model mean value (not the range), which should be interpreted as the direction of projected change rather than the actual expected value.

Literature Cited

Abatzoglou JT, Battisti DS, Williams AP, Hansen WD, Harvey BJ, Kolden CA. 2021a. Projected increases in western US forest fire despite growing fuel constraints. *Communications Earth & Environment*, 2(1): 1–8. https://doi.org/10.1038/s43247-021-00299-0.

Abatzoglou JT, Brown TJ. 2012. A comparison of statistical downscaling methods suited for wildfire applications. *International Journal of Climatology*, 32: 772–780. https://doi.org/10.1002/joc.2312.

Abatzoglou JT, Rupp DE, O'Neill LW, Sadegh M. 2021b. Compound extremes drive the western Oregon wildfires of September 2020. *Geophysical Research Letters*, 48(8): e2021GL092520. https://doi.org/10.1029/2021GL092520.

Abatzoglou JT, Williams AP. 2016. Impact of anthropogenic climate change on wildfire across western US forests. *Proceedings of the National Academy of Sciences*, 113: 11770–11775. https://doi.org/10.1073/pnas.1607171113.

Alizadeh MR, Adamowski J, Nikoo MR, AghaKouchak A, Dennison P, Sadegh M. 2020. A century of observations reveals increasing likelihood of continental-scale compound dry-hot extremes. *Science Advances*, 6(39): eaaz4571. https://doi.org/10.1126/sciadv.aaz4571.

Allen I, Chhin S, Zhang J. 2019. Fire and forest management in montane forests of the northwestern states and California, USA. *Fire*, 2(2): 17. https://doi.org/10.3390/fire2020017.

American Lung Association. 2022. *State of the air*. https://www.lung.org/research/sota. Accessed 28 March 2023.

Anderegg WRL, Abatzoglou JT, Anderegg LDL, Bielory L, Kinney PL, Ziska L. 2021. Anthropogenic climate change is worsening North American pollen seasons. *Proceedings of the National Academy of Sciences*, 118(7): e2013284118. https://doi.org/10.1073/pnas.2013284118.

Anderson RC, Anderson MR, Bauer JT, Loebach C, Mullarkey A, Engelhardt M. 2021. Response of the invasive *Alliaria petiolata* to extreme temperatures and drought. *Ecosphere*, 12(5): e03510. https://doi.org/10.1002/ecs2.3510.

Anfodillo T, Olson ME. 2021. Tree mortality: testing the link between drought, embolism vulnerability, and xylem conduit diameter remains a priority. *Frontiers in Forests and Global Change*, 4: 704670. https://doi.org/10.3389/ffgc.2021.704670.

ATSDR. 2022. *CDC/ATSDR Social Vulnerability Index*. Centers for Disease Control and Prevention (CDC), Agency for Toxic Substance and Disease Registry (ATSDR).

https://www.atsdr.cdc.gov/placeandhealth/svi/index.html. Accessed 8 March 2023.

Bai P, Liu X, Zhang Y, Liu C. 2018. Incorporating vegetation dynamics noticeably improved performance of hydrological model under vegetation greening. *Science of the Total Environment*, 643: 610–622. https://doi.org/10.1016/j.scitotenv.2018.06.233.

Baker JP, Hulse DW, Gregory SV, White D, Van Sickle J, Berger PA, Dole D, Schumaker NH. 2004. Alternative futures for the Willamette River Basin, Oregon. *Ecological Applications*, 14: 313–324. https://doi.org/10.1890/02-5011.

Balch JK, Abatzoglou JT, Joseph MB, Koontz MJ, Mahood AL, McGlinchy J, Cattau ME, Williams AP. 2022. Warming weakens the night-time barrier to global fire. *Nature*, 602: 442–448. https://doi.org/10.1038/s41586-021-04325-1.

Balch JK, Bradley BA, Abatzoglou JT, Nagy RC, Fusco EJ, Mahood AL. 2017. Human-started wildfires expand the fire niche across the United States. *Proceedings of the National Academy of Sciences*, 114: 2946–2951. https://doi.org/10.1073/pnas.1617394114.

Balch JK, Bradley BA, D'Antonio CM, Gómez-Dans J. 2013. Introduced annual grass increases regional fire activity across the arid western USA (1980-2009). *Global Change Biology*, 19: 173–183. https://doi.org/10.1111/gcb.12046.

Baxendale VJ, Tessier JT. 2015. Duration of freezing necessary to damage the leaves of *Fallopia japonica* (Houtt.) Ronse Decraene. *Plant Species Biology*, 30: 279–284. https://doi.org/10.1111/1442-1984.12068.

BCHD. 2017. *Benton County community health assessment 2017–2021*. Benton County Health Department (BCHD): Corvallis, Oregon. https://www.co.benton.or.us/sites/default/files/fileattachments/health_departme nt/page/201/benton_cha_2017_final_11_7_2017.pdf.

Berghuijs WR, Woods RA, Hutton CJ, Sivapalan M. 2016. Dominant flood generating mechanisms across the United States. *Geophysical Research Letters*, 43: 4382–4390. https://doi.org/10.1002/2016GL068070.

Bernert JA, Eilers JM, Eilers BJ, Blok E, Daggett SG, Bierly KF. 1999. Recent wetlands trends (1981/82–1994) in the Willamette Valley, Oregon, USA. *Wetlands*, 19: 545–559. https://doi.org/10.1007/BF03161692.

Blossey B, Nuzzo V, Dávalos A. 2017. Climate and rapid local adaptation as drivers of germination and seed bank dynamics of *Alliaria petiolata* (garlic mustard) in North America. *Journal of Ecology*, 105: 1485–1495. https://doi.org/10.1111/1365-2745.12854.

Boughton DA. 1999. Empirical evidence for complex source–sink dynamics with alternative states in a butterfly metapopulation. *Ecology*, 80: 2727–2739. https://doi.org/10.1890/0012-9658(1999)080[2727:EEFCSS]2.0.CO;2.

Bowman DMJS, Kolden CA, Abatzoglou JT, Johnston FH, van der Werf GR, Flannigan M. 2020. Vegetation fires in the Anthropocene. *Nature Reviews Earth and Environment*, 1: 500–515. https://doi.org/10.1038/s43017-020-0085-3.

Bradley B, Curtis C, Chambers J. 2016. Bromus response to climate and projected changes with climate change. In: Germino MJ, Chambers JC and Brown CS (eds) *Exotic brome-grasses in arid and semiarid ecosystems of the western US.* Springer: Zurich, 257–274. https://doi.org/10.1007/978-3-319-24930-8_9.

Bradshaw LS, Deeming JE, Burgan RE, Cohen JD. 1984. *The 1978 National Fire-Danger Rating System: technical documentation*. General Technical Report INT-169. U.S. Department of Agriculture, Forest Service, Intermountain Forest and Range Experiment Station: Ogden, Utah. https://doi.org/10.2737/INT-GTR-169.

Brewer MC, Mass CF. 2016. Projected changes in heat extremes and associated synoptic- and mesoscale conditions over the Northwest United States. *Journal of Climate*, 29: 6383–6400. https://doi.org/10.1175/JCLI-D-15-0641.1.

Brown EK, Wang J, Feng Y. 2021. US wildfire potential: a historical view and future projection using high-resolution climate data. *Environmental Research Letters*, 16(3): 034060. https://doi.org/10.1088/1748-9326/aba868.

Buchholz RR, Park M, Worden HM, Tang W, Edwards DP, Gaubert B, Deeter MN, Sullivan T, Ru M, Chin M, Levy RC, Zheng B, Magzamen S. 2022. New seasonal pattern of pollution emerges from changing North American wildfires. *Nature Communications*, 13(1): 2043. https://doi.org/10.1038/s41467-022-29623-8.

Cascio WE. 2018. Wildland fire smoke and human health. *Science of the Total Environment*, 624: 586–595. https://doi.org/10.1016/j.scitotenv.2017.12.086.

CDC. n.d. *Estimating the number of pregnant women in a geographic area*. Centers for Disease Control and Prevention (CDC). https://www.cdc.gov/reproductivehealth/emergency/pdfs/pregnacyestimatobrochure508.pdf.

Chambers JC, Maestas JD, Pyke DA, Boyd CS, Pellant M, Wuenschel A. 2017. Using resilience and resistance concepts to manage persistent threats to sagebrush ecosystems and Greater Sage-Grouse. *Rangeland Ecology & Management*, 70: 149–164. https://doi.org/10.1016/j.rama.2016.08.005.

Chambers JC, Roundy BA, Blank RR, Meyer SE, Whittaker A. 2007. What makes Great Basin sagebrush ecosystems invasible by *Bromus tectorum*? *Ecological Monographs*, 77: 117–145. https://www.jstor.org/stable/27646075.

Chang H, Loikith P, Messer L. 2021. The June 2021 extreme heat event in Portland, OR, USA: its impacts on ecosystems and human health and potential adaptation strategies. *Journal of Extreme Events*, 08(03): 2175001. https://doi.org/10.1142/S2345737621750014.

Chegwidden OS, Nijssen B, Rupp DE, Arnold JR, Clark MP, Hamman JJ, Kao S-C, Mao Y, Mizukami N, Mote PW, Pan M, Pytlak E, Xiao M. 2019. How do modeling decisions affect the spread among hydrologic climate change projections? Exploring a large ensemble of simulations across a diversity of hydroclimates. *Earth's Future*, 7: 623–637. https://doi.org/10.1029/2018EF001047.

Chegwidden OS, Rupp DE, Nijssen B. 2020. Climate change alters flood magnitudes and mechanisms in climatically-diverse headwaters across the northwestern United States. *Environmental Research Letters*, 15(9): 094048. https://doi.org/10.1088/1748-9326/ab986f.

Chen J, Burns E, Fleming M, Patterson E. 2020. Impact of climate change on population dynamics and herbicide resistance in kochia (*Bassia scoparia* (L.) A. J. Scott). *Agronomy*, 10(11): 1700. https://doi.org/10.3390/agronomy10111700.

Chen L. 2020. Impacts of climate change on wind resources over North America based on NA-CORDEX. *Renewable Energy*, 153: 1428–1438. https://doi.org/10.1016/j.renene.2020.02.090.

Chiodi AM, Potter BE, Larkin NK. 2021. Multi-decadal change in western US nighttime vapor pressure deficit. *Geophysical Research Letters*, 48(15): e2021GL092830. https://doi.org/10.1029/2021GL092830.

Christy JA, Alverson ER. 2011. Historical vegetation of the Willamette Valley, Oregon, circa 1850. *Northwest Science*, 85: 93–107. https://doi.org/10.3955/046.085.0202.

Clements DR, DiTommaso A. 2012. Predicting weed invasion in Canada under climate change: evaluating evolutionary potential. *Canadian Journal of Plant Science*, 92: 1013–1020. https://doi.org/10.4141/cjps2011-280.

Colautti RI, Ågren J, Anderson JT. 2017. Phenological shifts of native and invasive species under climate change: insights from the Boechera–Lythrum model. *Philosophical Transactions of the Royal Society B: Biological Sciences*, 372(1712): 20160032. https://doi.org/10.1098/rstb.2016.0032.

Colautti RI, Barrett SCH. 2013. Rapid adaptation to climate facilitates range expansion of an invasive plant. *Science*, 342: 364–366. https://doi.org/10.1126/science.1242121.

Colautti RI, Eckert CG, Barrett SCH. 2010. Evolutionary constraints on adaptive evolution during range expansion in an invasive plant. *Proceedings of the Royal Society B: Biological Sciences*, 277: 1799–1806. https://doi.org/10.1098/rspb.2009.2231.

Compagnoni A, Adler PB. 2014. Warming, competition, and *Bromus tectorum* population growth across an elevation gradient. *Ecosphere*, 5(9): art121. https://doi.org/10.1890/ES14-00047.1.

Conlon KC, Rajkovich NB, White-Newsome JL, Larsen L, O'Neill MS. 2011. Preventing cold-related morbidity and mortality in a changing climate. *Maturitas*, 69: 197–202. https://doi.org/10.1016/j.maturitas.2011.04.004.

Coop JD, Parks SA, Stevens-Rumann CS, Ritter SM, Hoffman CM. 2022. Extreme fire spread events and area burned under recent and future climate in the western USA. *Global Ecology and Biogeography*, 31: 1949–1959. https://doi.org/10.1111/geb.13496.

Daggett S, Boulé M, Bernert JA, Eilers JM, Blok E, Peters D, Morlan JC. 1998. *Wetland and land use change in the Willamette Valley, Oregon: 1982 to 1994.* Oregon Division of State Lands: Salem, Oregon. https://www.fws.gov/wetlands/Documents/Wetland-and-Land-Use-Change-in-the-Willamette-Valley-Oregon-1982-to-1994.pdf.

Dalton M, Chang H, Hatchett B, Loikith PC, Mote PW, Queen LE, Rupp DE. 2021. State of climate science. In: Dalton M and Fleishman E (eds) *Fifth Oregon Climate Assessment*. Oregon Climate Change Research Institute, Oregon State University: Corvallis, Oregon, 11–30. https://doi.org/10.5399/osu/1160.

Dalton M, Fleishman E (eds). 2021. *Fifth Oregon Climate Assessment*. Oregon Climate Change Research Institute, Oregon State University: Corvallis, Oregon. https://doi.org/10.5399/osu/1160.

Dalton M, Loikith PC. 2021. Extreme heat. In: Dalton M and Fleishman E (eds) *Fifth Oregon Climate Assessment*. Oregon Climate Change Research Institute, Oregon State University: Corvallis, Oregon, 31–35. https://doi.org/10.5399/osu/1160.

Dalton MM, Bachelet D. 2023. Understanding the most current climate projections. In: Fleishman E (ed) *Sixth Oregon Climate Assessment*. Oregon Climate Change Research Institute, Oregon State University: Corvallis, Oregon, 21–39. https://doi.org/10.5399/osu/1161.

Dalton MM, Dello KD, Hawkins L, Mote PW, Rupp DE. 2017. *The Third Oregon Climate Assessment Report*. Oregon Climate Change Research Institute, Oregon State University: Corvallis, Oregon. https://doi.org/10.5399/osu/1158.

D'Amato G, Chong-Neto HJ, Monge Ortega OP, Vitale C, Ansotegui I, Rosario N, Haahtela T, Galan C, Pawankar R, Murrieta-Aguttes M, Cecchi L, Bergmann C, Ridolo E, Ramon G, Gonzalez Diaz S, D'Amato M, Annesi-Maesano I. 2020. The effects of climate change on respiratory allergy and asthma induced by pollen and mold allergens. *Allergy*, 75: 2219–2228. https://doi.org/10.1111/all.14476.

De Frenne P, Kolb A, Verheyen K, Brunet J, Chabrerie O, Decocq G, Diekmann M, Eriksson O, Heinken T, Hermy M, Jõgar Ü, Stanton S, Quataert P, Zindel R, Zobel M, Graae BJ.

2009. Unravelling the effects of temperature, latitude and local environment on the reproduction of forest herbs. *Global Ecology and Biogeography*, 18: 641–651. https://doi.org/10.1111/j.1466-8238.2009.00487.x.

Dech JP, Nosko P. 2004. Rapid growth and early flowering in an invasive plant, purple loosestrife (*Lythrum salicaria* L.) during an El Niño spring. *International Journal of Biometeorology*, 49: 26–31. https://doi.org/10.1007/s00484-004-0210-x.

Dennison PE, Brewer SC, Arnold JD, Moritz MA. 2014. Large wildfire trends in the western United States, 1984–2011. *Geophysical Research Letters*, 41: 2014GL059576. https://doi.org/10.1002/2014GL059576.

Descamps C, Boubnan N, Jacquemart A-L, Quinet M. 2021. Growing and flowering in a changing climate: effects of higher temperatures and drought stress on the bee-pollinated species *Impatiens glandulifera* Royle. *Plants*, 10(5): 988. https://doi.org/10.3390/plants10050988.

Dlugosch KM, Cang FA, Barker BS, Andonian K, Swope SM, Rieseberg LH. 2015. Evolution of invasiveness through increased resource use in a vacant niche. *Nature Plants*, 1: 15066. https://doi.org/10.1038/nplants.2015.66.

Doblas-Reyes FJ, Sorensson AA, Almazroui M, Dosio A, Gutowski WJ, Haarsma R, Hamdi R, Hewitson B, Kwon W-T, Lamptey BL, Maraun D, Stephenson T, Takayabu I, Terray L, Turner A, Zuo Z. 2021. Linking global to regional climate change. In: Masson-Delmotte V, Zhai P, Pirani, Connors SL, Péan C, Berger, Caud N, Chen Y, Goldfarb L, Gomis MI, Huang M, Leitzell K, Lonnoy E, Matthews JBR, Maycock TK, Waterfield T, Yelekçi R, Yu R and Zhou B (eds) *Climate change 2021: the physical science basis. Contribution of Working Group I to the Sixth Assessment Report of the Intergovernmental Panel on Climate Change*. Cambridge University Press: Cambridge and New York, 1363–1512. https://dx.doi.org/10.1017/9781009157896.012.

Dodson EK, Root HT. 2015. Native and exotic plant cover vary inversely along a climate gradient 11 years following stand-replacing wildfire in a dry coniferous forest, Oregon, USA. *Global Change Biology*, 21: 666–675. https://doi.org/10.1111/gcb.12775.

Downing WM, Dunn CJ, Thompson MP, Caggiano MD, Short KC. 2022. Human ignitions on private lands drive USFS cross-boundary wildfire transmission and community impacts in the western US. *Scientific Reports*, 12(1): 2624. https://doi.org/10.1038/s41598-022-06002-3.

Drake SA, Rupp DE, Thomas CK, Oldroyd HJ, Schulze M, Jones JA. 2022. Increasing daytime stability enhances downslope moisture transport in the subcanopy of an even-aged conifer forest in western Oregon, USA. *Journal of Geophysical Research: Atmospheres*, 127(9): e2021JD036042. https://doi.org/10.1029/2021JD036042.

Dukes JS, Chiariello NR, Loarie SR, Field CB. 2011. Strong response of an invasive plant species (*Centaurea solstitialis* L.) to global environmental changes. *Ecological Applications*, 21: 1887–1894. https://doi.org/10.1890/11-0111.1.

Dwire KA, Mellmann-Brown S, Gurrieri JT. 2018. Potential effects of climate change on riparian areas, wetlands, and groundwater-dependent ecosystems in the Blue Mountains, Oregon, USA. *Climate Services*, 10: 44–52. https://doi.org/10.1016/j.cliser.2017.10.002.

EIA. 2022. *Residential Energy Consumption Survey (RECS), 2020 RECS Survey Data*. U.S. Energy Information Administration (EIA). https://www.eia.gov/consumption/residential/data/2020/index.php?view=state. Accessed 8 March 2023.

Fann N, Brennan T, Dolwick P, Gamble JL, Ilacqua V, Kolb L, Nolte CG, Spero TL, Ziska L. 2016. Air quality impacts. In: Crimmins A, Balbus J, Gamble JL, Beard CB, Bell JE, Dodgen D, Eisen RJ, Fann N, Hawkins MD, Herring SC, Jantarasami L, Mills DM, Saha S, Sarofim MC, Trtanj J and Ziska L (eds) *The Impacts of Climate Change on Human Health in the United States: A Scientific Assessment*. US Global Change Research Program: Washington, DC, 69–98. http://dx.doi.org/10.7930/J0GQ6VP6.

Fickas KC, Cohen WB, Yang Z. 2016. Landsat-based monitoring of annual wetland change in the Willamette Valley of Oregon, USA from 1972 to 2012. *Wetlands Ecology and Management*, 24: 73–92. https://doi.org/10.1007/s11273-015-9452-0.

Ficklin DL, Novick KA. 2017. Historic and projected changes in vapor pressure deficit suggest a continental-scale drying of the United States atmosphere. *Journal of Geophysical Research: Atmospheres*, 122: 2061–2079. https://doi.org/10.1002/2016JD025855.

First Street Foundation. 2023. *Flood risk overview: Benton County, Oregon*. https://riskfactor.com/county/benton-county-oregon/41003_fsid/flood. Accessed 28 March 2023.

Flanagan BE, Gregory EW, Hallisey EJ, Heitgerd JL, Lewis B. 2011. A social vulnerability index for disaster management. *Journal of Homeland Security and Emergency Management*, 8(1): 0000102202154773551792. https://doi.org/10.2202/1547-7355.1792.

Fleishman E (ed). 2023. *Sixth Oregon Climate Assessment*. Oregon Climate Change Research Institute, Oregon State University: Corvallis, Oregon. https://doi.org/10.5399/osu/1161.

Fleishman E, Murphy DD. 2012. Minimizing uncertainty in interpreting responses of butterflies to climate change. In: Beever E and Belant J (eds) *Ecological consequences of climate change: mechanisms, conservation, and management*. Taylor & Francis:

London, 55–66. https://www.routledge.com/Ecological-Consequences-of-Climate-Change-Mechanisms-Conservation-and/Beever-Belant/p/book/9781138114692.

Footitt S, Huang Z, Ölcer-Footitt H, Clay H, Finch-Savage WE. 2018. The impact of global warming on germination and seedling emergence in *Alliaria petiolata*, a woodland species with dormancy loss dependent on low temperature. *Plant Biology*, 20: 682–690. https://doi.org/10.1111/plb.12720.

Forster PM, Storelvmo T, Armour KC, Collins WD, Dufresne J-L, Frame D, Lunt DJ, Mauritsen T, Palmer MD, Watanabe M, Wild M, Zhang H. 2021. The Earth's energy budget, climate feedbacks, and climate sensitivity. In: Masson-Delmotte V, Zhai P, Pirani, Connors SL, Péan C, Berger, Caud N, Chen Y, Goldfarb L, Gomis MI, Huang M, Leitzell K, Lonnoy E, Matthews JBR, Maycock TK, Waterfield T, Yelekçi R, Yu R and Zhou B (eds) *Climate change 2021: the physical science basis. Contribution of Working Group I to the Sixth Assessment Report of the Intergovernmental Panel on Climate Change.* Cambridge University Press: Cambridge and New York, 923–1054. https://dx.doi.org/10.1017/9781009157896.009.

Fox N, Jönsson AM. 2019. Climate effects on the onset of flowering in the United Kingdom. *Environmental Sciences Europe*, 31: 89. https://doi.org/10.1186/s12302-019-0271-4.

García RA, Pauchard A, Escudero A. 2014. French broom (*Teline monspessulana*) invasion in south-central Chile depends on factors operating at different spatial scales. *Biological Invasions*, 16: 113–124. https://doi.org/10.1007/s10530-013-0507-y.

Garton EO, Connelly, J.W., Horne JS, Hagen CA, Moser A, Schroeder MA. 2011. Greater Sage-Grouse population dynamics and probability of persistence. In: Knick ST and Connelly, J.W. (eds) *Greater Sage-Grouse: ecology and conservation of a landscape species and its habitats. Studies in Avian Biology 38.* University of California Press: Berkeley, CA, 292–381. https://doi.org/10.1525/california/9780520267114.003.0016.

Ge Z-M, Kellomäki S, Zhou X, Peltola H, Wang K-Y, Martikainen PJ. 2012. Seasonal physiological responses and biomass growth in a bioenergy crop (*Phalaris arundinacea* L.) under elevated temperature and CO_2, subjected to different water regimes in boreal conditions. *BioEnergy Research*, 5: 637–648. https://doi.org/10.1007/s12155-011-9170-2.

Gergel DR, Nijssen B, Abatzoglou JT, Lettenmaier DP, Stumbaugh MR. 2017. Effects of climate change on snowpack and fire potential in the western USA. *Climatic Change*, 141: 287–299. https://doi.org/10.1007/s10584-017-1899-y.

Goodman AC, Segura C, Jones JA, Swanson FJ. 2023. Seventy years of watershed response to floods and changing forestry practices in western Oregon, USA. *Earth Surface Processes and Landforms*, early view. https://doi.org/10.1002/esp.5537.

Grantz DA, Shrestha A. 2006. Tropospheric ozone and interspecific competition between yellow nutsedge and pima cotton. *Crop Science*, 46: 1879–1889. https://doi.org/10.2135/cropsci2005.06.0167.

Gray AN. 2005. Eight nonnative plants in western Oregon forests: associations with environment and management. *Environmental Monitoring and Assessment*, 100(1): 109–127. https://doi.org/10.1007/s10661-005-7060-9.

Greaver TL, Clark CM, Compton JE, Vallano D, Talhelm AF, Weaver CP, Band LE, Baron JS, Davidson EA, Tague CL, Felker-Quinn E, Lynch JA, Herrick JD, Liu L, Goodale CL, Novak KJ, Haeuber RA. 2016. Key ecological responses to nitrogen are altered by climate change. *Nature Climate Change*, 6: 836–843. https://doi.org/10.1038/nclimate3088.

Green A. 2020. *Air quality in Portland and parts of Oregon is worse than in Beijing or Mexico City, due to wildfire smoke.* The Oregonian. https://www.oregonlive.com/news/2020/09/air-quality-in-portland-is-worse-than-in-beijing-mumbai-or-mexico-city-due-to-wildfire-smoke.html. Accessed 15 March 2023.

Gynn EG, Richards AJ. 1985. *Acaena novae-zelandiae* T. Kirk. *Journal of Ecology*, 73: 1055–1063. https://doi.org/10.2307/2260167.

Halofsky JE, Peterson DL, Ho JJ. 2019. *Climate change vulnerability and adaptation in south-central Oregon*. General Technical Report PNW-GTR-974. U.S. Department of Agriculture, Forest Service, Pacific Northwest Research Station: Portland, OR. https://doi.org/10.2737/PNW-GTR-974.

Hausfather Z, Marvel K, Schmidt GA, Nielsen-Gammon JW, Zelinka M. 2022. Climate simulations: recognize the 'hot model' problem. *Nature*, 605: 26–29. https://doi.org/10.1038/d41586-022-01192-2.

Hawkins LR, Abatzoglou JT, Li S, Rupp DE. 2022. Anthropogenic influence on recent severe autumn fire weather in the West Coast of the United States. *Geophysical Research Letters*, 49(4): e2021GL095496. https://doi.org/10.1029/2021GL095496.

Hayhoe K, Edmonds J, Kopp RE, LeGrande AN, Sanderson BE, Wehner MF, Wuebbles DJ. 2017. Climate models, scenarios, and projections. In: Wuebbles DJ, Fahey DW, Hibbard KA, Dokken DJ, Stewart BC and Maycock TK (eds) *Climate Science Special Report: Fourth National Climate Assessment Volume I*. US Global Change Research Program: Washington, DC, USA, 133–160. https://science2017.globalchange.gov/chapter/4/.

Heeter KJ, Harley GL, Abatzoglou JT, Anchukaitis KJ, Cook ER, Coulthard BL, Dye LA, Homfeld IK. 2023. Unprecedented 21st century heat across the Pacific Northwest of North America. *npj Climate and Atmospheric Science*, 6(1): 1–9. https://doi.org/10.1038/s41612-023-00340-3.

Heidari H, Arabi M, Warziniack T. 2021. Effects of climate change on natural-caused fire activity in western U.S. National Forests. *Atmosphere*, 12(8): 981. https://doi.org/10.3390/atmos12080981.

Henderson SB. 2020. The COVID-19 pandemic and wildfire smoke: potentially concomitant disasters. *American Journal of Public Health*, 110: 1140–1142. https://doi.org/10.2105/AJPH.2020.305744.

Higuera PE, Abatzoglou JT. 2021. Record-setting climate enabled the extraordinary 2020 fire season in the western United States. *Global Change Biology*, 27: 1–2. https://doi.org/10.1111/gcb.15388.

Ho TH, York E, Hystad P. 2021. Public health. In: Dalton M and Fleishman E (eds) *Fifth Oregon Climate Assessment*. Oregon Climate Change Research Institute, Oregon State University: Corvallis, Oregon, 137–156. https://doi.org/10.5399/osu/1160.

Hogenbirk JC, Wein RW. 1991. Fire and drought experiments in northern wetlands: a climate change analogue. *Canadian Journal of Botany*, 69: 1991–1997. https://doi.org/10.1139/b91-250.

Hogg BN, Moran PJ. 2020. Combined effects of drought stress and psyllid herbivory on the invasive weed Scotch broom, *Cytisus scoparius. Entomologia Experimentalis et Applicata*, 168: 209–220. https://doi.org/10.1111/eea.12880.

Holz A, Halofsky JE, Nanavati W, Platt L, Gleason K. 2021. Wildfire. In: Dalton M and Fleishman E (eds) *Fifth Oregon Climate Assessment*. Oregon Climate Change Research Institute, Oregon State University: Corvallis, Oregon, 47–65. https://doi.org/10.5399/osu/1160.

IHME. 2016. *US county profile: Benton County, Oregon*. Institute for Health Metrics and Evaluation (IHME): Seattle, Washington. https://www.healthdata.org/sites/default/files/files/county_profiles/US/2015/County_Report_Benton_County_Oregon.pdf.

IPCC. 2013. Summary for policymakers. In: Stocker TF, Qin D, Plattner G-K, Tignor M, Allen SK, Boschung J, Nauels A, Xia Y, Bex V and Midgley PM (eds) *Climate Change 2013: The Physical Science Basis. Contribution of Working Group I to the Fifth Assessment Report of the Intergovernmental Panel on Climate Change*. Cambridge University Press: Cambridge and New York, 3–29. https://www.ipcc.ch/site/assets/uploads/2018/02/WG1AR5_SPM_FINAL.pdf.

IPCC. 2021. Summary for policymakers. In: Masson-Delmotte V, Zhai P, Pirani, Connors SL, Péan C, Berger, Caud N, Chen Y, Goldfarb L, Gomis MI, Huang M, Leitzell K, Lonnoy E, Matthews JBR, Maycock TK, Waterfield T, Yelekçi R, Yu R and Zhou B (eds) *Climate change 2021: the physical science basis. Contribution of Working Group I to the Sixth Assessment Report of the Intergovernmental Panel on Climate Change*. Cambridge

University Press: Cambridge and New York, 3–32.
https://dx.doi.org/10.1017/9781009157896.001.

IPRE. 2021. *Impacts to Oregon's wine industry: Covid-19 and the 2020 wildfires*. University of Oregon, Institute for Policy Research and Engagement (IPRE): Eugene, Oregon. https://industry.oregonwine.org/wp-content/uploads/sites/2/2020-Vineyard-and-Winery-Report-COVID-and-Wildfire-Impacts-09-07-21.pdf.

Jeong DI, Sushama L. 2019. Projected changes to mean and extreme surface wind speeds for North America based on regional climate model simulations. *Atmosphere*, 10(9): 497. https://doi.org/10.3390/atmos10090497.

Jolly WM, Cochrane MA, Freeborn PH, Holden ZA, Brown TJ, Williamson GJ, Bowman DMJS. 2015. Climate-induced variations in global wildfire danger from 1979 to 2013. *Nature Communications*, 6: 7537. https://doi.org/10.1038/ncomms8537.

Jones MW, Abatzoglou JT, Veraverbeke S, Andela N, Lasslop G, Forkel M, Smith AJP, Burton C, Betts RA, van der Werf GR, Sitch S, Canadell JG, Santín C, Kolden C, Doerr SH, Le Quéré C. 2022. Global and regional trends and drivers of fire under climate change. *Reviews of Geophysics*, 60(3): e2020RG000726. https://doi.org/10.1029/2020RG000726.

Juang CS, Williams AP, Abatzoglou JT, Balch JK, Hurteau MD, Moritz MA. 2022. Rapid growth of large forest fires drives the exponential response of annual forest-fire area to aridity in the western United States. *Geophysical Research Letters*, 49(5): e2021GL097131. https://doi.org/10.1029/2021GL097131.

Kalashnikov DA, Schnell JL, Abatzoglou JT, Swain DL, Singh D. 2022. Increasing co-occurrence of fine particulate matter and ground-level ozone extremes in the western United States. *Science Advances*, 8(1): eabi9386. https://doi.org/10.1126/sciadv.abi9386.

Kerns BK, Tortorelli C, Day MA, Nietupski T, Barros AMG, Kim JB, Krawchuk MA. 2020. Invasive grasses: a new perfect storm for forested ecosystems? *Forest Ecology and Management*, 463: 117985. https://doi.org/10.1016/j.foreco.2020.117985.

Khatana SAM, Werner RM, Groeneveld PW. 2022. Association of extreme heat with all-cause mortality in the contiguous US, 2008-2017. *JAMA Network Open*, 5(5): e2212957. https://doi.org/10.1001/jamanetworkopen.2022.12957.

Knapp PA. 1998. Spatio-temporal patterns of large grassland fires in the Intermountain West, U.S.A. *Global Ecology and Biogeography Letters*, 7: 259–272. https://doi.org/10.2307/2997600.

Konrad CP, Dettinger MD. 2017. Flood runoff in relation to water vapor transport by atmospheric rivers over the western United States, 1949–2015. *Geophysical Research Letters*, 44: 11,456-11,462. https://doi.org/10.1002/2017GL075399.

Koo E, Pagni PJ, Weise DR, Woycheese JP. 2010. Firebrands and spotting ignition in large-scale fires. *International Journal of Wildland Fire*, 19: 818–843. https://doi.org/10.1071/WF07119.

Kossin JP, Hall T, Knutson T, Kunkel KE, Trapp RJ, Waliser DE, Wehner MF. 2017. Extreme storms. In: Wuebbles DJ, Fahey DW, Hibbard KA, Dokken DJ, Stewart BC and Maycock TK (eds) *Climate Science Special Report: Fourth National Climate Assessment Volume I*. US Global Change Research Program: Washington, DC, 257–276. https://science2017.globalchange.gov/chapter/9/.

Larson CD, Lehnhoff EA, Rew LJ. 2017. A warmer and drier climate in the northern sagebrush biome does not promote cheatgrass invasion or change its response to fire. *Oecologia*, 185: 763–774. https://doi.org/10.1007/s00442-017-3976-3.

Leavesley GH, Lichty RW, Troutman BM, Saindon LG. 1983. *Precipitation-runoff modeling system - user's manual*. U.S. Geological Survey, Water Resources Division: Denver, Colorado. https://doi.org/10.3133/wri834238.

Lee S-Y, Ryan ME, Hamlet AF, Palen WJ, Lawler JJ, Halabisky M. 2015. Projecting the hydrologic impacts of climate change on montane wetlands. *PLoS ONE*, 10(9): e0136385. https://doi.org/10.1371/journal.pone.0136385.

Liang X, Lettenmaier DP, Wood EF, Burges SJ. 1994. A simple hydrologically based model of land surface water and energy fluxes for general circulation models. *Journal of Geophysical Research*, 99: 14415–14428. https://doi.org/10.1029/94JD00483.

Liu JC, Mickley LJ, Sulprizio MP, Dominici F, Yue X, Ebisu K, Anderson GB, Khan RFA, Bravo MA, Bell ML. 2016. Particulate air pollution from wildfires in the western US under climate change. *Climatic Change*, 138: 655–666. https://doi.org/10.1007/s10584-016-1762-6.

Liu JC, Peng RD. 2019. The impact of wildfire smoke on compositions of fine particulate matter by ecoregion in the Western US. *Journal of Exposure Science & Environmental Epidemiology*, 29: 765–776. https://doi.org/10.1038/s41370-018-0064-7.

Luís M de, Raventós J, González-Hidalgo JC, Luís M de, Raventós J, González-Hidalgo JC. 2005. Fire and torrential rainfall: effects on seedling establishment in Mediterranean gorse shrublands. *International Journal of Wildland Fire*, 14: 413–422. https://doi.org/10.1071/WF05037.

MacDonald GM. 2010. Global warming and the Arctic: a new world beyond the reach of the Grinnellian niche? *Journal of Experimental Biology*, 213: 855–861. https://doi.org/10.1242/jeb.039511.

MacDonald GM, Bennett KD, Jackson ST, Parducci L, Smith FA, Smol JP, Willis KJ. 2008. Impacts of climate change on species, populations and communities:

palaeobiogeographical insights and frontiers. *Progress in Physical Geography: Earth and Environment*, 32: 139–172. https://doi.org/10.1177/0309133308094081.

Manzanedo RD, Ballesteros-Cánovas J, Schenk F, Stoffel M, Fischer M, Allan E. 2018. Increase in CO2 concentration could alter the response of *Hedera helix* to climate change. *Ecology and Evolution*, 8: 8598–8606. https://doi.org/10.1002/ece3.4388.

Mass C, Dotson B. 2010. Major extratropical cyclones of the northwest United States: historical review, climatology, and synoptic environment. *Monthly Weather Review*, 138: 2499–2527. https://doi.org/10.1175/2010MWR3213.1.

Mass CF, Ovens D, Conrick R, Saltenberger J. 2021. The September 2020 wildfires over the Pacific Northwest. *Weather and Forecasting*, 36: 1843–1865. https://doi.org/10.1175/WAF-D-21-0028.1.

Mass CF, Salathé EP, Steed R, Baars J. 2022. The mesoscale response to global warming over the Pacific Northwest evaluated using a regional climate model ensemble. *Journal of Climate*, 35: 2035–2053. https://doi.org/10.1175/JCLI-D-21-0061.1.

Maurer EP, Kayser G, Gabel L, Wood AW. 2018. Adjusting flood peak frequency changes to account for climate change impacts in the western United States. *Journal of Water Resources Planning and Management*, 144(3): 05017025. https://doi.org/10.1061/(ASCE)WR.1943-5452.0000903.

Meyer SE, Garvin SC, Beckstead J. 2001. Factors mediating cheatgrass invasion of intact salt desert shrubland. In: McArthur ED and Fairbanks DJ (eds) *Shrubland ecosystem genetics and biodiversity: proceedings*. US Department of Agriculture Forest Service, Rocky Mountain Research Station: Provo, Utah, 224–232. https://www.fs.usda.gov/research/treesearch/29312.

Miles-Novelo A, Anderson CA. 2019. Climate change and psychology: effects of rapid global warming on violence and aggression. *Current Climate Change Reports*, 5: 36–46. https://doi.org/10.1007/s40641-019-00121-2.

Mitchell NJ, Janzen FJ. 2010. Temperature-dependent sex determination and contemporary climate change. *Sexual Development: Genetics, Molecular Biology, Evolution, Endocrinology, Embryology, and Pathology of Sex Determination and Differentiation*, 4(1–2): 129–140. https://doi.org/10.1159/000282494.

Mote P, Brekke L, Duffy PB, Maurer E. 2011. Guidelines for constructing climate scenarios. *Eos, Transactions American Geophysical Union*, 92: 257–258. https://doi.org/10.1029/2011EO310001.

Mote PW, Abatzoglou JT, Dello KD, Hegewisch K, Rupp DE. 2019. *Fourth Oregon Climate Assessment Report*. Oregon Climate Change Research Institute, Oregon State University: Corvallis, Oregon. https://doi.org/10.5399/osu/1159.

Mote PW, Abatzoglou JT, Kunkel KE. 2013. Climate: variability and change in the past and the future. In: Dalton MM, Mote PW and Snover AK (eds) *Climate Change in the Northwest: Implications for Our Landscapes, Waters, and Communities*. Island Press: Washington, DC, 25–40. https://doi.org/10.5822/978-1-61091-512-0.

Musselman KN, Lehner F, Ikeda K, Clark MP, Prein AF, Liu C, Barlage M, Rasmussen R. 2018. Projected increases and shifts in rain-on-snow flood risk over western North America. *Nature Climate Change*, 8: 808–812. https://doi.org/10.1038/s41558-018-0236-4.

Najafi MR, Moradkhani H. 2015. Multi-model ensemble analysis of runoff extremes for climate change impact assessments. *Journal of Hydrology*, 525: 352–361. https://doi.org/10.1016/j.jhydrol.2015.03.045.

Naz BS, Kao S-C, Ashfaq M, Rastogi D, Mei R, Bowling LC. 2016. Regional hydrologic response to climate change in the conterminous United States using high-resolution hydroclimate simulations. *Global and Planetary Change*, 143: 100–117. https://doi.org/10.1016/j.gloplacha.2016.06.003.

NCHH. 2022. *Emergency preparedness and response: extreme cold*. National Center for Healthy Housing (NCHH). https://nchh.org/information-and-evidence/learn-about-healthy-housing/emergencies/extreme-cold/. Accessed 8 March 2023.

Nolte CG, Dolwick PD, Fann N, Horowitz LW, Naik V, Pinder RW, Spero TL, Winner DA, Ziska LH. 2018. Air quality. In: Reidmiller DR, Avery CW, Easterling DR, Kunkel KE, Lewis KLM, Maycock TK and Stewart BC (eds) *Impacts, Risks, and Adaptation in the United States: Fourth National Climate Assessment, Volume II*. U.S. Global Change Research Program: Washington, DC, 512–538. https://nca2018.globalchange.gov/chapter/13/.

ODFW. 2016. *Oregon Conservation Strategy*. Oregon Department of Fish and Wildlife: Salem, Oregon. https://www.dfw.state.or.us/conservationstrategy/.

OED. 2023. *Occupational employment projections for Northwest (Benton, Clatsop, Columbia, Lincoln and Tillamook Counties), 2021–2031*. Oregon Employment Department (OED), Workforce and Economic Research Division. www.qualityinfo.org/northwest-oregon.

OHA. 2019. *Estimates of the homeless population by county, Oregon, 2017*. Oregon Health Authority (OHA). https://www.oregon.gov/oha/PH/ABOUT/Documents/indicators/homeless-county.pdf.

Olson ME, Soriano D, Rosell JA, Anfodillo T, Donoghue MJ, Edwards EJ, León-Gómez C, Dawson T, Camarero Martínez JJ, Castorena M, Echeverría A, Espinosa CI, Fajardo A, Gazol A, Isnard S, Lima RS, Marcati CR, Méndez-Alonzo R. 2018. Plant height and

hydraulic vulnerability to drought and cold. *Proceedings of the National Academy of Sciences*, 115: 7551–7556. https://doi.org/10.1073/pnas.1721728115.

O'Neill LW, Hatchett B, Dalton M. 2021. Drought. In: Dalton M and Fleishman E (eds) *Fifth Oregon Climate Assessment*. Oregon Climate Change Research Institute, Oregon State University: Corvallis, Oregon, 37–45. https://doi.org/10.5399/osu/1160.

O'Neill LW, Siler N. 2023. Drought. In: Fleishman E (ed) *Sixth Oregon Climate Assessment*. Oregon Climate Change Research Institute, Oregon State University: Corvallis, Oregon, 52–59. https://doi.org/10.5399/osu/1161.

O'Neill LW, Siler N, Loikith PC, Arends A. 2023. Extreme temperatures. In: Fleishman E (ed) *Sixth Oregon Climate Assessment*. Oregon Climate Change Research Institute, Oregon State University: Corvallis, Oregon, 40–51. https://doi.org/10.5399/osu/1161.

Oregon DEQ. 2016. *2015 Oregon Air Quality Data Summaries*. Oregon Department of Environmental Quality: Portland, Oregon. http://www.deq.state.or.us/aq/forms/2015AQDataSummaryReport.pdf.

Oregon DEQ. 2022. *Wildfire smoke trends and the air quality index*. Oregon Department of Environmental Quality: Hillsboro, Oregon. https://www.oregon.gov/deq/wildfires/Documents/WildfireSmokeTrendsReport.pdf.

Oregon Explorer. 2023. *Advanced Oregon wildfire risk explorer*. Oregon Explorer. https://tools.oregonexplorer.info/OE_HtmlViewer/index.html?viewer=wildfireplanning. Accessed 2 March 2023.

Parepa M, Fischer M, Bossdorf O. 2013. Environmental variability promotes plant invasion. *Nature Communications*, 4(1): 1604. https://doi.org/10.1038/ncomms2632.

Parker LE, Abatzoglou JT. 2016. Spatial coherence of extreme precipitation events in the northwestern United States. *International Journal of Climatology*, 36: 2451–2460. https://doi.org/10.1002/joc.4504.

Parks SA, Abatzoglou JT. 2020. Warmer and drier fire seasons contribute to increases in area burned at high severity in western US forests from 1985 to 2017. *Geophysical Research Letters*, 47(22): e2020GL089858. https://doi.org/10.1029/2020GL089858.

Paudel B, Chu T, Chen M, Sampath V, Prunicki M, Nadeau KC. 2021. Increased duration of pollen and mold exposure are linked to climate change. *Scientific Reports*, 11(1): 12816. https://doi.org/10.1038/s41598-021-92178-z.

Pearson DE, Ortega YK, Maron JL. 2017. The tortoise and the hare: reducing resource availability shifts competitive balance between plant species. *Journal of Ecology*, 105: 999–1009. https://doi.org/10.1111/1365-2745.12736.

Philip SY, Kew SF, van Oldenborgh GJ, Anslow FS, Seneviratne SI, Vautard R, Coumou D, Ebi KL, Arrighi J, Singh R, van Aalst M, Pereira Marghidan C, Wehner M, Yang W, Li S, Schumacher DL, Hauser M, Bonnet R, Luu LN, Lehner F, Gillett N, Tradowsky JS, Vecchi GA, Rodell C, Stull RB, Howard R, Otto FEL. 2022. Rapid attribution analysis of the extraordinary heat wave on the Pacific coast of the US and Canada in June 2021. *Earth System Dynamics*, 13: 1689–1713. https://doi.org/10.5194/esd-13-1689-2022.

Pickering CM, Mount A, Wichmann MC, Bullock JM. 2011. Estimating human-mediated dispersal of seeds within an Australian protected area. *Biological Invasions*, 13: 1869–1880. https://doi.org/10.1007/s10530-011-0006-y.

Potter KJB, Kriticos DJ, Watt MS, Leriche A. 2009. The current and future potential distribution of *Cytisus scoparius*: a weed of pastoral systems, natural ecosystems and plantation forestry. *Weed Research*, 49: 271–282. https://doi.org/10.1111/j.1365-3180.2009.00697.x.

PRC. 2023a. *Population estimate reports, 2022 certified population estimates*. Portland State University, Population Research Center (PRC). https://www.pdx.edu/population-research/population-estimate-reports.

PRC. 2023b. *Population forecasts, current forecast summaries for all areas*. Portland State University, Population Research Center (PRC). https://www.pdx.edu/population-research/population-forecasts.

PRC. 2023c. *Population forecasts, Oregon final forecast table by age*. Portland State University, Population Research Center (PRC). https://www.pdx.edu/population-research/population-forecasts.

Pryor SC, Barthelmie RJ, Schoof JT. 2012. Past and future wind climates over the contiguous USA based on the North American Regional Climate Change Assessment Program model suite. *Journal of Geophysical Research: Atmospheres*, 117: D19119. https://doi.org/10.1029/2012JD017449.

Queen LE, Mote PW, Rupp DE, Chegwidden O, Nijssen B. 2021. Ubiquitous increases in flood magnitude in the Columbia River basin under climate change. *Hydrology and Earth System Sciences*, 25: 257–272. https://doi.org/10.5194/hess-25-257-2021.

Radeloff VC, Helmers DP, Kramer HA, Mockrin MH, Alexandre PM, Bar-Massada A, Butsic V, Hawbaker TJ, Martinuzzi S, Syphard AD, Stewart SI. 2018. Rapid growth of the US wildland-urban interface raises wildfire risk. *Proceedings of the National Academy of Sciences*, 115: 3314–3319. https://doi.org/10.1073/pnas.1718850115.

Rahe M. 2018. *Estimates of migrant and seasonal farmworkers in agriculture, 2018 update*. Oregon Health Authority. https://www.ohdc.org/uploads/1/1/2/4/11243168/05-24-18-awhft-oregon-msfw-enumeration-study_2.pdf.

Rao K, Williams AP, Diffenbaugh NS, Yebra M, Konings AG. 2022. Plant-water sensitivity regulates wildfire vulnerability. *Nature Ecology & Evolution*, 6: 332–339. https://doi.org/10.1038/s41559-021-01654-2.

Rastogi D, Lehner F, Ashfaq M. 2020. Revisiting recent U.S. heat waves in a warmer and more humid climate. *Geophysical Research Letters*, 47(9): e2019GL086736. https://doi.org/10.1029/2019GL086736.

Raymondi RR, Cuhaciyan JE, Glick P, Capalbo SM, Houston LL, Shafer SL, Grah O. 2013. Water resources: implications of changes in temperature and precipiptation. In: Dalton MM, Mote PW and Snover AK (eds) *Climate Change in the Northwest: Implications for Our Landscapes, Waters, and Communities*. Island Press: Washington, DC, 41–66. https://doi.org/10.5822/978-1-61091-512-0.

Read W. 2003. *The Willamette Valley's strongest windstorms 1950–2002*. www.climate.washington.edu/stormking/WillametteValBigStorms.html. Accessed 27 February 2023.

Read W. 2007. *The strongest windstorms in the western Pacific Northwest 1950–2004*. www.climate.washington.edu/stormking/PNWStormRanks.html. Accessed 27 February 2023.

Redmond KT. 2002. The depiction of drought: a commentary. *Bulletin of the American Meteorological Society*, 83: 1143–1148. https://doi.org/10.1175/1520-0477-83.8.1143.

Reilly MJ, McCord MG, Brandt SM, Linowksi KP, Butz RJ, Jules ES. 2020. Repeated, high-severity wildfire catalyzes invasion of non-native plant species in forests of the Klamath Mountains, northern California, USA. *Biological Invasions*, 22: 1821–1828. https://doi.org/10.1007/s10530-020-02227-3.

Reilly MJ, Zuspan A, Halofsky JS, Raymond C, McEvoy A, Dye AW, Donato DC, Kim JB, Potter BE, Walker N, Davis RJ, Dunn CJ, Bell DM, Gregory MJ, Johnston JD, Harvey BJ, Halofsky JE, Kerns BK. 2022. Cascadia burning: the historic, but not historically unprecedented, 2020 wildfires in the Pacific Northwest, USA. *Ecosphere*, 13(6): e4070. https://doi.org/10.1002/ecs2.4070.

Reisner MD, Grace JB, Pyke DA, Doescher PS. 2013. Conditions favouring *Bromus tectorum* dominance of endangered sagebrush steppe ecosystems. *Journal of Applied Ecology*, 50: 1039–1049. https://doi.org/10.1111/1365-2664.12097.

RMJOC. 2018. *Climate and hydrology datasets for RMJOC long-term planning studies, second edition: part 1 - hydroclimate projections and analyses*. River Management Joint Operating Committeehttps://www.bpa.gov/p/Generation/Hydro/Pages/Climate-670 Change-FCRPS-Hydro.aspx.

Rohlman D, Attridge S, O'Malley K, Anderson KA. 2023. Composition of wildfire smoke and health risks. In: Fleishman E (ed) *Sixth Oregon Climate Assessment*. Oregon Climate Change Research Institute, Oregon State University: Corvallis, Oregon, 192–206. https://doi.org/10.5399/osu/1161.

Rothermel RC. 1991. *Predicting behavior and size of crown fires in the northern Rocky Mountains*. Research Paper INT-438. U.S. Department of Agriculture, Forest Service, Intermountain Research Station: Ogden, Utah. https://doi.org/10.2737/INT-RP-438.

Rupp DE. 2019. *Projected climate change impacts on water demand and supply for the city of Corvallis, Oregon: report to Carollo Engineers, Inc.* Oregon Climate Change Research Institute: Corvallis, Oregon.

Rupp DE, Hawkins LR, Li S, Koszuta M, Siler N. 2022. Spatial patterns of extreme precipitation and their changes under ~ 2 °C global warming: a large-ensemble study of the western USA. *Climate Dynamics*, 59: 2363–2379. https://doi.org/10.1007/s00382-022-06214-3.

Rupp DE, Holz A. 2023. Wildfire trends and drivers. In: Fleishman E (ed) *Sixth Oregon Climate Assessment*. Oregon Climate Change Research Institute, Oregon State University: Corvallis, Oregon, 94–102. https://doi.org/10.5399/osu/1161.

Rupp DE, Schmittner A. 2023. Arctic amplification. In: Fleishman E (ed) *Sixth Oregon Climate Assessment*. Oregon Climate Change Research Institute, Oregon State University: Corvallis, Oregon, 14–17. https://doi.org/10.5399/osu/1161.

Safeeq M, Grant GE, Lewis SL, Staab B. 2015. Predicting landscape sensitivity to present and future floods in the Pacific Northwest, USA. *Hydrological Processes*, 29: 5337–5353. https://doi.org/10.1002/hyp.10553.

Salathé EP, Hamlet AF, Mass CF, Lee S-Y, Stumbaugh M, Steed R. 2014. Estimates of twenty-first-century flood risk in the Pacific Northwest based on regional climate model simulations. *Journal of Hydrometeorology*, 15: 1881–1899. https://doi.org/10.1175/JHM-D-13-0137.1.

Seager R, Hooks A, Williams AP, Cook B, Nakamura J, Henderson N. 2015. Climatology, variability, and trends in the U.S. vapor pressure deficit, an important fire-related meteorological quantity. *Journal of Applied Meteorology and Climatology*, 54: 1121–1141. https://doi.org/10.1175/JAMC-D-14-0321.1.

Sedano F, Randerson JT. 2014. Multi-scale influence of vapor pressure deficit on fire ignition and spread in boreal forest ecosystems. *Biogeosciences*, 11: 3739–3755. https://doi.org/10.5194/bg-11-3739-2014.

Seiler C, Zwiers FW. 2016. How will climate change affect explosive cyclones in the extratropics of the Northern Hemisphere? *Climate Dynamics*, 46: 3633–3644. https://doi.org/10.1007/s00382-015-2791-y.

Seneviratne SI, Zhang X, Adnan M, Badi W, Dereczynski C, Di Luca A, Ghosh S, Iskandar I, Kossin J, Lewis S, Otto F, Pinto I, Satoh M, Vicente-Serrano SM, Wehner M, Zhou B. 2021. Weather and climate extreme events in a changing climate. In: Masson-Delmotte V, Zhai P, Pirani, Connors SL, Péan C, Berger, Caud N, Chen Y, Goldfarb L, Gomis MI, Huang M, Leitzell K, Lonnoy E, Matthews JBR, Maycock TK, Waterfield T, Yelekçi R, Yu R and Zhou B (eds) *Climate change 2021: the physical science basis. Contribution of Working Group I to the Sixth Assessment Report of the Intergovernmental Panel on Climate Change*. Cambridge University Press: Cambridge and New York, 1513–1766. https://dx.doi.org/10.1017/9781009157896.013.

Sheehan T, Bachelet D, Ferschweiler K. 2015. Projected major fire and vegetation changes in the Pacific Northwest of the conterminous United States under selected CMIP5 climate futures. *Ecological Modelling*, 317: 16–29. https://doi.org/10.1016/j.ecolmodel.2015.08.023.

Short KC. 2022. *Spatial wildfire occurrence data for the United States, 1992-2020 [FPA_FOD_20221014]. 6th Edition.* Forest Service Research Data Archive: Fort Collins, Colorado. https://doi.org/10.2737/RDS-2013-0009.6.

Siirila-Woodburn ER, Rhoades AM, Hatchett BJ, Huning LS, Szinai J, Tague C, Nico PS, Feldman DR, Jones AD, Collins WD, Kaatz L. 2021. A low-to-no snow future and its impacts on water resources in the western United States. *Nature Reviews Earth & Environment*, 2: 800–819. https://doi.org/10.1038/s43017-021-00219-y.

Singer MC. 2017. Shifts in time and space interact as climate warms. *Proceedings of the National Academy of Sciences*, 114: 12848–12850. https://doi.org/10.1073/pnas.1718334114.

Skelly DK, Joseph LN, Possingham HP, Freidenburg LK, Farrugia TJ, Kinnison MT, Hendry AP. 2007. Evolutionary responses to climate change. *Conservation Biology*, 21: 1353–1355. https://doi.org/10.1111/j.1523-1739.2007.00764.x.

Stechemesser A, Levermann A, Wenz L. 2022. Temperature impacts on hate speech online: evidence from 4 billion geolocated tweets from the USA. *The Lancet Planetary Health*, 6(9): e714–e725. https://doi.org/10.1016/S2542-5196(22)00173-5.

Stevens JT, Latimer AM. 2015. Snowpack, fire, and forest disturbance: interactions affect montane invasions by non-native shrubs. *Global Change Biology*, 21: 2379–2393. https://doi.org/10.1111/gcb.12824.

Stevenson S, Coats S, Touma D, Cole J, Lehner F, Fasullo J, Otto-Bliesner B. 2022. Twenty-first century hydroclimate: a continually changing baseline, with more frequent

extremes. *Proceedings of the National Academy of Sciences*, 119(12): e2108124119. https://doi.org/10.1073/pnas.2108124119.

Still CJ, Sibley A, DePinte D, Busby PE, Harrington CA, Schulze M, Shaw DR, Woodruff D, Rupp DE, Daly C, Hammond WM, Page GFM. 2023. Causes of widespread foliar damage from the June 2021 Pacific Northwest heat dome: more heat than drought. *Tree Physiology*, 43: 203–209. https://doi.org/10.1093/treephys/tpac143.

Storey MA, Price OF, Bradstock RA, Sharples JJ. 2020. Analysis of variation in distance, number, and distribution of spotting in southeast Australian wildfires. *Fire*, 3(2): 10. https://doi.org/10.3390/fire3020010.

Stowell JD, Yang C-E, Fu JS, Scovronick NC, Strickland MJ, Liu Y. 2021. Asthma exacerbation due to climate change-induced wildfire smoke in the Western US. *Environmental Research Letters*, 17(1): 014023. https://doi.org/10.1088/1748-9326/ac4138.

Strelau M, Clements DR, Benner J, Prasad R. 2018. The Biology of Canadian Weeds: 157. *Hedera helix* L. and *Hedera hibernica* (G. Kirchn.) Bean. *Canadian Journal of Plant Science*, 98: 1005–1022. https://doi.org/10.1139/cjps-2018-0009.

Surfleet CG, Tullos D. 2013. Variability in effect of climate change on rain-on-snow peak flow events in a temperate climate. *Journal of Hydrology*, 479: 24–34. https://doi.org/10.1016/j.jhydrol.2012.11.021.

Thomas JW, Maser C, Rodiek JE. 1979. *Wildlife habitats in managed rangelands—the Great Basin of southeastern Oregon: riparian zones.* U.S. Department of Agriculture Forest Service, Pacific Northwest Research Station: Portland, Oregon. https://www.fs.usda.gov/research/treesearch/4964.

Thorne JH, Morgan BJ, Kennedy JA. 2008. Vegetation change over sixty years in the central Sierra Nevada, California, USA. *Madroño*, 55: 223–237. https://doi.org/10.3120/0024-9637-55.3.223.

Titus JH, Christy JA, VanderScaaf D, Kagan JS, Alverson ER. 1996. *Native wetland, riparian, and upland plant communities and their biota in the Willamette Valley, Oregon*. The Nature Conservancy: Portland, Oregon. https://ir.library.oregonstate.edu/concern/technical_reports/mp48sk06n.

Tohver IM, Hamlet AF, Lee S-Y. 2014. Impacts of 21st-century climate change on hydrologic extremes in the Pacific Northwest region of North America. *Journal of the American Water Resources Association*, 50: 1461–1476. https://doi.org/10.1111/jawr.12199.

Tørresen KS, Fykse H, Rafoss T, Gerowitt B. 2020. Autumn growth of three perennial weeds at high latitude benefits from climate change. *Global Change Biology*, 26: 2561–2572. https://doi.org/10.1111/gcb.14976.

Tortorelli CM, Krawchuk MA, Kerns BK. 2020. Expanding the invasion footprint: *Ventenata dubia* and relationships to wildfire, environment, and plant communities in the Blue Mountains of the inland Northwest, USA. *Applied Vegetation Science*, 23: 562–574. https://doi.org/10.1111/avsc.12511.

Touma D, Stevenson S, Swain DL, Singh D, Kalashnikov DA, Huang X. 2022. Climate change increases risk of extreme rainfall following wildfire in the western United States. *Science Advances*, 8(13): eabm0320. https://doi.org/10.1126/sciadv.abm0320.

U.S. Census Bureau. 2023. *Quick Facts, Benton County, Oregon*. U.S. Census Bureau. https://www.census.gov/quickfacts/fact/table/bentoncountyoregon/SBO010217. Accessed 8 March 2023.

Van Wagner CE. 1987. *Development and structure of the Canadian Forest Fire Weather Index System*. Forestry Technical Report 35. Canadian Forestry Service: Ottawa, Canada. https://d1ied5g1xfgpx8.cloudfront.net/pdfs/19927.pdf.

Vins H, Bell J, Saha S, Hess JJ. 2015. The mental health outcomes of drought: a systematic review and causal process diagram. *International Journal of Environmental Research and Public Health*, 12: 13251–13275. https://doi.org/10.3390/ijerph121013251.

Vose RS, Easterling DR, Kunkel KE, LeGrande AN, Wehner MF. 2017. Temperature changes in the United States. In: Wuebbles DJ, Fahey DW, Hibbard KA, Dokken DJ, Stewart BC and Maycock TK (eds) *Climate Science Special Report: Fourth National Climate Assessment, Volume 1*. U.S. Global Change Research Program: Washington, DC, 185–206. https://science2017.globalchange.gov/chapter/6/.

Walsh J, Wuebbles D, Hayhoe K, Kossin J, Kunkel K, Stephens G, Thorne P, Vose R, Wehner M, Willis J, Anderson D, Kharin V, Knutson T, Landerer F, Lenton T, Kennedy J, Somerville R. 2014. Appendix 4: frequently asked questions. In: Melillo JM, Richmond TC and Yohe GW (eds) *Climate Change Impacts in the United States: The Third National Climate Assessment*. U.S. Global Change Research Program, 790–820. http://nca2014.globalchange.gov/report/appendices/faqs.

Walsworth TE, Schindler DE, Colton MA, Webster MS, Palumbi SR, Mumby PJ, Essington TE, Pinsky ML. 2019. Management for network diversity speeds evolutionary adaptation to climate change. *Nature Climate Change*, 9: 632–636. https://doi.org/10.1038/s41558-019-0518-5.

Wang J, Stern MA, King VM, Alpers CN, Quinn NWT, Flint AL, Flint LE. 2020. PFHydro: a new watershed-scale model for post-fire runoff simulation. *Environmental Modelling & Software*, 123: 104555. https://doi.org/10.1016/j.envsoft.2019.104555.

Way DA, Stinziano JR, Berghoff H, Oren R. 2017. How well do growing season dynamics of photosynthetic capacity correlate with leaf biochemistry and climate fluctuations? *Tree Physiology*, 37: 879–888. https://doi.org/10.1093/treephys/tpx086.

Westerling AL. 2016. Increasing western US forest wildfire activity: sensitivity to changes in the timing of spring. *Philosophical Transactions of the Royal Society B*, 371(1696): 20150178. https://doi.org/10.1098/rstb.2015.0178.

Willette DAS, Tucker JK, Janzen FJ. 2005. Linking climate and physiology at the population level for a key life-history stage of turtles. *Canadian Journal of Zoology*, 83: 845–850. https://doi.org/10.1139/z05-078.

Williams AP, Abatzoglou JT. 2016. Recent advances and remaining uncertainties in resolving past and future climate effects on global fire activity. *Current Climate Change Reports*, 2: 1–14. https://doi.org/10.1007/s40641-016-0031-0.

Williams AP, Livneh B, McKinnon KA, Hansen WD, Mankin JS, Cook BI, Smerdon JE, Varuolo-Clarke AM, Bjarke NR, Juang CS, Lettenmaier DP. 2022. Growing impact of wildfire on western US water supply. *Proceedings of the National Academy of Sciences*, 119(10): e2114069119. https://doi.org/10.1073/pnas.2114069119.

Williams AP, Seager R, Berkelhammer M, Macalady AK, Crimmins MA, Swetnam TW, Trugman AT, Buenning N, Hryniw N, McDowell NG, Noone D, Mora CI, Rahn T. 2014. Causes and implications of extreme atmospheric moisture demand during the record-breaking 2011 wildfire season in the southwestern United States. *Journal of Applied Meteorology and Climatology*, 53: 2671–2684. https://doi.org/10.1175/JAMC-D-14-0053.1.

Willis KJ, MacDonald GM. 2011. Long-term ecological records and their relevance to climate change predictions for a warmer world. *Annual Review of Ecology, Evolution, and Systematics*, 42: 267–287. https://doi.org/10.1146/annurev-ecolsys-102209-144704.

Willis SG, Hulme PE. 2002. Does temperature limit the invasion of *Impatiens glandulifera* and *Heracleum mantegazzianum* in the UK? *Functional Ecology*, 16: 530–539. https://doi.org/10.1046/j.1365-2435.2002.00653.x.

Wilmot TY, Hallar AG, Lin JC, Mallia DV. 2021. Expanding number of Western US urban centers face declining summertime air quality due to enhanced wildland fire activity. *Environmental Research Letters*, 16(5): 054036. https://doi.org/10.1088/1748-9326/abf966.

Wilmot TY, Mallia DV, Hallar AG, Lin JC. 2022. Wildfire plumes in the Western US are reaching greater heights and injecting more aerosols aloft as wildfire activity intensifies. *Scientific Reports*, 12(1): 12400. https://doi.org/10.1038/s41598-022-16607-3.

Winde J, Sønderkær M, Nielsen KL, Pagter M. 2020. Is range expansion of introduced Scotch broom (*Cytisus scoparius*) in Denmark limited by winter cold tolerance? *Plant Ecology*, 221: 709–723. https://doi.org/10.1007/s11258-020-01044-x.

Winter M, Fiedler W, Hochachka WM, Koehncke A, Meiri S, De la Riva I. 2016. Patterns and biases in climate change research on amphibians and reptiles: a systematic review. *Royal Society Open Science*, 3(9): 160158. https://doi.org/10.1098/rsos.160158.

Wood AW, Leung LR, Sridhar V, Lettenmaier DP. 2004. Hydrologic implications of dynamical and statistical approaches to downscaling climate model outputs. *Climatic Change*, 62: 189–216. https://doi.org/10.1023/B:CLIM.0000013685.99609.9e.

Xie Y, Lin M, Decharme B, Delire C, Horowitz LW, Lawrence DM, Li F, Séférian R. 2022. Tripling of western US particulate pollution from wildfires in a warming climate. *Proceedings of the National Academy of Sciences*, 119(14): e2111372119. https://doi.org/10.1073/pnas.2111372119.

York E, Braun MJF, Goldfarb GG, Sifuentes JE. 2020. *Climate and health in Oregon: 2020 report.* Oregon Health Authority: Portland, Oregon. https://www.oregon.gov/oha/PH/HEALTHYENVIRONMENTS/CLIMATECHANGE/Pages/profile-report.aspx.

Young SL, Clements DR, DiTommaso A. 2017. Climate dynamics, invader fitness, and ecosystem resistance in an invasion-factor framework. *Invasive Plant Science and Management*, 10: 215–231. https://doi.org/10.1017/inp.2017.28.

Zhou X, Josey K, Kamareddine L, Caine MC, Liu T, Mickley LJ, Cooper M, Dominici F. 2021. Excess of COVID-19 cases and deaths due to fine particulate matter exposure during the 2020 wildfires in the United States. *Science Advances*, 7(33): eabi8789. https://doi.org/10.1126/sciadv.abi8789.

Zhuang Y, Fu R, Santer BD, Dickinson RE, Hall A. 2021. Quantifying contributions of natural variability and anthropogenic forcings on increased fire weather risk over the western United States. *Proceedings of the National Academy of Sciences*, 118(45): e2111875118. https://doi.org/10.1073/pnas.2111875118.

Ziska LH. 2002. Influence of rising atmospheric CO_2 since 1900 on early growth and photosynthetic response of a noxious invasive weed, Canada thistle (*Cirsium arvense*). *Functional Plant Biology*, 29: 1387–1392. https://doi.org/10.1071/FP02052.

Ziska LH, Epstein PR, Schlesinger WH. 2009. Rising CO_2, climate change, and public health: exploring the links to plant biology. *Environmental Health Perspectives*, 117: 155–158. https://doi.org/10.1289/ehp.11501.

Ziska LH, Faulkner S, Lydon J. 2004. Changes in biomass and root:shoot ratio of field-grown Canada thistle (*Cirsium arvense*), a noxious, invasive weed, with elevated CO_2: implications for control with glyphosate. *Weed Science*, 52: 584–588. https://doi.org/10.1614/WS-03-161R.